Identification and analysis of novel virulence-defective Rhodococcus fascians mutants

Adriana Sofia Silva Cabecinhas

Thesis submitted in partial fulfillment of the requirements for the degree of Master of Applied Biotechnology

Promotor: Doctor Danny Vereecke
Co-Promotor: Doctor Américo Rodrigues

2014

Title: Identification and analysis of novel virulence-defective *Rhodococcus fascians* mutants

This work was conducted at the Laboratory of Applied *in vitro* Plant Biotechnology at the Campus Schoonmeersen of the Ghent University.

Part of the work was also conducted at the department of Plant Systems Biology (PSB) of the Flanders Institute for Biotechnology (Vlaams Instituut voor Biotechnologie - VIB).

Acknowledgments

First of all, thanks a lot to Danny Vereecke, my scientific mum, to be not only a spectacular promotor, that guided and supported me through all the different stages of the thesis, but also a remarkable touristic guide, gastronomic advisor and a big friend. Thanks a lot for everything that you taught me, for all the input that you have asked from me and, specially, for all the effort that you have put into my thesis and to always believe in me. Thanks to Katrien to always have a big smile, to annoy me when I was trying to work and to try to put everyone speaking in English and encourage me to give it a try on the Dutch. Thanks to Joris to improve the quality of my photos and to bake cakes (or at least promise to). Thanks Nina that was in Belgium for a short time but was a big support for me. Thanks to the girls (Halima, Salima, Nandini and Mirni) for the support when I was really busy and tired, the company, the funny moments and to allow me to try a bit of your culture. Thanks Stefaan to let me working in your lab and for the relaxing effect that you have by always saying that "it is ok" even when it is not.

Thanks to Stephen to allow me work at your bench in VIB and be always available to help. Thanks a lot to Annick for the advice in the clonings, to take care of me when I had to work with the radioactive compounds and to help me at any time. Thanks Belén, not only for the company at weird hours at VIB but also to be always with a smile and able to help me even in the most busy days. Thanks to Pieter for the "ai, ai, ai…" and the nice conversations in the lab. Thanks to Hans and Stephanie because the party is also an important part of the work. Thanks to the Portuguese people that I met here. You made me feel at home in a country that is not ours. Thanks to Maria's (Fonseca and Fuller, my adopted mum), my two pillars that kept me straight and never allowed me to fall. Thanks for the awesome company, the nice food and all the support. Thanks to my Erasmus friends (José, Inês, Sónia, Vicky, Olívia), it would definitely not have been the same without you. A special thank to Vicky for being the exception.

Obrigada aos Doutores Américo Rodrigues, pelo apoio prestado ao longo deste trabalho, e Marco Lemos, pela permanente disponibilidade. Por último, mas não menos importante, obrigada aos meus pais pois sem eles não estaria aqui. Obrigada mãe por não ser preciso uma palavra para me entenderes. Obrigada pai pelo apoio. Obrigada aos dois por me terem

dado fortes raízes mas também por não me terem cortado as asas. Um grande obrigada ao João, meu amigo, companheiro e confidente. Obrigada por seres o meu porto de abrigo, me dares todo o apoio, acreditares em mim e teres sempre uma palavra positiva para me dizer. Obrigada manas por, cada uma à sua maneira, me darem força todos os dias para continuar. Obrigada Nádia pelas estrelinhas que me guiaram ao longo de todo o caminho e por estares sempre disposta a ouvir-me. Obrigada padrinhos pela ajuda, obrigada avó pelos miminhos e obrigada tios e primos pelo amparo. Obrigada amigos (Serguei, Dani, SaSilva, Rute, Tilui, Rita Pascoal, Joana Patriarca e Sarah Azinheiro) por terem sempre disponibilidade para mim e por nada mudar mesmo após meses de ausência.

Words do not come easy to me and it is impossible to say all the names that were important in this process. I will always be grateful to all of you.

Dank u wel

Muito obrigada

Abstract

The phytopathogenic actinomycete *Rhodococcus fascians* induces a disease, known as leafy gall, characterized by the induction of multiple shoots, on a broad variety of dicotyledonous herbaceous plants. The main pathogenicity factor of the bacterium is the production of a mixture of 6 cytokinins encoded by the genes of the *fas* operon which is located on a linear virulence plasmid pFiD188. This research aimed to analyze two novel virulence loci of the linear plasmid: *GT1* encoding a glycosyltransferase and the highly homologous *mtr1* and *mtr2* genes encoding SAM-dependent methyltransferases.

Previous data showed that the glycosyltransferase mutant 21D5 had a modified colony morphology and formed aggregates in liquid cultures. We established that these characteristics did not affect growth on rich media, but lead to the inability to proliferate under nutrient deprivation, strongly impacting epiphytic fitness. The latter was illustrated by the strongly attenuated virulence of 21D5, which was accompanied by a defective expression of the essential virulence genes *fas* and *att*, and the consequent reduced capacity to invade plant tissues and produce virulence factors. *GT1* expression proved to be induced by compounds that accumulate in plants very early upon infection, placing the GT1 function at the onset of the interaction.

Just like *R. fascians*, *Streptomyces turgidiscabies* carries a *fas* operon and two associated *mtr* genes. Mutants in these *mtr*'s in *R. fascians* have lost all ability to provoke symptoms, but still produce 2MeS-cytokinins, implying that other methylated cytokinins are imperative for disease induction. By analysing the cytokinin profiles via TLC of a set of *R. fascians* strains grown under *fas*-inducing conditions and of *S. turgidiscabies* fed with ^{14}C-labelled SAM and adenine we tried to uncover the elusive reaction products of the MTRs. Unfortunately, no *fas*- or *mtr*-dependent compounds were detected in the supernatants. By determining the expression pattern of the *mtr* genes *in vitro* and *in planta* it became clear that the regulatory aspects of these genes are very complex, limiting their expression to *R. fascians* cells that reside on the host. To open the path to the identification of the MTR reaction products, we succeeded in developing an assay in which the *in planta* expression can be brought *in vitro* so that the labelling experiments can be repeated.

Keywords: glycosyltransferase; methyltransferase; *att* operon; *fas* operon; cytokinins.

Resumo

Rhodococcus fascians é uma actinomiceta fitopatogénica que induz uma doença, conhecida como irritação frondosa, caracterizada pela indução de múltiplos rebentos, numa vasta gama de plantas herbáceas dicotiledóneas. O principal factor de patogenicidade da bactéria é a produção de uma mistura de 6 citoquininas codificadas pelos genes do operão *fas* que está localizado num plasmídeo linear associado à virulência, pFiD188. Este trabalho teve como objectivo a análise de dois novos loci deste plasmídeo associados à virulência: *GT1* que codifica uma glicosiltransferase e os genes *mtr1* e *mtr2*, grandemente homólogos, que codificam metiltransferases dependentes de SAM.

Trabalhos prévios com 21D5, mutante na glicosiltransferase, mostraram que possui uma morfologia de colónia modificada e forma agregados em culturas líquidas. Neste trabalho demonstrou-se que essas características não afectam o crescimento em meio de cultura rico, mas levam à incapacidade de proliferação em condições de privação de nutrientes, tendo um impacto forte na competência epifítica. Este impacto foi demostrado pela atenuação severa da virulência em 21D5, que foi acompanhada de uma expressão alterada dos genes *fas* e *att*, essenciais para a virulência, e consequente redução da capacidade de invasão dos tecidos da planta e de produção dos factores de virulência. Demonstrou-se também que a expressão de *GT1* é induzida por compostos que são acumulados em plantas nas fases iniciais da infecção, colocando a função de GT1 no começo da interacção.

Tal como *R. fascians*, *Streptomyces turgidiscabies* possui um operão *fas* e dois genes *mtr* associados. *R. fascians* mutantes nestes genes *mtr*'s perderam a capacidade de provocar sintomas, mas produziram 2MeS-citoquininas, implicando que outras citoquininas metiladas são cruciais para a indução da doença. De modo a identificar os produtos de reacção das MTRs procedeu-se à análise do perfil de citoquininas de *R. fascians* em condições que induzem a expressão dos genes do operão *fas* e de *S. turgidiscabies* alimentados com SAM e adenina marcadas com ^{14}C em TLC. No entanto, não foi possível a identificação de compostos dependentes de *fas* ou *mtr* nos sobrenadantes. Pela determinação do perfil de expressão dos genes *mtr in vitro* e *in planta* tornou-se claro que a regulação destes genes é muito complexa, sendo a sua expressão limitada a células de *R. fascians* que colonizam o hospedeiro. Para possibilitar a identificação dos produtos de recção de MTR, desenvolveu-se um protocolo que permite a expressão *in planta* em condições *in vitro*, o que permitirá a repetição dos ensaios de marcação com ^{14}C.

Palavras-chave: glicosiltransferase; metiltransferase; operão *att*; operão *fas*; citoquininas.

Part of this work is published in:

2014 - **Adriana Cabecinhas**, Petr Tarkowski, Ine Pertry, Stefaan Werbrouck, and Danny Vereecke "Methylated cytokinins: the secret weapon of the phytopathogen *Rhodococcus fascians*?" – Auxins and cytokinins in plant development, International Symposium

Table of contents

List of figures

List of tables

List of frequently used abbreviations

2-iP	2-isopentenyladenine
2MeS	Methylthio-derivatives
Amp	Ampicillin
att	Attenuation
CKX	Cytokinin oxidase/dehydrogenase
Cm	Chloramphenicol
*c*Z	*cis*-zeatin
DNA	Deoxyribonucleic acid
dpi	Days post-infection
fas	Fasciation
GT	Glycosyltransferase
GUS	β-Glucuronidase
His	Histidine
IM	Induction medium
Km	Kanamycin
LB	Luria broth
MES	2-(*N*-morpholino)ethanesulfonic acid
MTR	Methyltransferase
OD	Optical density
Phleo	Phleomycin
Pyr	Pyruvate
SAM	S-adenosyl methionine
TLC	Thin layer chromatography
*t*Z	*trans*-zeatin
YEB	Yeast extract broth

1. Introduction

Organisms living together in ecosystems can interact with each other in different ways. Mutualism is the interaction where both organisms benefit from the relation. Commensalism benefits one organism and does not bring advantage or disadvantage for the other. Pathogenic interactions benefit one of the organisms (the pathogen) and is disadvantageous for the other (the host) (Rédei, 2008). Pathogens can be differentiated according to the mechanism used to obtain nutrients. Necrotrophic pathogens kill the host or the cells of the invaded tissues through the secretion of toxic compounds. Biotrophic organisms extract nutrients directly from living cells (Dyakov et al., 2007).

Pathogens that affect plants are called phytopathogens. Those interactions have important economic implications since diseased plants are unfit for consumption or ornamental purposes (Depuydt et al., 2008). Bacterial interactions with plants can be compatible or incompatible. Compatible interactions happen when the bacteria infect susceptible host plants and are able to cause disease symptoms (Collmer, 1998). Incompatible interactions occur when the bacteria are not able to cause symptoms, because they cannot invade the plant tissues or because the plant secretes compounds that are toxic for the bacterium or that interfere with the pathogen's virulence mechanism.

A. Rhodococcus fascians, causative agent of the leafy gall syndrome

R. fascians is a phytopathogenic Gram-positive, rod-shaped, aerobic, nonmotile, and nonsportulating bacterium that forms orange colonies (Pertry et al., 2010; Stes et al., 2011; Tilford, 1936; Vandeputte et al., 2005) (Figure 1.1.A). The taxonomic position of the bacterium was a matter of debate for several years. Based on phenotypic, biochemical and genetic data the phytopathogen was positioned within the Actinomycetales in the genus *Rhodococcus* (Goodfellow, 1984). Bacteria from the genus *Rhodococcus* are known because of their medical, environmental and industrial implications (Gürtler et al., 2004). Despite the advances in the study of the genus and reports referring to plant-association, *R. fascians* is the only pathogenic member (Stes et al., 2011).

When infecting plants, *R. fascians* induces the development of leafy galls (Figure 1.1.B), structures consisting of clusters of small often deformed shoots of which further outgrowth

is inhibited (Crespi et al., 1992; Vereecke et al., 2000). Generally, plant tissues first grow by cell division and then by cell expansion (Donnelly et al., 1999), but in the formed structures there is continuous growth through cell proliferation (Depuydt et al., 2009a; Vereecke et al., 2002b). Although the important role of cytokinins in the development of those symptoms is established, there is evidence that other hormones are involved as well (Depuydt et al., 2008; Simón-Mateo et al., 2006). Other gall-inducing pathogens, such as bacteria of the genera *Agrobacterium*, *Pantoea*, and *Pseudomonas*, cause the proliferation of undifferentiated tissues (Pitzschke and Hirt, 2010). *R. fascians* is the only hyperplasia-inducing bacterium that causes differentiated galls (Vereecke et al., 2000), inducing the formation of shoots from existing and newly formed meristems (de O Manes et al., 2004). The leafy galls represent a niche with the perfect conditions for the survival and maintenance of the pathogen (Bailey et al., 2009; Hayward and Stone, 2005). Other symptoms observed in plants infected with *R. fascians* are the deformation of the leaves and swelling of the vascular tissues (Stes et al., 2011) (Figure 1.1.C). Symptom development (time to appear and aggressiveness) depends on the infection success, which is influenced by the initial amount of bacteria, the susceptibility of the plant, and the general efficiency of the interaction between the plant and the bacterium.

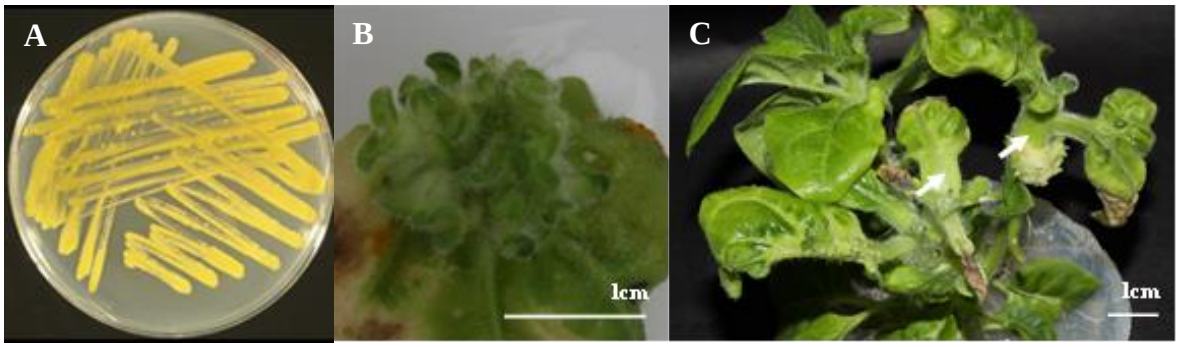

Figure 1.1 Typical growth of *R. fascians* on YEB and symptoms on *Nicotiana tabacum* infected with the wild-type strain D188 at 28 dpi.
(A) *R. fascians* grown on YEB; (B) Leafy gall on infected leaf (ISO 100, Diaphragm 16 and closing time 1/100sec); (C) Leaf deformation and swelling of the vascular tissue (arrow) on decapitated plants (ISO 100, Diaphragm 32 and closing time 2,5sec).

With the increase of transport of ornamental plants, this pathogen has become a worldwide threat in horticulture, leading to significant economic losses (Depuydt et al., 2008; Putnam and Miller, 2007). Infections have been recorded throughout the world but are mainly present in temperate regions (CBI, 2006) The reported host range of *R. fascians* encompasses 164 different plant species belonging to 43 families, mono- and

dicotyledonous, but this number is most probably an underestimation of the pathological potential of the species (Depuydt, 2008). Few reports describe plants that are resistant to the morphologic alterations caused by the bacteria. For instance, *Dalbergia pervillei* synthesizes a compound - perbergin - that is able to inhibit the expression of the virulence genes of the bacteria (Rajaoson et al., 2011).

The bacteria can stay on the plant surface for months before symptoms become visible (Cornelis et al., 2001). Therefore, the propagation of contaminated material is the main transmission way in horticultural practices (Miller et al., 2007). Moreover, the phytohormones that are extensively used in horticulture for plant propagation induce morphological changes that are similar to the ones caused by *R. fascians*. In that way, infected symptomatic plants can be mistaken for plants deformed by the exogenous hormones. Moreover, other pathogens or herbicides can cause *R. fascians*-like deformations (Miller et al., 2008; Putnam and Miller, 2006). Altogether, because of these complications, it is likely that the problem with *R. fascians* in horticulture is underestimated and a good diagnosis combined with strict sanitary measures are imperative to prevent infection spread to other plants (Miller et al., 2007).

Proper diagnosis of the plants is based on the combination of different methods. The traditional method to isolate the bacteria from the plant has proven to be difficult and can lead to false negative results. Additionally, non-pathogenic strains can be obtained as well and, therefore, the pathogenicity of the isolates has to be confirmed by molecular methods which are time consuming, yet extremely sensitive (Lacey, 1961). Pathogenicity can also be established by infecting a plant from the same species as the original host (Putnam, 2014; Vereecke et al., 2000). Finally, serological tests, based on the detection of fluorescent antibodies, are used but those methods are laborious and can raise false results (de Boer et al., 1988). Adding to the complexity, recent work developed at the Oregon State University indicated that the causative agent of the leafy gall syndrome is not a single organism, but two genetically very different bacterial species (Putnam, 2014).

Some plants do not react to the phytohormone-based methods used in *in vitro* propagation and hence cannot be propagated artificially (Kevers et al., 2004). Since *R. fascians* triggers vegetative multiplication through the action of phytohormones, this pathology also has a putative positive side and might be useful in different plant research areas. A first line of

research is to understand the role of plant hormones in regular plant development. Currently this question is addressed by using plant mutants or exogenous hormones. An alternative approach is to use *R. fascians* as a source of phytohormones that are delivered directly into the plant tissues in a much more controlled and biologically relevant concentration than exogenous addition (Depuydt et al., 2009a). The direct application of *R. fascians* in *in vitro* technologies still lies far ahead because the leafy gall syndrome is the result of a complex interaction between the pathogen and its host, and therefore it is very difficult if not impossible to mimic the shoot formation induced by *R. fascians* by exogenous hormone addition. Leafy galls induced by *R. fascians* bacteria on diverse medicinal plants have been reported to generate intact plants without phenotypical abnormalities upon repeated antibiotic treatments (Vereecke et al., 2000). However, it is difficult to convince plant growers to use a phytopathogenic bacterium to propagate their plants. Nevertheless, it is worthwhile to continue exploring the possibilities of implementing *R. fascians* and/or its morphogens in tissue culture practices since the very broad host range of the pathogen suggests that it might bring solutions for recalcitrant plants (Tarkowski and Vereecke, 2014). Consequently, it is imperative to complete the knowledge on the mechanism of leafy gall development and to get insight into putative novel virulence factors (Depuydt et al., 2008).

B. The molecular basis of the phytopathogenicity of R. fascians strain D188

A common strategy in plant-associated microbes is the secretion of phytohormones (Francis et al., 2010). Generally the genes responsible for hormone production are on large circular plasmids (Nester and Kosuge, 1981), but in *R. fascians* they are uniquely encoded by a linear plasmid (Francis et al., 2007). The wild-type *R. fascians* strain D188 has a genome consisting of a circular chromosome and two plasmids, one linear, pFiD188, associated with the pathogenicity, and one circular, pD188, related with cadmium resistance (Crespi et al., 1994; Desomer et al., 1988). Two different regions can be considered in the linear plasmid: R regions conserved in other rhodococcal linear plasmids, involved in the plasmid maintenance functions, and U regions unique to *R. fascians* (Francis et al., 2012) (Figure 1.2).

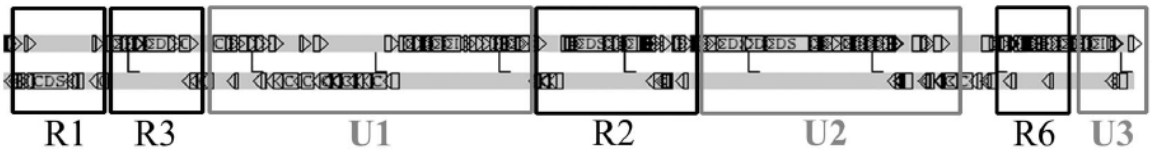

Figure 1.2 Representation of the linear plasmid pFiD188 of *R. fascians* strain D188. Conserved (R) and unique (U) regions are indicated (Francis et al., 2012).

Unique region U1 is the largest and contains the loci *attenuation* (*att*) and *fasciation* (*fas*), described later in this section (Figure 1.3), and *hyp*, involved in post transcriptional control of virulence-related genes (Crespi et al., 1992; Maes et al., 2001; Rajaoson et al., 2011). Since region U1 contains all genes encoding the known virulence factors and pathogenicity regulators, this region is considered to be the main pathogenicity region on pFiD188. So far, no virulence-associated genes have been identified in the unique regions U2 en U3.

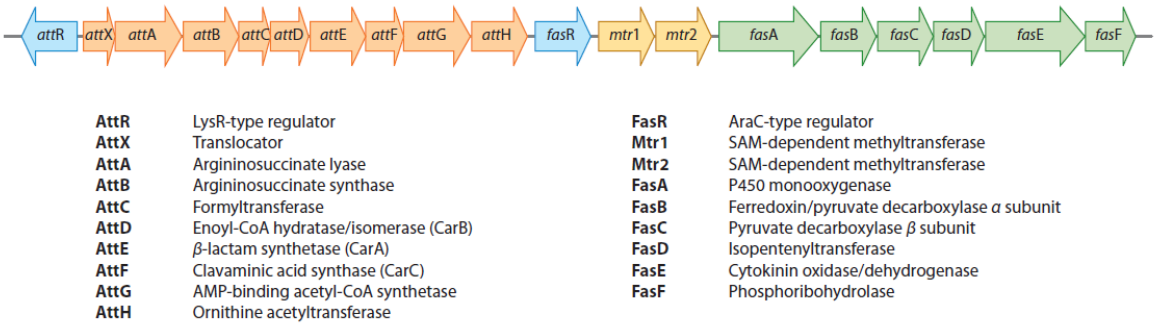

Figure 1.3 Organization and homologies of the *fas* and *att* loci located in region U1 of pFiD188, the linear plasmid of *R. fascians* strain D188 (Stes et al., 2011).

Infection of a host starts with an epiphytic colonization. *R. fascians* has several characteristics that are beneficial for a successful establishment of the interaction. For instance, the orange carotenoid pigments (Figure 1.1.A) provide protection against ultraviolet radiation during the establishment of epiphytic colonies on the stems and leaves of the host (Ichiyama et al., 1989; Sundin and Jacobs, 1999). *R. fascians* produces the hormone indole-3-acetic acid (IAA), an auxin that triggers nutrient release from and suppresses the defense responses mounted by plant cells (Cornelis et al., 2001; Depuydt et al., 2009a; Vandeputte et al., 2005). The formation of a biofilm that is surrounded by a slime layer, probably composed by exopolysaccharides, protects the bacterial cells against environmental conditions and improves the attachment to the plant (Cornelis et al., 2001; Miller et al., 2007; Pertry et al., 2010). All these features are encoded by chromosomal

genes because linear plasmid-free bacteria have similar colonization capacities as the wild-type strain (Cornelis et al., 2001).

During the epiphytic colonization the primary metabolism of the host changes. In this process the plant increases the production of carbon and nitrogen sources, which is thought to facilitate the bacterial colonization (Depuydt et al., 2009a). The bacteria sense these metabolic changes of the plant and perceive it as a signal that a compatible host has been found (Maes et al., 2001). The active role of the host in the infection process is very important and complex. However, since the focus of this work is the phytopathogen and not the plant, we will not elaborate on the plant side of the interaction. Information about this topic can be found in recent review articles (Stes et al., 2013; Stes et al., 2011).

When a specific combination of carbon and nitrogen sources is detected, *att* gene expression is activated in *R. fascians* (Figure 1.4.A). This expression is controlled by AttR, a LysR-type transcriptional regulator (Stes et al., 2011). The *att* operon is essential at the onset of the infection and the first locus to be expressed in this process (Cornelis et al., 2002). An initially low concentration of the *att* compound is sufficient to activate the expression of the *att* biosynthetic genes. With this positive feedback mechanism, the production of high amounts of the *att* compound is established (Figure 1.4.B)(Stes et al., 2013). Such an autoregulatory mechanism resembles the quorum sensing classical concept, a phenomenon that allows the cells to act as a community rather than as single cells. In *R. fascians* the *att* autoregulatory mechanism is not considered as genuine quorum sensing since the presence of the plant is required to activate the expression and there is no cell density-dependent production of the regulatory compound (Maes et al., 2001). The *att* regulatory compound is responsible for the activation of the *fas* operon (Figure 1.4.C). This operon encodes the genes responsible for the synthesis of the cytokinins and will be described later (Depuydt et al., 2008). The *att* knockouts require wounding of the plant tissues to infect the plant and therefore it is believed that the regulatory compound also affects, directly or indirectly, the entrance of the bacteria into the plant tissues. Although the exact mechanism is unknown, it is hypothesized that the *att* compound itself breaks the plant cuticula by phytotoxicity or activates the expression of plant cell wall degrading enzyme genes (Stes et al., 2011). As soon as the bacteria engage in an endophytic stage, *att* expression is switched off (Cornelis et al., 2002).

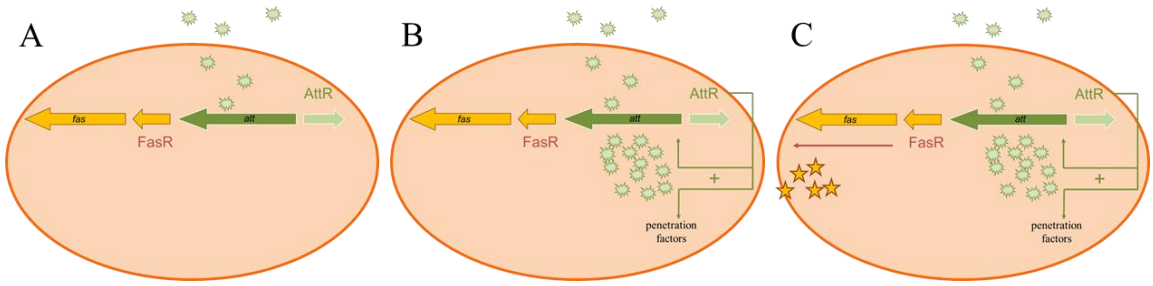

Figure 1.4 Representation of the molecular processes occurring after the infection of a host plant by *R. fascians*.
(A) After contact with a compatible host, the expression of the *att* genes is increased and the *att* compound is produced; (B) the accumulation of the *att* compound triggers the formation of penetration factors and stimulates the production of high amounts of the *att* compound through a positive feedback; (C) the *att* compound triggers the expression of the *fas* genes, responsible for the symptom development (Modified from Stes et al., 2013).

The main pathogenicity strategy of *R. fascians* is the production of shoot-inducing cytokinins, triggered by the expression of *fas* operon genes (Stes et al., 2010) (Figure 1.3). *fas* expression is tightly controlled and involves the AttR regulator and FasR, an AraC-type transcriptional regulator (Temmerman et al., 2000) (Figure 1.4.C). *In planta*, the *fas* genes are active both in the epiphytic and the endophytic populations (Cornelis et al., 2002). Through biochemical data and the analysis of cytokinin profiles it was possible to understand that the Fas proteins lead the synthesis of six distinct cytokinins: 2-isopentenyladenine (2-iP), *cis*-zeatin (*c*Z), *trans*-zeatin (*t*Z) and their methylthio-derivatives – 2MeSiP, 2MeS*c*Z and 2MeS*t*Z (Figure 1.5) (Pertry et al., 2009). In contrast to earlier ideas, the virulence depends more on the cytokinin concentration and ratio of the different compounds that the host is exposed to, than on the production of specialized molecules by the bacterium (Pertry et al., 2009). FasD, an isopentenyltransferase, is the key enzyme in the process. This enzyme synthesizes 2-iP which is the precursor for the other Fas enzymes (Pertry et al., 2009). FasE is a cytokinin oxidase/dehydrogenase (CKX) with a strong affinity for 2-iP-type cytokinins and thought to be required for the optimal functioning of the FasD enzyme. FasA is a putative P450 monooxygenase that hydroxylates 2-iP to form *t*Z and *c*Z. This enzyme can also hydroxylate 2MeSiP, allowing the formation of 2MeS*c*Z and 2MeS*t*Z. FasA is absolutely required for the virulence of the phytopathogen (Crespi et al., 1994). FasB and FasC are homologous to the α- and β-subunit of pyruvate decarboxylase, respectively, and are thought to be accessory proteins of FasA providing the required electrons (Crespi et al., 1994; Goethals et al., 2001). The enzymes involved in the direct methylthiolation of 2-iP, *t*Z, and *c*Z to produce their 2MeS

derivatives remain to be identified. FasF is a phophoribohydrolase and represents a complementary pathway for the formation of Z-type cytokinins. This enzyme directly releases cytokinin bases from their nucleotide precursors and is crucial for symptoms maintenance (Figures 1.3 and 1.5) (Stes et al., 2011).

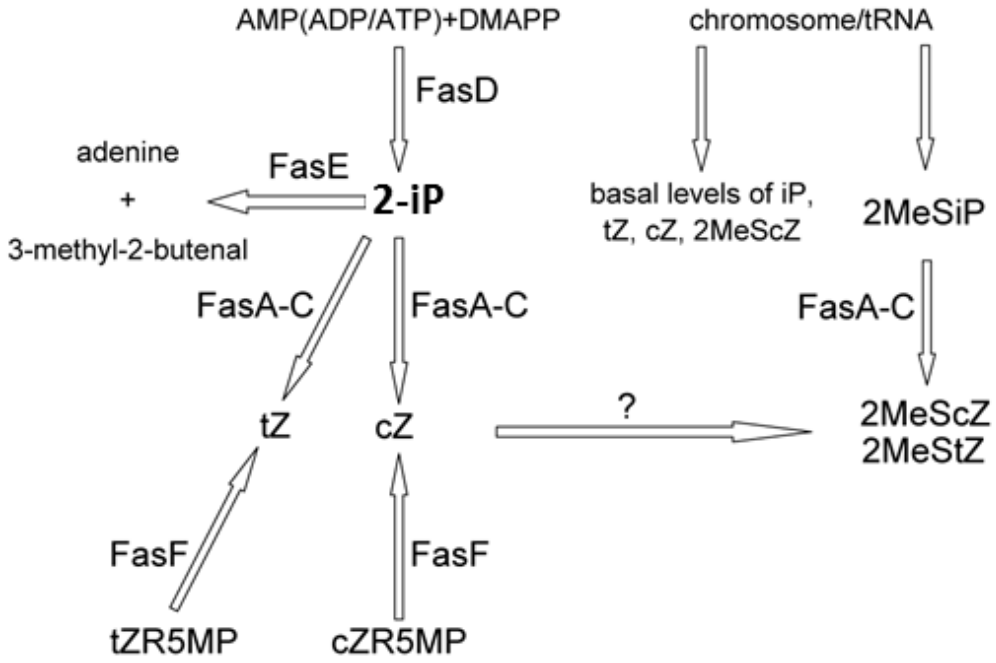

Figure 1.5 Representation of the cytokinin biosynthetic pathway encoded by the *fas* operon of *R. fascians* D188 (Stes et al., 2011).

The production of a mixture of cytokinins instead of the production of large amounts of a single one has several advantages. In plants, the CKX enzymes are responsible for the degradation of cytokinins and cytokinin homeostasis. Previous work showed that each CKX enzyme has a particular substrate specificity and, consequently, the capacity of different plant tissues and species to degrade specific cytokinins can differ (Galuszka et al., 2007). In *Arabidopsis* the activation of the CKX enzymes effectively reduces the *in planta* levels of most of the bacterially produced cytokinins, but they are unable to efficiently degrade *c*Z and 2MeS*c*Z. The CKX enzymes of *Nicotiana tabacum*, however, are ineffective against 2-iP (Pertry et al., 2009). Thus, with the strategy of producing a cytokinin mixture, some bacterial cytokinins will always be able to accumulate in the infected plant tissues. The *R. fascians* cytokinin mixture also modulates the sensitivity of the plant for those morphogens. In *Arabidopsis*, when infection by the bacteria occurs, the secreted cytokinins are perceived by two of the three cytokinin receptors, the ARABIDOPSIS HISTIDINE KINASES (AHK). At the onset of the interaction, 2-iP

strongly accumulates and the upregulation of the *AHK3* and especially *AHK4* receptor genes occurs. Consequently, even with a relatively low amount of secreted cytokinins, the cytokinin sensitivity of the plant is the highest when symptoms need to be initiated (Pertry et al., 2009; Pertry et al., 2010). Finally, adding to the efficiency of producing a cytokinin mixture, the equimolar mix of the six cytokinins proved to have a stronger effect than an equal final concentration of the individual molecules in different bioassays (Pertry et al., 2009; Stes et al., 2011). *R. fascians* produces its cytokinins in a very controlled and dynamic way. In the initiation process it secretes mainly high amounts of 2-iP, *t*Z and *c*Z and later it produces a maintenance flow consisting of *t*Z, 2MeS*t*Z, *c*Z and 2MeS*c*Z (Pertry et al., 2010).

During the endophytic colonization, the bacteria undergo a series of adaptations. In order to adapt to the new environment, the intercellular spaces of plant tissues, their cell wall is modulated (Cornelis et al., 2001) or lost (Lacey, 1961) and their metabolism shifts to the use of C2 compounds (Forizs et al., 2009; Vereecke et al., 2002a; Vereecke et al., 2002b). While the epiphytic bacterial subpopulation triggers the onset of symptoms development, the maintenance of the symptoms depends on the endophytic population (Stes et al., 2011).

C. Glycosyltransferase (GT1), a novel player in the pathology of R. fascians

The molecular identification of the *R. fascians* virulence determinants started in 1988 with the elimination of both plasmids from strain D188 (Desomer et al., 1988). Recently, a large collection of mutants from this strain has been generated by transposon mutagenesis in the laboratory of Professor Jaziri at the Université Libre de Bruxelles. *R. fascians* shifts its metabolism during the interaction with plants from the Krebs cycle to the glyoxylate shunt, which allows the bacteria to grow on C2 compounds that are thought to be enriched in infected tissues (Forizs et al., 2009). Due to this link between the glyoxylate shunt and virulence, the obtained mutants were screened for their ability to grow on acetate. Twenty six mutants out of approximately 1400 screened, were unable to grow on acetate, although their growth on rich medium was not seriously affected. From those, strain 21D5 was the only mutant that could not induce malformations on infected plants. The mutation in 21D5 was mapped on pFiD188 (Forizs, 2012).

Sequencing of the flanking regions of the transposon located the mutation in 21D5 in a

gene of unique region U2 of pFiD188 (Forizs, 2012). Interestingly, this region had not been associated with pathogenicity before. In the mutant library, three additional strains, 45F10, 41H2 and 40G10, were identified with a transposon insertion at different positions in the same gene (Figure 1.6) (Forizs, 2012). The disrupted gene, *pFi_136*, encodes a putative glycosyltransferase (GT) and was named *Rf_GT1*. The gene is translationally coupled to the upstream gene, *pFi_135*, which encodes a putative integral membrane protein. Based on this configuration, it was postulated that these two genes might constitute an operon. Upstream from this putative operon, there are two genes that comprise a two-component regulatory system: *pFi_133*, a putative sensor histidine kinase and *pFi_134*, its cognate response regulator that has a LuxR type DNA binding domain. These four genes have the same transcriptional orientation and are flanked by genes with an opposite transcriptional orientation. Altogether this might indicate that they act in the same pathway (Figure 1.6). The current hypothesis is that the sensor kinase (*pFi_133*) recognizes specific environmental signals and triggers the phosphorylation of the response regulator (*pFi_134*). This component will then activate de transcription of *pFi_135* and *Rf_GT1* (Forizs, 2012).

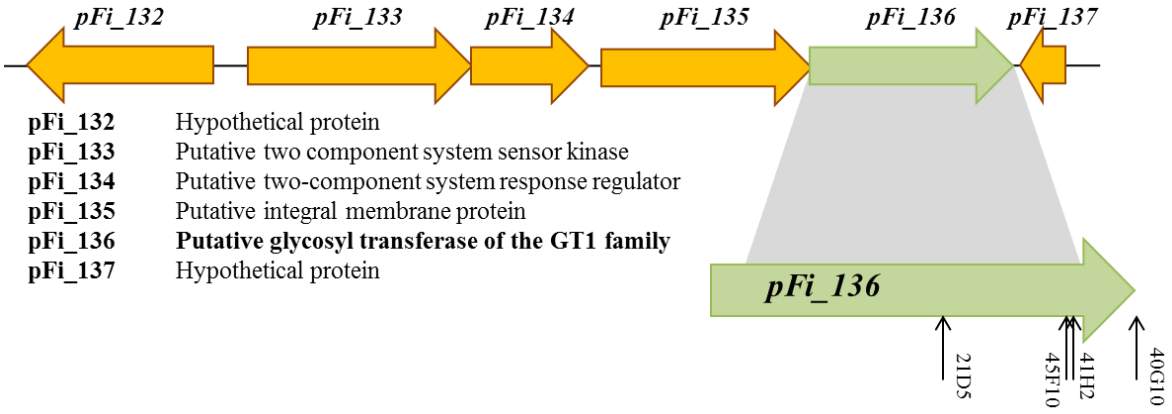

Figure 1.6 Organization and homologies of the *GT* locus genes in *R. fascians*.
The arrows in *pFi_136* represent the location of the mutations from the different *GT1* mutants studied in this work. The mutation in 40G10 is located in the stop codon.

Besides the virulence defect, the colonies formed by 21D5 on rich LB medium had a very different morphology compared to that of the wild-type strain D188. In liquid cultures the mutant cells formed aggregates that precipitated in the medium. An intriguing observation was that the colony morphology and the behavior in liquid cultures of the plasmid-free *R. fascians* strain D188-5, where *Rf_GT1* is also absent, was not similar to that of 21D5. It

was hypothesized that other genes located on pFiD188 were involved in the production of the matrix as substrates of *Rf_GT1*. D188-5 does not make those substrates of *Rf_GT1*, due to the fact that it does not possess pFiD188, and the pathway cannot be deregulated as in 21D5 (Forizs, 2012).

GTs are a large family of enzymes responsible for diverse transglycosylation reactions, involved in the biosynthesis of oligosaccharides, polysaccharides, and glycoconjugates (Berg et al., 2007; Taniguchi et al., 2002). Many of these compounds are cell wall components (Badreddine et al., 2008; Schaeffer et al., 1999; Wagner and Pesnot, 2010) that are critical not only in the maintenance of the structural integrity of cell membranes, but also in the modulation of molecular recognition events (Albesa-Jové et al., 2014). Obtaining a high level of expression, purification and crystallization were the main bottlenecks in the crystal structure determination for GT enzymes, but eventually two structural super-families were identified: GT-A and GT-B. When compared with other protein sequences, Rf-GT1 belongs to the B-fold GTs which consists of two separated Rossmann domains with a connecting linker region and a catalytic site located between these domains (Figure 1.7). Typically, the two Rossmann domains have a high structural homology, but a minimal sequence homology (Hu et al., 2003).

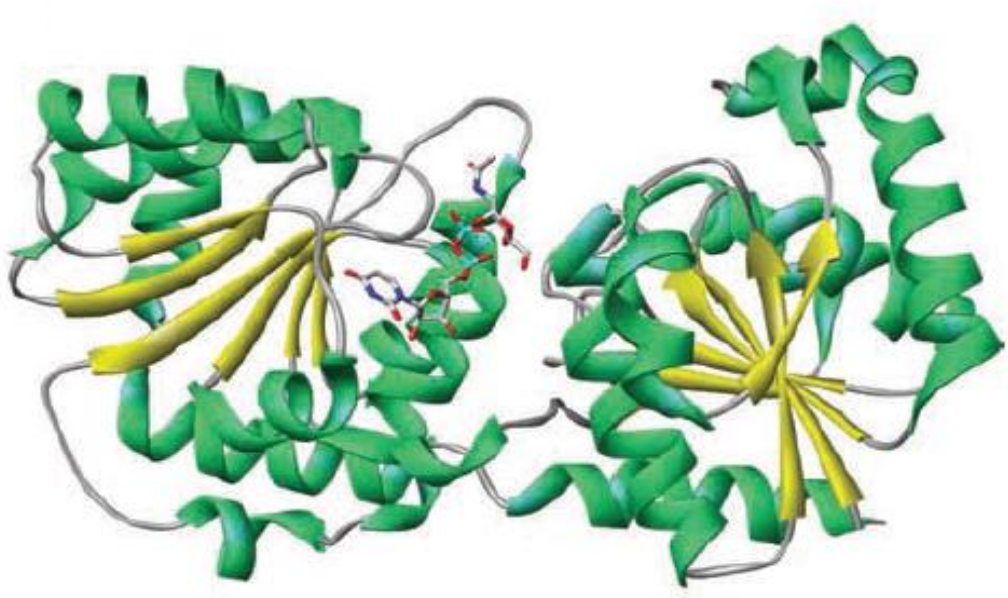

Figure 1.7 The protein structure of *Escherichia coli* MurG, a typical B-fold GT, in complex with its donor substrate, UDP-GlcNAc (Hu et al., 2003).

Nevertheless, some of the conserved amino acid residues are thought to be important for catalysis in GT-B glycosyltransferases. When aligning the *R. fascians* GT1 and related GTs from other organisms, such as *Streptomyces vitaminophilus*, *S. niveus*, and *Mycobacterium smegmatis*, with MurG of *E. coli* (Guerin et al., 2007), conserved glutamic acid, proline, and glycine residues could be identified in the *R. fascians* enzyme (Figure 1.8).

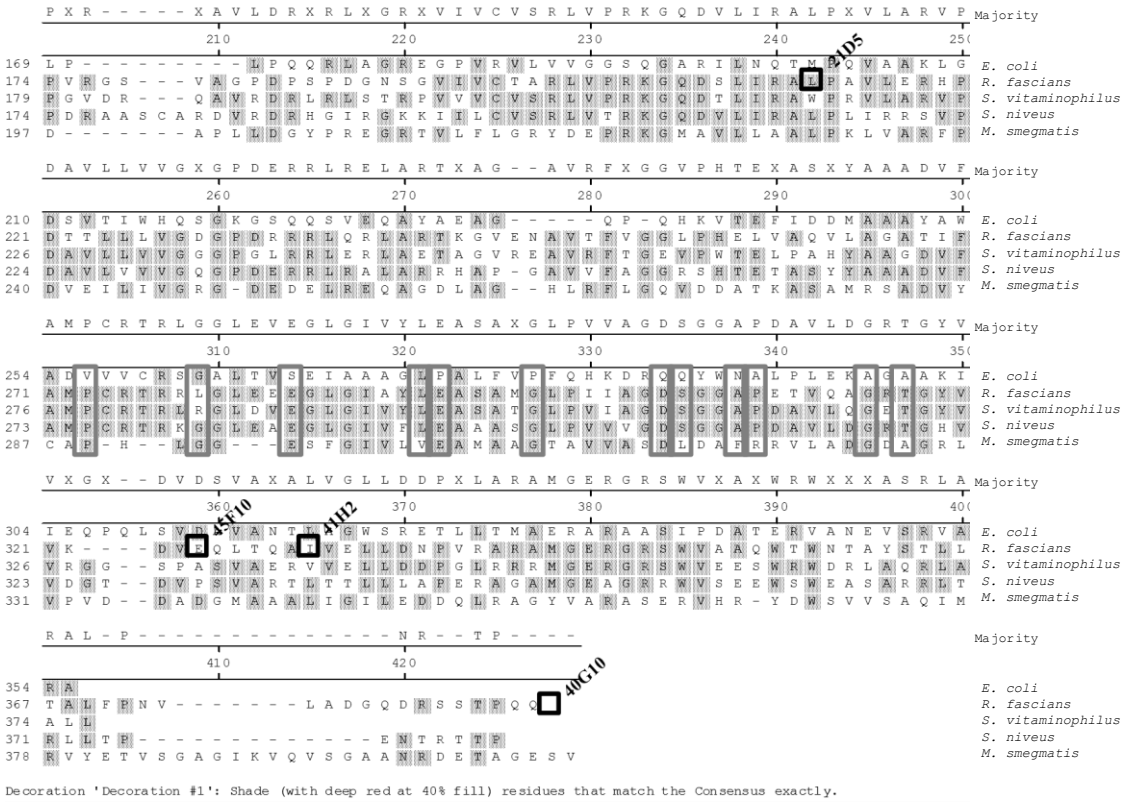

Figure 1.8 Sequence alignment of selected GT-B superfamily members.
Conserved residues are boxed in grey and transposon mutations in *R. fascians* in black. The sequence accession numbers are: P17443 of *E. coli*, WP_015586190 of *R. fascians*, WP_018382616.1 of *S. vitaminophilus*), WP_023538738 of *S. niveus*), and 2GEJ_A of *M. smegmatis*.

Another classification system based on amino acid sequence similarities has been proposed for GT function prediction (Campbell et al., 1997; Coutinho et al., 2003). With this sequence-based classification method 92 GT families have been identified. GTs belonging to family 1, to which the protein encoded by *pFi_136* of *R. fascians* belongs, are named GT1 and are typically responsible for the transfer of a saccharide from a glycosyl donor to an acceptor, that can be another saccharide, a protein, a peptide, a lipid or a secondary metabolite (Wagner and Pesnot, 2010).

In pathogenic organisms, the molecules involved in host recognition, adhesion, and colonization, as well as the antigens that target host responses are all located in the cell wall (Albesa-Jové et al., 2014; Netea et al., 2008). The expanding bacterial sequence dataset coupled with developments in mass spectrometry and analytical glycosciences has identified protein glycosylation systems in most bacterial pathogens (Cuccui and Wren, 2013). Those systems have proven to be essential for viability and virulence (Cuccui and Wren, 2013; Dover et al., 2004). As an example, in *Streptococcus mutans*, a mutant defective in a GT exhibited a modified colony morphology and an impaired aggregation (Kuramitsu, 1976; Taniguchi et al., 2010). In other pathogens as well, including phytopathogens, protein glycosylation systems were shown to be required for biofilm formation and virulence (Cuccui and Wren, 2013). In the pathogen *Burkholderia cepacia* (*Bcc*), the inability to produce exopolysaccharide (EPS) was correlated with a deletion in the *bceB* gene, which encodes a GT. EPS is a putative *Bcc* virulence factor that is involved in bacterial persistence, interaction with antimicrobial peptides, and biofilm formation (Bartholdson et al., 2008). *Xanthomonas campestris* causes citrus canker, a leaf-spotting and fruit rind-blemishing disease that can lead to defoliation, shoot dieback and fruit drop when conditions are highly favorable for infection (Gottwald et al., 2002). In this pathogen, silencing of the *gpsX* gene, that encodes a GT, resulted in a reduction in the amount of EPS and lipopolysaccharides (LPS) in the cell wall, defects in biofilm formation, delayed growth, a higher sensitivity to various stress compounds, and reduced symptoms on the host plant (Chou et al., 1997; Dow et al., 2003; Li and Wang, 2012). Similarly, in *Xanthomonas citri*, another citrus pathogen causing citrus canker, the knock-out of *gpsX*, also leads to a decreased biofilm formation and a reduced virulence. Nonetheless, quantitative PCR revealed that the mutation had no effect on the expression of the virulence genes (Li and Wang, 2012).

D. Two methyltransferases, intriguing members of the fas locus

As described above, previous studies on the *fas* operon identified the functions of all of the Fas proteins in the production of the cytokinin mixture (Pertry, 2009; Pertry et al., 2010). In between *fasR*, encoding the main regulator of *fas* gene expression, and *fasA*, the first gene on the *fas* operon, two genes are located that are homologous to putative S-adenosyl methionine (SAM)-dependent methyltransferases (MTRs), *pFi_075* and *pFi_076* (*mtr1* and *mtr2*) (Figure 1.3) (Stes et al., 2011).

These genes are conserved in the *fas* operon of the phytopathogen *Streptomyces turgidiscabies* (Joshi and Loria, 2007) (Figure 1.9). This organism is the causative agent of potato scab disease, a pathology that leads to significant annual losses to potato growers world-wide. The disease symptoms, characterized by erumpent lesions on the tubers (Figure 1.9-right), is caused by the main phytopathogenicity factor produced by *S. turgidiscabies*, i.e. the toxin thaxtomin (Loria et al., 2006). Although there are no reports for gall formation caused by this phytopathogen in nature, *S. turgidiscabies* has a *fas* operon that strongly resembles and is largely collinear to the one of *R. fascians* (Figure 1.9-middle). Furthermore, infection of *Nicotiana tabacum* and *Arabidopsis thaliana* with a thaxtomin-deficient mutant, lead to the formation of leafy galls similar with those induced by *R. fascians* (Figure 1.9-left and right). Intriguingly, upstream of the *fas* operon of *S. turgidiscabies* there are two *mtr* genes highly homologous to those of *R. fascians* (Joshi and Loria, 2007; Kers et al., 2005) (Figure 1.9-middle). Altogether, these observations suggest that the *mtr* gene products are involved in cytokinin production and/or pathogenicity. Indeed, preliminary data revealed that mutations in the *mtr* genes in *R. fascians* cause a complete loss of virulence (Pertry, 2009).

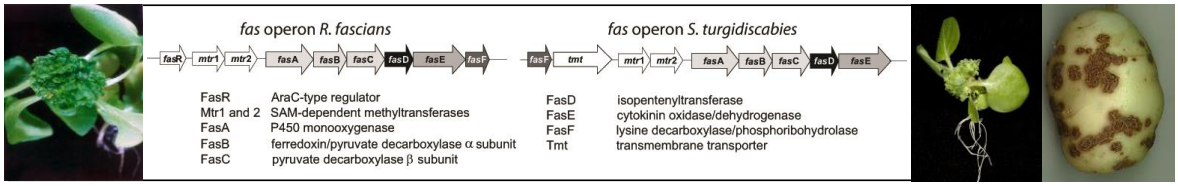

Figure 1.9 Organization of the *fas* loci of and induced symptoms by *R. fascians* strain D188 (left) and *S. turgidiscabies* (right).

Methyltransferases are a large family of enzymes that catalyze the transfer of a methyl group from a donor to an acceptor. Those enzymes can be divided in several subclasses based on their structural features and used substrates. Most common are the number I methyltransferases, encompassing by SAM-dependent enzymes with a Rossman fold (Katz et al., 2003). SAM-dependent methyl transfers are found in different pathways and mutations is the corresponding genes cause severe or complete impairment of regular behavior of the organism (Struck et al., 2012).

Although it is unlikely to be the case for *R. fascians*, in other pathogens MTRs are often linked to cell wall formation. In diverse plant pathogens, such as the gram-negative *Xanthomonas oryzae*, *Xanthomonas campestris*, *Pseudomonas syringae*, and *Ralstonia*

solanacearum, MTRs have been associated with the methylation of LPS (Whitfield et al., 1997) which have been shown to be critical virulence determinants and control a number of defense-related responses in plants (Desaki et al., 2006). It has also been suggested that LPS are likely to be involved in the association of bacteria with plant cell walls during the infection process (Boher et al., 1997). In the phytopathogen *Xanthomonas albilineans* MTRs are important in the biosynthesis of the key pathogenicity factor, i.e. the toxin albicidin (Birch, 2001; Hashimi and Birch, 2010). MTRs in *Candida albicans*, an opportunistic pathogen, are important for the maintenance of cellular homeostasis and regulation of intra- and interspecies interactions. It was found that those enzymes are also important for virulence-related processes, such as adhesion and membrane transport (Lissina et al., 2014). A gene that encodes a specialized o-methyltransferase is present in all virulent lineages from *Francisella*, a bacterial human pathogen (Champion, 2011), and therefore is assumed to be related with pathogenicity. Finally, in the gram-positive human pathogen *Mycobacterium tuberculosis*, MTRs are involved in the biosynthesis of mycolic acids, major components of the cell wall also present in the cell wall of members of the genus *Rhodococcus* (Nishiuchi et al., 2000). The envelope from *M. tuberculosis* is partly responsible for its resistance to antibiotics and plays a major role in the virulence and the persistence of the pathogen (Cantaloube et al., 2011; Simeone et al., 2013).

2. Aim of this work

Despite extensive mutagenesis screens, the main pathogenicity factors of *R. fascians* appeared to be linked to unique region U1 of the linear plasmid. Nevertheless, for the majority of genes on pFiD188, the function in the life style of *R. fascians* remains to be determined. Recently, two loci on pFiD188 were shown to be essential for the pathology of the bacteria: the glycosyltransferase *GT1* (*pFi_136*), situated in unique region U2, and two methyltransferases *mtr1* and *mtr2* (*pFi_075* and *pFi_076*), located immediately upstream of the *fas* operon. Here we aim to get insight into the role of GT1 and the two MTRs in the phytopathogenicity of *R. fascians*.

Preliminary data on *GT1* revealed that mutants in the gene have a strong colony phenotype and a severe loss of pathogenicity. Till today, virulence defects of *R. fascians* are either linked with cytokinin production and the regulation thereof (*fas*, *att*, *hyp*) or with *in planta* survival (*vic*) (Stes et al., 2012). GTs are known to glycosylate secondary metabolites. The *fas* cytokinins can be considered as secondary metabolites of *R. fascians* and it is currently unknown if their secretion into the environment is active or passive. Moreover, high cytokinin concentrations are toxic for living cells (Pertry et al., 2009). Based on this information we postulated a first working hypothesis that the *GT1* mutant 21D5 is non-pathogenic because it is defective in cytokinin production or secretion. The second working hypothesis is based on the knowledge that *R. fascians* forms an epiphytic biofilm prior to plant tissue penetration (Cornelis et al., 2001) and the finding that, in other pathogens, GTs are important for the survival in host tissues (see Introduction). So, we postulated that the inability of 21D5 to cause disease is the result of a severely impaired capacity to survive on or in the plant tissues. Before testing these hypotheses, we will first confirm the virulence defect by assessing symptom formation upon infection of *Nicotiana tabacum* cv. Havana and Xanthi (seedlings, decapitated plants and leaves) and *Arabidopsis thaliana* plants with strain 21D5. We will also evaluate the colony morphology on different defined media. Both phenotypes will be compared to the wild-type strain D188 and its plasmid-free non-pathogenic derivative D188-5; virulence will also be compared to the attenuated *att* mutant and the non-pathogenic *fas* mutant. With these experiments, we will get insight into the behavior of the mutant 21D5. The first hypothesis will be tested by measuring the expression of the *fas* and *att* genes in the 21D5 mutant, both *in vitro* and *in planta* using quantitative assays and histochemical stainings. The secretion of cytokinins

will be addressed by determining the cytokinin profile of 21D5 supernatants (in collaboration with Petr Tarkowski, Laboratory of Growth Regulators, Palacký University, Olomouc, Czech Republic). The secretion of the *att* compound by 21D5 will be verified by assessing the inducing capacity of extracts of plant tissues infected with 21D5. To test the second hypothesis, we will infect tobacco plants with 21D5 and quantify the endophytic and epiphytic populations after different time points. We will also evaluate the behavior of 21D5 on the plant tissues by scanning electron microscopy. Finally, the regulation of *GT1* expression will be determined by introducing a transcriptional *GT1:GUS* fusions into strains D188, D188-5, D188-Δ*attR*, and D188-Δ*fasR* and performing *in vitro* GUS assays with these reporter strains. As a result, we will hopefully have established how the gene is regulated and get some insight on when and where it is expressed during the interaction with a host.

Concerning the MTRs, their location upstream of the *fas* operon, their conservation in *S. turgidiscabies*, and the complete loss of phytopathogenicity upon their mutation, strongly indicate that they are involved in the biosynthesis of an essential cytokinin. Based on their homology we postulated that the reaction product of these enzymes is a methylated cytokinin. This hypothesis will be tested by comparing the cytokinin production of *R. fascians* strains D188, D188-5, D188-*fas1*, the two *mtr* mutants D188-*mtr1* and D188-*mtr2*, and two *S. turgidiscabies* strains containing a *fas* operon and the *mtr* genes (Aittamaa et al., 2010). Therefore, the bacteria will be grown under particular conditions, fed with labeled precursors, and the partially purified supernatants will be evaluated by thin layer chromatography. We will also assess the regulation of the *mtr* genes both *in vitro* and *in planta* by using available translational *mtr:GUS* reporter strains. As such, we hope to be able to answer the question whether methylated cytokinins are the secret weapon of *R. fascians*.

Based on the obtained data on *GT1* and the *mtr*'s we anticipate to make a considerable contribution to the understanding of the pathogenicity process of *R. fascians* and to open new research perspectives that might enable the use of *R. fascians* or its morphogens in tissue culture practices or help horticulturists in safe-guarding their ornamental crops from *R. fascians*.

3. Materials and methods

3.1 Bacterial strains and growth conditions

An overview of the bacterial strains used in this study is given in Table 3.1.

The *R. fascians* strains were grown on Yeast Extract Broth (YEB) (5g/L beef extract (Sigma-Aldrich, Mexico), 1g/L yeast extract (Oxoid, England), 5g/L peptone (Duchefa Biochemie, The Netherlands), 5g/L sucrose ($C_{12}H_{22}O_{11}$, Grand Pont®, Belgium)**,** 500mg/L magnesium sulfate heptahydrate ($MgSO_4.7H_2O$, purity >99%, Duchefa Biochemie, The Netherlands) and 15g/L agar (micro agar, Lab associates, The Netherlands) when solid medium was prepared) for two days at 28ºC. Suspension cultures were grown in 5ml liquid YEB and grown for two days at 28ºC under gentle agitation (160 rpm). Bacterial stocks were kept in glycerol (glycerine anhydrous, purity >95%, Duchefa Biochemie, The Netherlands) (25% final volume) at -80ºC.

The *S. turgidiscabies* strains were grown on Glucose-Yeast-Malt (GYM) medium (4g/L glucose ($C_6H_{12}O_6$, purity >99.5%, Duchefa Biochemie, The Netherlands), 4g/L yeast extract and 10g/L malt extract (Duchefa Biochemie, The Netherlands), pH set at 7.2 with potassium hydroxide (KOH, purity 85%, Duchefa Biochemie, The Netherlands) and 2g/L calcium carbonate ($CaCO_3$, purity >99%, UCB, Belgium) and 12g/L agar when solid medium was prepared) for three days at 28ºC. A spore solution stock was prepared to store the *S. turgidiscabies*. Vegetative mycelium was plated in sporulation medium (for 500mL: 250mL solution with 10g mannitol (purity >98%, Duchefa Biochemie, The Netherlands), 10g agar and 2.5mL of 2M magnesium chloride ($MgCl_2$, UCB, Belgium) added to 250mL solution with 10g soy flower (local bioshop) and grown at 28ºC for seven days. The spore solution was obtained by successive washings of the spores scraped gently with 7mL of sterile water (3mL, 2mL and 2mL). The resulting solution was vortexed, poured over sterile cheesecloth and centrifuged at 14 000rpm for 10min at 4ºC. The obtained pellet was resuspended in 1mL sterile 20% glycerol at 4ºC, divided over 3 eppendorfs in aliquots of 250µL and 500µL and stored at -80ºC.

The *E. coli* strains were grown on Luria Broth (LB) (1g/L glucose, 10g/L tryptone (Duchefa Biochemie, The Netherlands), 5g/L yeast extract, 10g/L sodium chloride (NaCl, purity ≥95%, Carl Roth) and 15g/L agar when solid medium was prepared) for one day at 37ºC with agitation (160 rpm). Bacterial stocks were kept in glycerol (25% final volume) at -80ºC.

Table 3.1 Characteristics of the bacterial strains used in this work.

	Bacterial strain	Construct	Vector	Description	Use	Selectable marker	Reference
Rhodococcus fascians	D188	none		*Rhodococcus fascians* , wild-type	Phenotype		Desomer et al., 1988
	D188-5	none		*Rhodococcus fascians* , plasmid-free derivative	Phenotype		Desomer et al., 1988
	D188-*att1*		pRF32	Original *att* mutant; D188-*att1*	Phenotype	Cm (25µg/ml)	Crespi et al. 1992
	D188-*fas1*		pRF32	Original *fas* mutant; D188-*fas1*	Phenotype	Cm (25µg/ml)	Crespi et al. 1992
	D188	21D5		Tn insertion mutant in GT1 (pFi_136) position 636; avirulent	Phenotype	Km (100µg/ml)	Forizs and Vandeputte
	D188	40G10		Tn insertion mutant in GT1 (pFi_136) position stop codon; virulent	Phenotype	Km (100µg/ml)	Forizs and Vandeputte
	D188	41H2		Tn insertion mutant in GT1 (pFi_136) position 993; attenuated	Phenotype	Km (100µg/ml)	Forizs and Vandeputte
	D188	45F10		Tn insertion mutant in GT1 (pFi_136) position 975; attenuated	Phenotype	Km (100µg/ml)	Forizs and Vandeputte
	D188	pJDGV5	pRF41	Replicating plasmid with translational *fasA:GUS* fusion	*fas* expression	Cm (25µg/ml)	Temmerman et al. 2000
	21D5	pJDGV5	pRF41	Replicating plasmid with translational *fasA:GUS* fusion	*fas* expression	Cm (25µg/ml)+Km (100µg/ml)	This work
	D188	pRFGusTM3	pRF37	Replicating *attA:GUS*	*att* expression	Phleo (1.5µg/ml)	Maes et al. 2001
	21D5	pRFGusTM3	pRF37	Replicating *attA:GUS*	*att* expression	Km (100µg/ml)+Phleo (1.5µg/ml)	This work
	D188-5	pRFGT2-1	pRF37	Transcriptional fusion of *GT1* gene	*GT1* expression	Phleo (1.5µg/ml)	This work
	D188-*att1*	pRFGT2-1	pRF37	Transcriptional fusion of *GT1* gene	*GT1* expression	Phleo (1.5µg/ml)	This work
	D188-*fas1*	pRFGT2-1	pRF37	Transcriptional fusion of *GT1* gene	*GT1* expression	Phleo (1.5µg/ml)	This work
	D188	pRFGT2-1	pRF37	Transcriptional fusion of *GT1* gene	*GT1* expression	Phleo (1.5µg/ml)	This work
	D188:*mtr1GUS*	mtr1GUSCm	pSP72	Integrated translational fusion	*mtr* expression	Cm (25µg/ml)	PhD thesis Ine Pertry
	D188:*mtr2GUS*	mtr2GUSCm	pSP72	Integrated translational fusion	*mtr* expression	Cm (25µg/ml)	PhD thesis Ine Pertry
Escherichia coli	DH5α	none		General cloning strain	Plasmid preparation		
	DH5α	pJDGV5		Replicating plasmid with translational *fasA:GUS* fusion	*fas* expression	Amp (100µg/ml)	Temmerman et al. 2000
	DH5α	pRFGusTM3	pRF37	Replicating *attA:GUS*	*att* expression	Amp (100µg/ml)	This work
	DH5α	pGUS1-GT2-1	pGUS1	Transcriptional fusion of *GT1* gene	*GT1* expression	Amp (100µg/ml)	O.Vandeputte
	DH5α		pGUS1	Cloning vector for translational *GUS* fusions	*GT1* expression	Amp (100µg/ml)	Peleman et al. 1989
	DH5α		pRF37	Bifunctional cloning vector *Ecoli/R. fascians*	*GT1* expression	Amp (100µg/ml)	Desomer et al 1992
	DH5α	pRFGT2-1	pRF37	Transcriptional fusion of *GT1* gene	*GT1* expression	Amp (100µg/ml)	This work
S.t	*S. turgidiscabies*	DSM 41990			Cytokinin profile		Aittamaa et al. 2010
	S. turgidiscabies	DSM 41997			Cytokinin profile		Aittamaa et al. 2010

All media were prepared with purified water (Synergy UV, Milipore) and supplemented with the following antibiotics when appropriate (Table 3.1): ampicillin (Amp) (ampicillin sodium, purity >91%, Duchefa Biochemie, The Netherlands), chloramphenicol (Cm) (Duchefa Biochemie, The Netherlands) phleomycin (Phleo) (Cayla, France), and kanamycin (Km) (kanamycin monosulfate, Sigma-Aldrich).

3.2 Determination of the colony morphology

For the determination of the colony morphology the *R. fascians* strains were grown as described above and washed once with sterile water. Then, serial dilutions were made from 10^0 till 10^{-8} in sterile water. For each dilution, three spots of 10µL were placed on seven different solid media: LB, YEB, Minimal A (10.5g/L dipotassium phosphate (K_2HPO_4, purity >98% UCB, Belgium), 4.5g/L monopotassium phosphate (KH_2PO_4, purity >99%, UCB, Belgium), 1g/L ammonium sulfate ($(NH_4)_2SO_4$, purity >99.5%, Fluka Chemie, Switzerland), 0.5g/L trisodium citrate ($Na_3C_6H_5O_7$, Duchefa Biochemie, The Netherlands), 2.5mL/L 10% magnesium sulfate heptahydrate, 2g/L glucose and 15g/L agar), and Minimal A supplemented with uninfected plant extract (20µl/mL), leafy gall extract (20µl/mL), pyruvate (20mM, sodium pyruvate, purity ≥99%, Sigma-Aldrich, Japan), or pyruvate/histidine (L-histidine, purity 98%, Janssen Chimica, Belgium) (20mM and 5mM, respectively). The filter sterilized compounds were added to the medium after autoclaving. Overview pictures were taken using a Canon OS 50D camera and detailed images were obtained using a binocular with LED light and the ProRes®CapturePro 2.8 software.

3.3 Plant material and growth conditions

Nicotiana tabacum cv. Havana and *N. tabacum* cv. Xanthi were grown in Murashige and Skoog (MS) medium (8g/L agar, 20g/L sucrose, 0.5g/L MES monohydrate (2-(N-Morpholino)ethanesulfonic acid, purity >99%, Duchefa Biochemie, The Netherlands), 0.1g/L myo-inositol (purity >97%, Duchefa Biochemie, The Netherlands); 4.4g/L MS salts (Duchefa Biochemie, The Netherlands), pH set at 5.7 with potassium hydroxide). Seeds were rinsed in sterile water and then submerged in 70% ethanol (C_2H_6O, purity 96%, Fiers) for 2min, 5% sodium hypochlorite (NaClO, local supermarket) with 0.05% Tween®80 (Ferak, Berlin) for 10min, rinsed again with sterile water three times, dried on sterile filter paper and kept in the dark.

Arabidopsis thaliana accession Col-0 was grown in ½ MS medium (identical to MS medium except for 10g/L sucrose and 2.2g/L MS salts). Seeds were submerged in 70% ethanol for 2min, 5% sodium hypochlorite with 0.05% Tween for 10min, 100% ethanol for 2 min, dried on sterile filter paper and kept in the dark.

For germination, seeds were placed in petri dishes with appropriate medium, vernalized for 3d at 4°C in the dark and then transferred to a growth chamber at 23ºC; with a light/dark cycle of 18/6 hours (Galbraith et al., 1995).

3.4 Infection procedures

The *R. fascians* strains were grown as described, collected by centrifugation, washed once with sterile water and concentrated 4 times. For all procedures, inoculation with water was used as a negative control. Infections with the wild-type strain D188 and its plasmid-free derivative D188-5 were used as references.

For *N. tabacum*, different infection procedures were followed to allow a quantification of the virulence of the different *R. fascians* strain. Seedlings were infected after radicle emergence (7d in growth chamber) with a drop of 20µL from each bacterial solution or water. Seedlings exhibiting normal growth, intermediate growth inhibition and full growth inhibition were scored at 24 and 45d after infection according to Pertry (2009). Three-week old *N. tabacum* cv. Xanthi plants were decapitated and infected with a drop of *R. fascians* solution or water. Leaves from three-week old plants were excised, placed on MS medium and infected with four drops of 10µL from each bacterial solution or water. The assay was done on wounded and intact leaves. For both experiments photos were taken 28d after the infection. Finally, for infection by dipping, plants or excised leaves were submerged in a washed *R. fascians* solution and placed on the appropriate medium.

14d-old *Arabidopsis thaliana* Col-0 plants were infected by placing 20µL of washed *R. fascians* culture in the heart of the rosette. Growth inhibition, anthocyanin accumulation, and serrated leaves were considered as symptoms. Symptomatic plants, non-symptomatic plants, and plants with axillary meristem activation were scored at 7, 14, 21 and 28d after infection. The number of shoots formed from activated axillary meristems was evaluated, under the binocular, 10d after infection.

3.5 SEM analysis

Epiphytic colonization was visualized by scanning electron microscopy (SEM). For this purpose *R. fascians* strains were grown as described above and 3-week old *N. tabacum* cv. *Xanthi* leaves were infected by dipping. After 7 weeks, the leaves were divided in sections and samples were analyzed with a Tabletop Microscope TM-1000 (Hitachi) without sample processing. Images were taken with the accompanying software.

3.6 Preparation of plant extracts

Infected plants or tissues were collected and macerated in a mortar using a pestle. The obtained pulp was collected in eppendorfs and centrifuged at 14 000rpm for 15min. The supernatant was collected, filter sterilized (0.45µm membrane, Chem-Lab), and stored at -20ºC until further use.

3.7 Transformation procedures and plasmid preparation

Constructs or ligation mixtures were introduced into available competent *E. coli* DH5α cells by heat shock transformation. Therefore, aliquots of competent cells were thaw, placed on ice, 100ng of the desired DNA added, and incubated on ice for 30min. Then cells were exposed to 42ºC for 30sec, placed back on ice, 300µL of SOC medium (Super Optimal Broth with Catabolite repression) (2% tryptone, 0.5% yeast extract, 10mM sodium chloride, 2.5mM potassium chloride (RPL, Belgium), 10mM $MgCl_2$, 10mM magnesium sulfate, and 20mM glucose) was added and the bacteria were placed at 37ºC for 60min. A 100µL-aliquot of the transformed bacteria was plated on LB with the appropriate antibiotics in triplicate and left at 37ºC overnight. At least six *E. coli* clones were subsequently grown on LB with the appropriate antibiotics at 37ºC overnight for plasmid preparation and construct verification. The plasmid preparations were done using the Pure YieldTM Plasmid Miniprep System by Promega.

R. fascians was transformed by electroporation. For this procedure the desired DNA was dialyzed for 1h on a Millipore membrane VS (0.025µm) and in the meantime, 0.2cm electrode gap electroporation cuvettes (BioRad) were cooled on ice. Bacteria were grown as described above, washed three times with ice cold sterile water, resuspended in the

initial volume, and placed on ice. 400µL-aliquots from these cells were transformed with 7µL (containing aprox. 1µg DNA) of dialyzed DNA using a Gene Pulser Xcell™ (Bio-Rad) with a voltage of 2500V, a capacity of 25µF, and a resistance of 400Ω. After the electroporation, 600µL of YEB was added to the bacteria and the mixture placed at 28ºC for 4h. 300µL-samples of the bacteria were plated in triplicate on YEB with the adequate antibiotics and placed at 28ºC until growth was observed (around 7d). At least six *R. fascians* clones were grown in YEB with the appropriate antibiotics at 28ºC for two days for further analysis or use.

3.8 In vitro expression analysis

R. fascians was grown as described above, washed with Induction medium (IM) (3.875g/L Gamborg B5 salts (Duchefa Biochemie, The Netherlands), 500mg/L MES monohydrate, 250mg/L ammonium nitrate (NH_4NO_3, purity >97.5%, Duchefa Biochemie, The Netherlands) and pH set at 5.5 with potassium hydroxide) and resuspended in the initial volume. For *GT1*, *mtr1*, and *mtr2* expression, bacterial cultures were concentrated 5 times in order to use a high bacteria concentration (2 times diluted as final concentration). In 24-well plates (VWR), the filter sterilized desired inducers, 900µL IM and 100µL-aliquots of washed bacteria were mixed and incubated at 28ºC overnight with agitation (100 rpm). The inducers used throughout the experiments were: 20mM pyruvate, 20mM histidine, 20mM sucrose, 20µl/mL uninfected plant extracts, 20µl/mL leafy gall extracts, (D-frutose ($C_6H_{12}O_6$, purity ≥ 99%, Fluka Chemie, Switzerland), 20mM citrate (trisodium citrate), 20mM fumarate (fumaric acid purity >99.5%, Fluka Chemie, Switzerland; pH set at 6 with 1M sodium hydroxide, measured with Universal Indicator Strips pH 0-14, Merck, Germany), 20mM malate (maleic acid, purity ≥99%, Sigma-Aldrich, United States of America; pH set at 7 with 1M sodium hydroxide), 20mM acetate (sodium acetate, purity >99%, Anala®, England), or 20mM succinate (succinic acid disodium salt hexahydrate, ICN Biomedicals Inc., United States of America; pH set at 7 with 1M sodium hydroxide).

3.8.1 *att* expression

For analysis of the *att* expression, cells were collected (2min centrifugation at 13000rpm, Microcentrifuge Eppendorf, 5417C, Rotor F45-30-10) and resuspended in 1mL of GUS buffer (for 50mL: 50mM sodium phosphate buffer pH=7.5 (in 100mL: 28mL 1M dipotassium phosphate and 72mL 1M monopotassium phosphate), 100µL 0.5M EDTA,

40µL 10mM β-mercaptoethanol (purity ≥99%, Fluka, Germany), 50µL 10% SDS (sodium dodecyl sulfate, purity >99%, Duchefa Biochemie, The Netherlands). A 100-µL sample was collected to determine the optical density at 600nm by diluting the solution twice with sterile water in a 96-well plate (Nunc^{TM}, Denmark)(Tunable microplate reader VERSAmax, Molecular devices). Then, 30µL of chloroform (purity 99.2%, VWR) was added to permeabilize the membrane of the cells and after 5min the reaction was started by adding the substrate, 1µL of 1M pNPG (*p*-nitrophenyl-β-D-glucuronide, purity ≥99%, Duchefa Biochemie, The Netherlands). The mixture was homogenized by inverting and incubated at 37ºC. The reactions were stopped with the addition of 400µL of 2-amino-2-methyl-1,3-propanediol (purity ≥99%, Sigma-Aldrich, Germany) when a clear yellow color was observed; the time was registered. After centrifugation (2min at 13000rpm), the optical density at 415nm of the supernatant was measured in 96-well plates. The β-glucuronidase (GUS) activity was calculated using the following formula: $OD_{415nm}/(OD_{600nm}$*dilution*time(min))*1000.

3.8.2 *fas*, *GT1*, *mtr1* and *mtr2* expression

For analysis of the *fas, GT1, and mtr1 and mtr2* expression the more sensitive MUG assay was used, which is more suitable for genes with a low expression. The cells were collected (2min centrifugation at 13000rpm) and resuspended in 1mL of MUG buffer (for 200mL: 50mM sodium phosphate pH=7, 160µL 10mM β-mercaptoethanol, 4mL 10mM EDTA, 2mL 10% SDS and 200µL 0.1% Triton X-100 (Acros organics, Belgium)). A 100µL-sample was taken to determine the optical density at 600nm by diluting the solution twice with sterile water in 96-well plates. The reaction was started by adding the substrate, 10µL of 100mM MUG (4-methylumbelliferyl-β-D-glucuronide, purity ≥99%, Sigma-Aldrich, UK) dissolved in DMSO (dimethyl sulfoxide, C_2H_6OS, purity >99.9%, Duchefa Biochemie, The Netherlands), inverting and incubating at 37ºC. The reaction was stopped at different time points (15, 30, and 60min) by taking 50µL-samples of the reaction mixture and adding it to 200µL of 200mM sodium carbonate (Na_2CO_3, purity ≥99.5%, Normapur®, France) in black Nunc Polysorb 96-well plates (ThermoFischer Scientific). The emitted fluorescence was measured after excitation at 355nm and emission at 460nm (FLUOstar OPTIMA reader, Isogen). The MUG activity was calculated using the following formula: fluorescence/(OD_{600nm}*dilution*time(min))*1000.

3.9 In planta expression analysis

3.9.1 Quantitative *in planta* expression analysis

To determine the *att*, *fas*, *GT1*, and *mtr1* and *mtr2* expression on the plant, 3-week old *N. tabacum* plants were infected by dipping in the appropriate bacterial suspension. After 7d, the leaves were crushed in eppendorf tubes and 500µL of sterile water was added. 10-µL-samples were taken from the plant extract and 490µL of sterile water was added as a start for 8 serial 10-fold dilutions to determine the colony forming units (CFUs). For *in planta* gene expression, 500µL of 2-times concentrated MUG buffer (100mM sodium phosphate (pH=7.0), 20mM β-mercaptoethanol, 20mM EDTA, 0.2% SDS) was added to the remaining plant extract. These mixtures were homogenized by vortexing and 10µL of 100mM MUG was added to start the reaction. The reaction mixtures were incubated at 37ºC and the reaction was stopped at 15, 30 and 60min by adding 50µL-samples of the reaction mixtures to 200µL of 200mM sodium carbonate in black Nunc Polysorb 96-well plates (ThermoFischer Scientific). Excitation at 365nm and measurement at 460nm was performed (FLUOstar OPTIMA reader, Isogen) and β-glucuronidase (GUS) activity was calculated as the measured emission/[time(min)*log(CFU)]. The presented results are the average of four biological repeats.

In order to bring the *in planta mtr* expression *in vitro*, excised leaves and complete plants were infected by dipping with D188-*mtr1*. After 7d, the plant material was either crushed or cut in small pieces and placed in 1mL IM medium. In some of the cases 100-µL aliquots of D188-*mtr1* cells grown *in vitro* were added to evaluate if in these cells *mtr1* gene expression could be activated. The expression analysis was as described above with MUG as a substrate. In these experiments, no normalization to OD600 or CFU was done, so the emitted fluorescence was, therefore, used as an approximation of the gene expression.

3.9.2 Histochemical *in planta* expression analysis

In order to locate the gene expression *in planta*, 3 week-old plants were infected by dipping. After 7d, plants were immerged in 90% acetone (C_3H_6O, purity ≥99.7%, Carl Roth) for 30min, washed three times with phosphate buffer ($NaPO_4$) (pH=7.2) and placed in 6 well-plates. Plants were submerged in staining buffer (50mM sodium phosphate buffer pH 7.2, 0.2% Triton X-100, 5mM potassium ferrocyanide ($K_4Fe(CN)_6.3H_2O$, Sigma-Aldrich, Japan), 5mM potassium ferricyanide ($K_3Fe(CN)_6$, purity 99.8%, Sigma-Aldrich,

Germany), 2mM X-gluc (purity ≥97%, Carl Roth)) and plates were covered with aluminum foil and left at 37ºC overnight. The staining buffer was replaced for 70% ethanol and the plates were placed at room temperature with low agitation (50rpm) until all the chlorophyll was extracted from the plant tissues. Gene expression was visible as a blue precipitate.

3.10 In planta survival

Complete 4 week-old tobacco plants were infected by dipping with the desired bacterial suspension. The CFUs of the total and the endophytic populations per gram fresh weight (FW) plant tissue were determined at different time points after infection: 2, 7, and 21d. Therefore, a minimum of four leaves was collected, divided in two, and their weight was measured. One half of each leaf was immersed in 6% sodium hypochloride for 1min and washed twice with sterile water; the other half was not treated. The resulting tissues were crushed and 10µL of the tissue fluid was diluted 100 times in sterile water. Serial dilutions from these tissue extracts were plated on YEB medium, the number of colonies counted, and the CFU's per gram of fresh plant tissue was calculated and logarithmically transformed.

3.11 Cloning of GT1:GUS fusions

A construct with a transcriptional fusion of *GT1* with *GUS*, pGUS1-GT2-1, was available in the *E. coli* vector pGUS1 (O. Vandeputte). To allow its introduction into *R. fascians*, the fusion were cloned in the bifunctional vector pRF37 which replicates both in *E. coli* and *R. fascians* (Figure 3.1.A). For this purpose the fusion was isolated from the construct and the vector pRF37 was linearized with the restriction enzymes *Hin*dIII (10U/µL, Invitrogen^{TM}) and *Xba*I (20U/µL, Biolabs, New England). The reaction mixtures contained: 20µL sterile water, 3µL NEBuffer 2.1 (Biolabs, New England), 1µg DNA and 1µL of each enzyme, and was placed at 37ºC for 60min. Then, 1µL GelRed (Biotium, Inc.) and 4µL LD (Blue Loading Dye, Promega, United States of America) was added to each sample. The fragments were subsequently separated by agarose gel electrophoresis (i-Mupid®, Japan): 1% agarose (Invitrogen^{TM}, UK) in 0.5x TAE buffer buffer (242g/L Tris, 51.7mL/L acetic acid, 100mL/L dissodic EDTA), the same running buffer, at 100V, for

30min. The lambda marker (λ DNA/*Pst*I, 0.5µg/µL, Fermentas) was used as molecular size marker (6µL marker, 1µL GelRed and 2µL LD). The linearized vector and the insert fragment of 4-kb were eluted using the Wizard SV Gel and PCR Clean-Up System by Promega. Prior to setting the ligation, the quality of the fragments was verified by electrophoresis (Figure 3.1.B; left part of the image). The ligation mixture contained 3µL sterile water, 2µL T4 DNA ligase buffer, 1µL vector DNA, 3µL GT2-1 insert DNA, and 1µL T4 DNA ligase (Invitrogen^{TM}, 1U/µL), and was kept overnight at room temperature. Then, competent *E. coli* DH5α cells were transformed by heat shock transformation with 1µL of the ligation mixture, plated on LB medium with ampicilline, and incubated at 37°C overnight. Twenty four clones were grown overnight on LB medium with ampicilline for plasmid preparation and the structure of the construct was analyzed by a *Hin*dIII/*Xba*I restriction digest and gel electrophoresis (Figure 3.1.B; right part of the image). The correct construct pRFGT2-1 was introduced into *R. fascians* by electroporation.

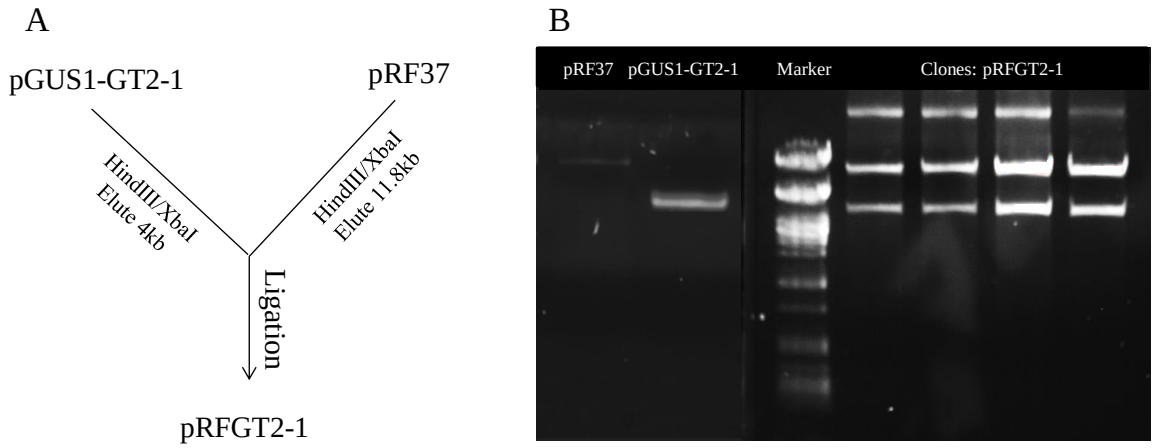

Figure 3.1 Cloning strategy for the generation of a construct carrying a transcriptional fusion between *GT1* and *GUS* in pRF37, a bifunctional vector for *E. coli* and *R. fascians.*
(A) Scheme of the cloning strategy; (B) DNA gel electrophoresis of the linearized vector and isolated insert (left) and *Hin*dIII/*Xba*I digest of few resulting clones (right) (image obtained with the software ChemiDoc™ MP imager).

3.12 TLC analysis of bacterial cytokinins

R. fascians was grown as described above, diluted 10 times in fresh YEB, and grown overnight. *S. turgidiscabies* was grown as described above. The bacteria from 5mL cultures were collected by centrifugation and resuspended in 1mL IM. Inductions were set in two-fold with the desired inducers, 900µL of IM and 100µL of bacterial solution in 24-

well plates. After 2h of growth at 28ºC with agitation, either 2.5µCi of ^{14}C labelled adenine (3301 Adenine [$^{14}C(U)$]hydrochloride, specific activity 238mCi/mL, purity 99%, ARC, United States of America) or 2.5µCi SAM (0344 Adenosyl-L-methionine, S-[methyl-^{14}C], specific activity 55mCi/mL, purity 99%, ARC, United States of America) were added and incubated overnight at 28ºC with agitation. Then, the induced cultures were collected in eppendorfs and centrifuged at 16 000rpm for 10min; both the pellet and the supernatants were kept for further processing. The supernatants were acidified with TFA (Trifluoroacetic acid, purity ≥99.9%, Carl Roth) (0.1% final volume). Sep-Pak Waters C18 Classic cartridges (Waters, Ireland) were activated with 3mL 100% methanol (CH_4O, purity>99.9%, Fluka, Germany) and equilibrated with 5mL 0.1% TFA in water. The acidified samples were loaded on the cartridges (maximum speed 1mL/min), washed with 6mL 0.01% TFA in water, and eluted with 6mL 80% methanol. The eluate was dried under vacuum (Speed Vac Concentrator, Savant) and resuspended in 30µL of a mixture of 0.1% TFA and 15% methanol in water. For the collected pellet, a volume of 100µL water and 100µL butanol (C_4H_9OH, purity 99.5%, Carl Roth) was added and the suspension was vigorously shaken for 60min. These suspensions were centrifuged at 16 000rpm for 10min, the upper butanolic phases collected, dried under vacuum, and the resulting fraction resuspended in 30µL of a mixture of 0.1% TFA and 15% methanol in water. Before use, the TLCs (Thin Layer Chromatography, Polygram Sil G/UV254, 20*20cm, Machery-Nagel) were washed with 100% methanol for 30min with slow shaking and dried to the air. In a first TLC, a volume of 10µL from each sample was loaded; the second TLC was loaded with the remaining 20µL (in 5µL-aliquots). Then, the TLCs were developed for 6h with a mobile phase consisting of the upper organic phase from butanol/water/ammonia 25% (purity 25%, RPL, Belgium) (4/2/1); the second TLCs were developed a second time with the same mobile phase for another 6h. The TLCs were air dried and placed in phosphor-imager cassette (445 SI, Molecular Dynamics) overnight. The banding pattern was visualized with the Image Quant software package. Only the results of the second TLCs are shown in the Results section.

4. Results

A. Functional analysis of the glycosyltransferase GT1

4.A.1. The colony morphology of *R. fascians* is defined by the medium composition and modified in the *GT1* mutant 21D5

The 21D5 mutant has been identified in a collection of transposon mutants of the wild-type *R. fascians* strain D188 based on its growth impairment in LB medium supplemented with acetate (Forizs, 2012). As a first step to understand if the observed modified colony morphology has biological relevance for the interaction with the host, the development of single colonies obtained through serial dilutions of *R. fascians* strain D188, its plasmid-free derivative D188-5 and mutant 21D5 was evaluated and compared on different media. On the one hand we tested the bacterial behavior on rich media, such as LB and YEB. On the other hand, since virulence gene expression can be induced under particular conditions mimicking the plant tissue environment (Temmerman et al., 2000), we also tested minimal medium supplemented or not with pyruvate, histidine, and extracts of non-infected plants and of leafy galls.

As shown in Figure 4.1, the medium composition had a strong impact on the colony morphology of all three strains. Although the colony diameter of strain D188-5 was generally half that of strain D188, the overall appearance of the colonies on rich media and minimal medium supplemented with plant-derived extracts was comparable for both strains: the bright orange-yellow colonies were convex and smooth and had a sharp edge (Figure 4.1). On the minimal media without plant-derived extracts, the colonies of D188-5 and D188 looked very different: their color was less pronounced and their surface appeared more fuzzy or rough, but the most striking characteristic was the elaboration of a thin protrusion layer surrounding the colonies. For strain D188 this protrusion layer was less pronounced than for strain D188-5; in the presence of histidine/pyruvate it was even almost absent (Figure 4.1).

The colony morphology of mutant 21D5 on LB medium confirmed the observations made by Forizs (2012) and resembled that of D188-5 and D188 on minimal media: the colonies

were pale with a fuzzy and rough surface and had a broad protrusion layer. On YEB, the colonies appeared very rough and flat and had a whitish yellow color. Whereas the colony morphology of 21D5 on minimal medium supplemented with leafy gall extract was comparable to that on the rich media, surprisingly, the morphology was largely restored to that of the wild-type in minimal medium supplemented with non-infected plant extract (Figure 4.1). Finally, the mutant was not able to grow on minimal medium without plan-derived extracts (Figures 4.1 and 4.2).

The colony morphology of other *R. fascians* mutants was evaluated as well on the same set of media. The attenuated D188-*att1* and the non-pathogenic D188-*fas1* mutants revealed a similar phenotype as the wild-type strain D188 on the rich media and the minimal medium supplemented with plant-derived extracts or with pyruvate. In contrast to D188, both mutants exhibited an extensive protrusion layer on minimal medium supplemented with histidine and pyruvate; the D188-*att1* mutant did not have the protrusions when grown on minimal medium alone (Figure 8.1 in the Annexes).

Interestingly, none of the other *GT1* transposon mutants, 45F10, 41H2 and 40G10 (Figure 8.2 in the Annexes), had a colony morphology defect like 21D5 when grown on rich media and minimal medium supplemented with plant-derived extracts. Moreover, unlike 21D5, the three mutants grew well on the minimal media without plant-derived extracts. As expected, 40G10 had a colony morphology similar to that of D188, except on minimal medium alone, where no protrusion layer was formed. On this medium, the other two *GT1* mutants did not exhibit the protrusion layer either. The colonies of 45F10 and 41H2 also differed from those of D188 and 40G10 on minimal medium supplemented with pyruvate and with histidine and pyruvate in the sense that no clear protrusion layer was formed (Figure 8.2 in the Annexes).

Although we currently have no information on which molecular mechanisms determine the colony morphology, our results clearly show that *R. fascians* can adjust its shape in response to particular conditions which might affect its capacity to interact with or survive on its host. Moreover, the mutation in the *GT1* gene in the 21D5 mutant must affect the activity of the protein in a much more profound way than in the other three *GT1* mutants, since it exhibits the strongest phenotype.

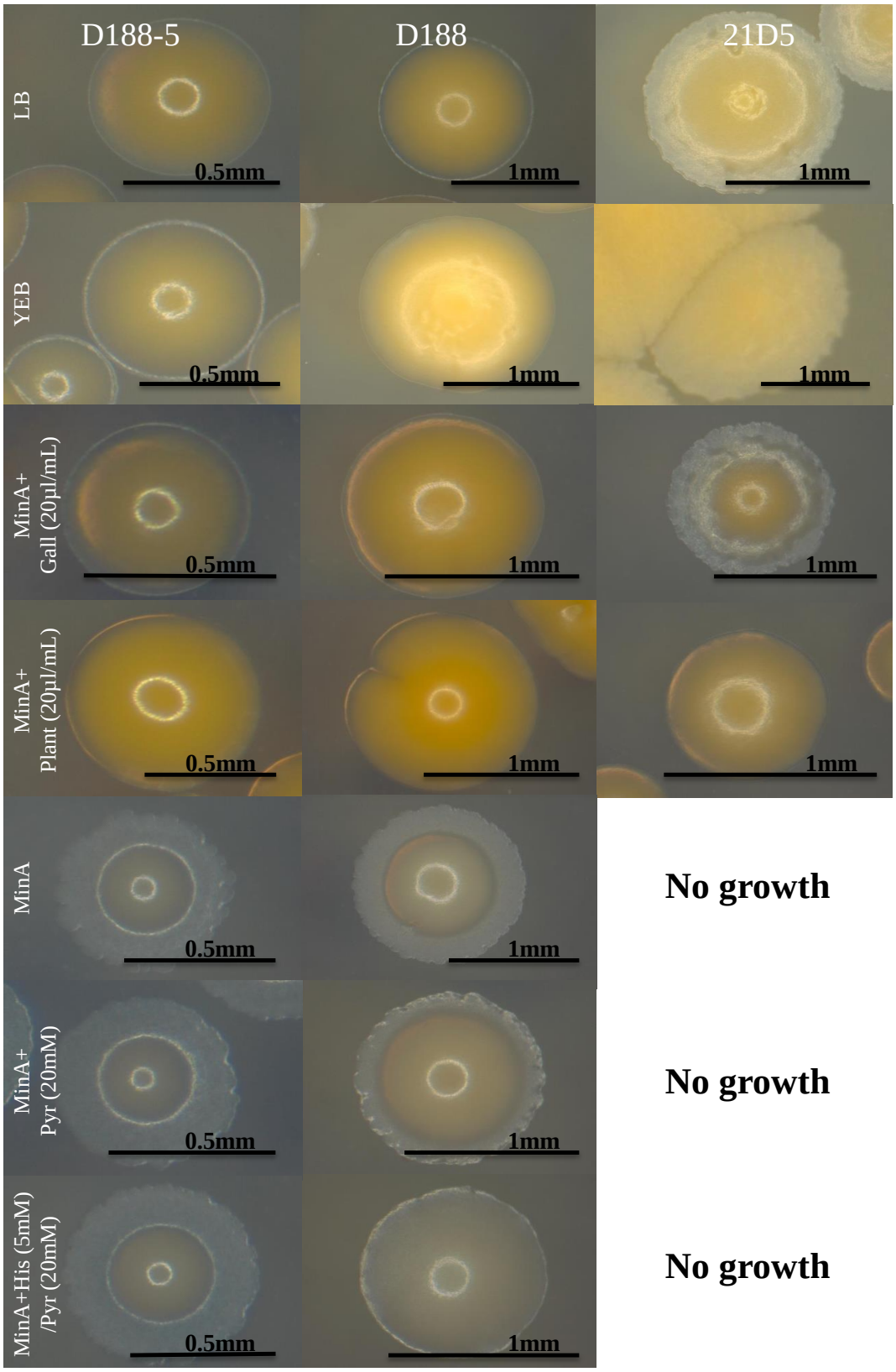

Figure 4.1 Colony morphology of the wild-type *R. fascians* strain D188, its plasmid-free derivative D188-5 and the transposon mutant 21D5 grown on different media.
Photos of representative colonies after 4 days of growth at 28°C were taken with a binocular and the ProRes®CapturePro 2.8 software (exposure time of 650ms). The experiment was performed once.

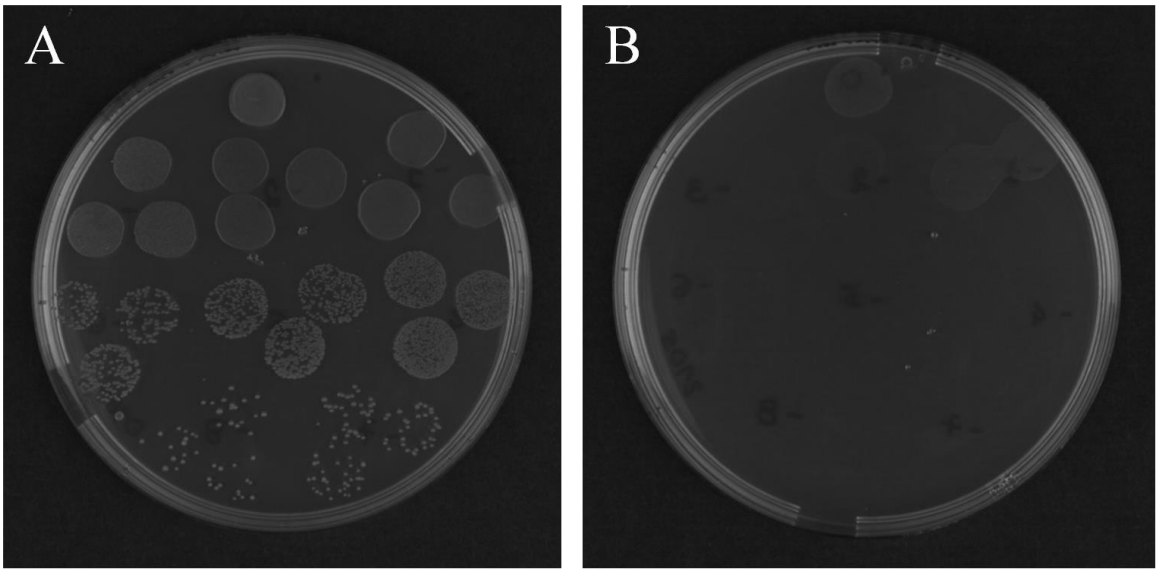

Figure 4.2 Overview of the growth of the wild-type *R. fascians* strain D188.
(A) and the transposon mutant 21D5 (B) on minimal medium supplemented with 20 mM pyruvate/5 mM histidine after 4 days incubation at 28°C. Photos were taken with a Canon OS 50D (ISO 100, Diaphragm 18 and closing time 1/13).

4.A.2. Growth capacity of different *R. fascians* strains on different media

Forisz (2012) noticed that mutant 21D5 formed aggregates when cultured in liquid LB medium. Essentially, the bacteria do not homogeneously spread in the medium, but coagulate and eventually precipitate. We confirmed this finding and observed the same behavior of 21D5 in YEB medium (data not shown). None of the other *GT1* mutants exhibited the coagulation behavior in liquid cultures which is in agreement with the lack of a colony morphology phenotype. To evaluate if the aggregate formation by 21D5 would reflect differences in growth capacity, we determined the CFUs on the plates of the previous experiment with the different media, set the growth on YEB at 100% because this is the standard growth medium for *R. fascians*, and compared the growth on the other media to that value (Table 4.1).

The data presented in Table 4.1 are the result of a single experiment and should be interpreted with some caution. For all strains, growth on MinA without any supplements was low, whereas the addition of plant-derived extracts, pyruvate, or histidine/pyruvate (partially) restored growth. When comparing the growth pattern of D188 with that of D188-5, it appears that the linear plasmid might encode functions that enable *R. fascians* to

grow better in minimal conditions. Moreover, the colony morphology of 21D5 nor its coagulation seemed to affect the capacity to grow on relatively rich media (including MinA with plant-derived extracts), although the GT1 mutation completely abolished growth under nutrient-restrictive conditions.

Table 4.1: Relative growth of different *R. fascians* strains on different media based on CFU's (%).

Strain	YEB	LB	MinA+ Gall (20µl/mL)	MinA+ Plant (20µl/mL)	MinA	MinA+ Pyr (20mM)	MinA+ His (5mM)/ Pyr (20mM)
D188	100	123	138	110	93	125	160
D188-5	100	72	13	11	0	81	68
D188-*att1*	100	97	84	106	16	69	91
D188-*fas1*	100	91	101	94	23	114	130
21D5	100	126	172	171	0	0	0
45F10	100	87	16	13	1	110	92
41H2	100	79	102	19	0	0	0
40G10	100	13	97	9	0	12	97

Based on these preliminary observations, we can postulate that 21D5 has no fitness defect when sufficient nutrients are provided.

4.A.3. Mutations in *GT1* seriously impair the virulence of *R. fascians*

To assess the effect of the mutation in *GT1* on the pathogenicity of the strains, we analyzed the response of Arabidopsis and tobacco plants at different time points after infection with 21D5, 45F10, 41H2, and 40G10 and compared it to the phenotypes induced by the wild-type strain D188, its non-pathogenic plasmid-free derivative D188-5, the non-pathogenic D188-*fas1* mutant, and the attenuated D188-*att1* mutant.

For Arabidopsis, 2-week old plants were infected by placing a 20-µl drop of bacterial suspension in the heart of the rosette. At 7, 14, 21 and 28 days post infection (dpi) the occurrence of different responses, such as stunted growth, leaf deformation, anthocyanin production, and serration of leaf margins, was scored by eye. When at least one of these responses occurred, the plants were considered symptomatic. When plants were symptomatic but also exhibited the most typical symptom, activation and neoformation of shoot meristems in the axillary regions, they were scored separately at each time point. Moreover, the degree of axillary activation was scored under the binocular at 10 dpi by counting the number of shoots that were formed in the axils.

Figure 4.3 shows a general overview of the infected plants at 28 dpi. Clearly, the strains D188-5 and D188-*fas1* could not provoke symptoms and the infected plants had a similar phenotype as the mock-inoculated control (water). The responses induced by D188-*att1* and 21D5 were limited to some axillary activation and anthocyanin accumulation that was not accompanied by leaf deformations (Figure 4.3). Infection with 45F10 lead to more pronounced axillary activation, but hardly no growth inhibition was observed. Finally, although 41H2 induced the full array of symptoms, the degree of symptom formation was lower than that upon infection with strains 40G10 and D188 (Figure 4.3).

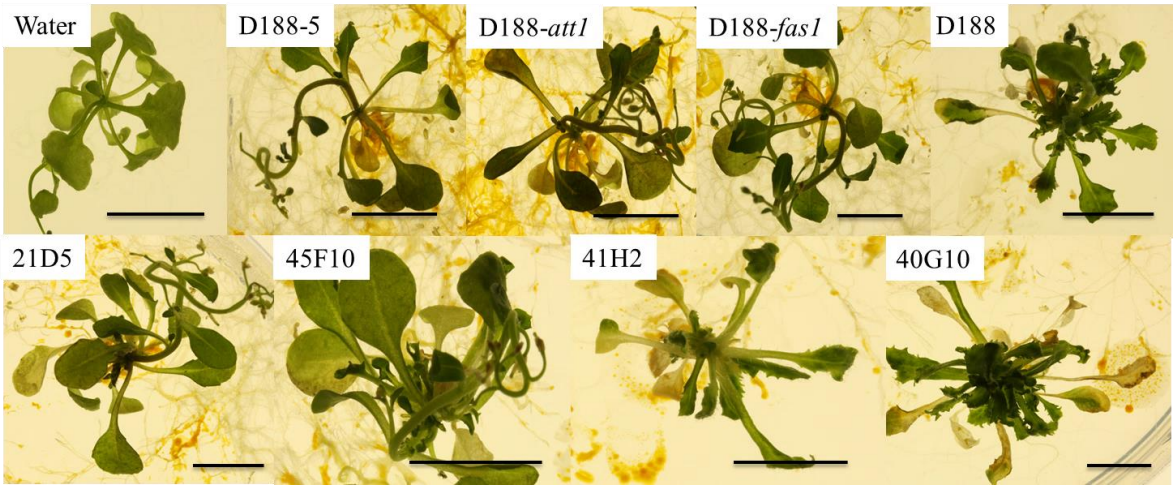

Figure 4.3 Symptoms on *A. thaliana* plants inoculated with different *R. fascians* strains at 28 dpi.
At least 50 seedlings were analyzed per treatment. Photos were taken with a Canon OS 50D (ISO 100, Diaphragm 16 and closing time 6 sec, except for 21D5, 41H2 and 45F10 which was 5sec). Bar=1cm.

Quantification of the axillary activation (Figure 4.4) showed that the activity of 41H2 was comparable to that of D188. 45F10 and 40G10 induced a response that resembled that of D188-*att1*, and 21D5 hardly induced shoot formation. D188-5 and D188-*fas1* could not activate the axillary region.

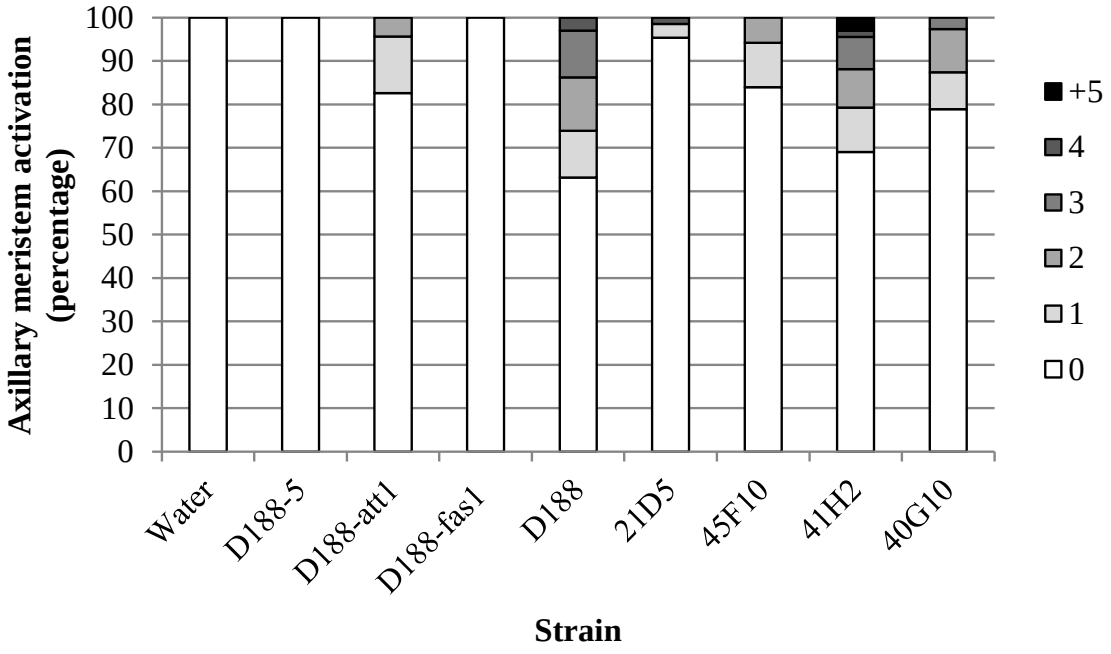

Figure 4.4 Axillary activation in *A. thaliana* plants inoculated with different *R. fascians* strains at 10 dpi.
At least 50 plants were scored per treatment.

When the kinetics of symptom formation were considered, all mutants, except for 41H2 and 40G10, were strongly delayed (Figure 4.5). The pattern of symptom development by 21D5 was similar to that of D188-*att1*, and, although 41H2 and 40G10 strongly activated the axillary region, the response was not as strong as that obtained by D188 infection (Figure 4.5).

From these data we can conclude that the *GT1* mutation in 21D5 severely attenuates the virulence capacity of *R. fascians*.

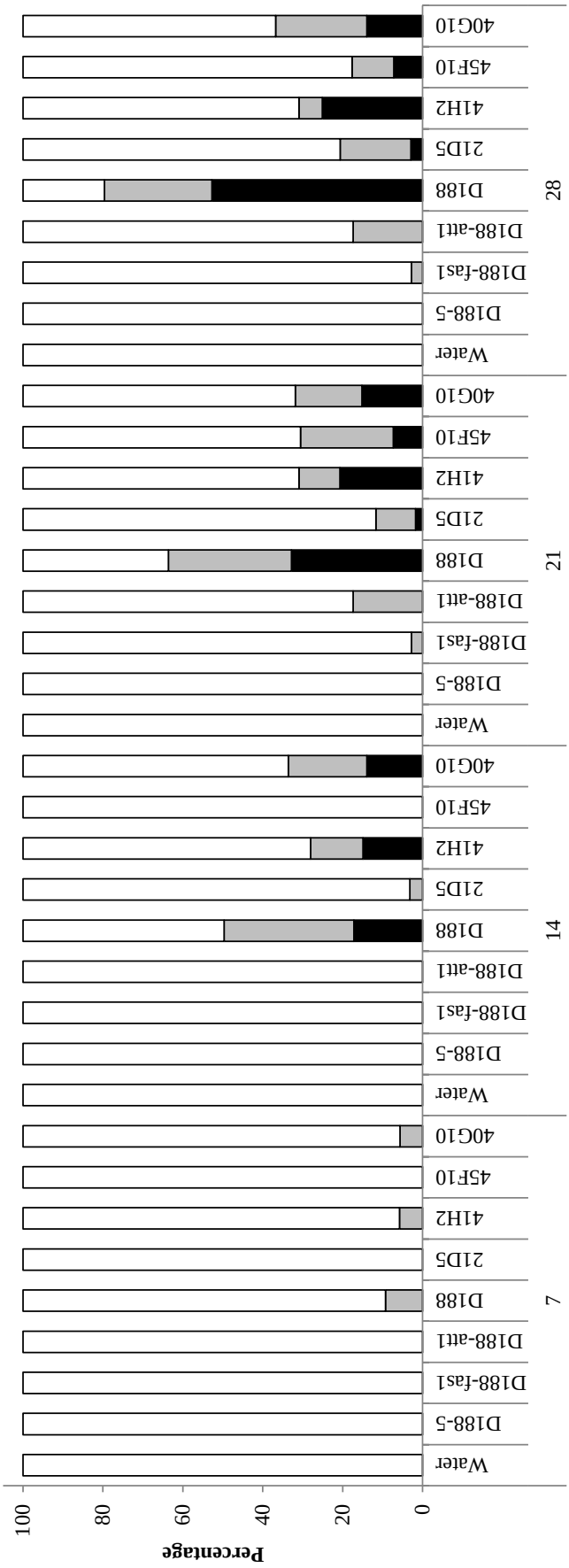

Figure 4.5 Kinetics of symptom development on *A. thaliana* plants inoculated with different *R. fascians* strains at 7, 14, 21 and 28 dpi.
White, non-symptomatic plants; grey, symptomatic plants exhibiting anthocyanin accumulation, swollen veins, and/or serrated leaves; black, symptomatic plants exhibiting activation of the axillary meristems. At least 50 plants were scored.

Because different hosts can respond differently, the virulence of the *R. fascians* strains was also assessed on tobacco plants using different infection procedures. Upon decapitation of the shoot apical meristem, *R. fascians* typically induces the formation of leafy galls (Vereecke et al., 2000). In this assay, 4-week old plants, decapitated and infected with water, D188-5, D188-*fas1* and 21D5 mutants did not develop leafy galls, but instead the first axillary meristem at the decapitation site developed into a normal shoot (Figure 4.6). Plants infected with D188-*att1* and 45F10 did not develop leafy galls either. Nevertheless, leaf deformations did occur, as well as swelling of the vascular tissues and the area at the infection site (Figure 4.6). Already at 7 dpi, infection with 41H2, 40G10, and D188, lead to swelling of the vasculature of newly formed leaves, severe leaf deformations, and the occurrence of dark green islands on the leaf lamina. At the end of the experiment, at 28 dpi, all three strains had induced leafy galls (Figure 4.6).

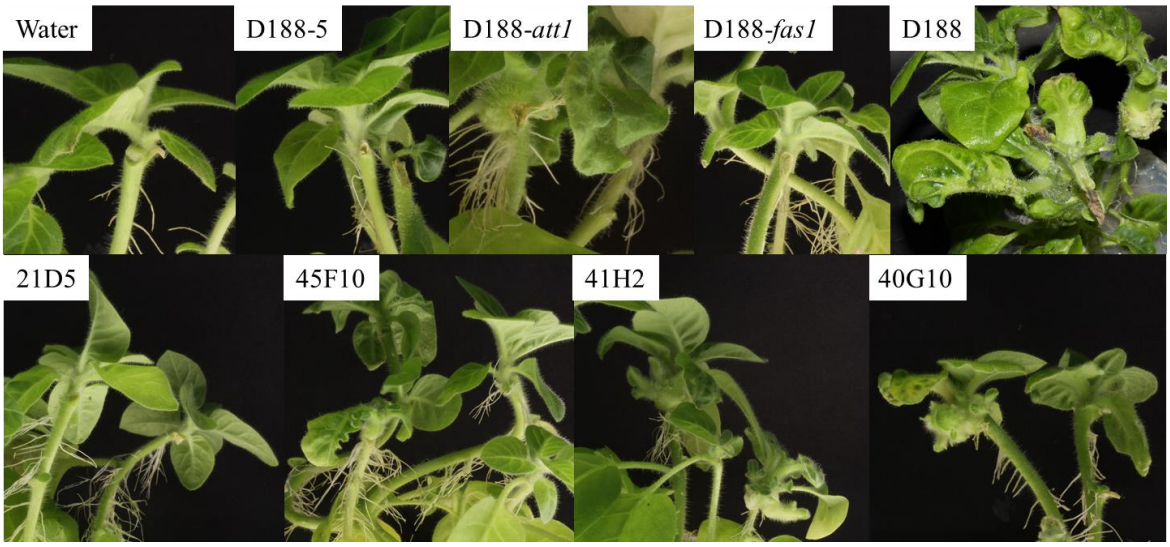

Figure 4.6 Symptom formation on decapitated *N. tabacum* xanthi plants inoculated when they were 4-week old with different *R. fascians* strains.
For each strain, 4 plants were infected. Photos were taken at 28 dpi with a Canon OS 50D (ISO 100, Diaphragm 32 and closing time 2,5sec).

Inoculation of excised leaves with or without wounding of the leaf lamina is a helpful assay to assess virulence potential: when the plant tissue is kept intact, the bacteria need to be able to overcome the physical barriers of the cuticula and epidermal cells in order to invade the plant tissues. In contrast, when the leaves are wounded, the first steps of the interaction with the host can be skipped and tissue penetration is gratuitous. Thus, infection of excised leaves not only allows to evaluate the capacity to induce shoots, but also to assess the invasion potential (Maes et al., 2001), two important yet distinct pathogenicity parameters.

Infection of wounded leaves largely confirmed the results obtained upon decapitation: D188-5 and D188-*fas1* did not provoke any symptoms, whereas D188, 45F10, 41H2, and 40G10 induced bumps (i.e. regions of increased cell division) and green islands at 7 dpi and, eventually at 28 dpi, leafy galls in almost all infected leaves (Figure 4.7). This assay also illustrated the attenuated virulence of the D188-*att1* mutant: although bumps and green islands were induced, only in 60% of the cases leafy galls formed, but they were much smaller than those induced by D188 (Figure 4.7). Similar observations were made for 21D5, but the primordial leafy galls only appeared in 20% of the cases (Figure 4.7), signifying extreme virulence attenuation and suggesting a defective production of morphogens

Infection of unwounded leaves corroborated the non-pathogenicity of D188-5 and D188-*fas1* (Crespi et al., 1992), the inability of D188-*att1* to invade plant tissues in the absence of wounds (Maes et al., 2001), and the wound-independence of D188, 41H2, and 40G10 to induce leafy galls (Figure 4.7). Interestingly, both 21D5 and 45F10 were unable to cause leafy galls if the plant tissue was intact (Figure 4.7), implying that their penetration capacity is impaired.

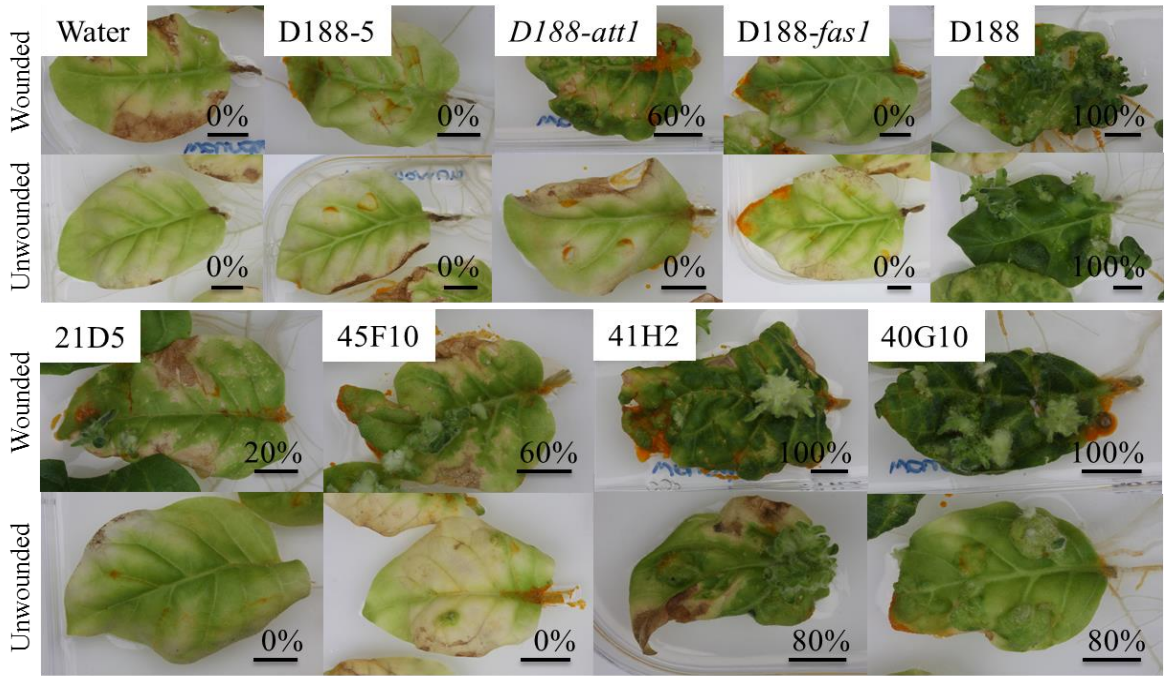

Figure 4.7 Symptoms on wounded or intact excised leaves of 4-week old *N. tabacum* xanthi plants inoculated with different *R. fascians* strains at 28 dpi.
For each strain and each condition, five leaves were infected. The percentage given with each image represents the occurrence of leafy gall formation. Photos were taken with a Canon OS 50D ISO 100 (Diaphragm 16 and closing time 1/100sec). Bar=1cm.

Altogether, the virulence assessment on different hosts using different infection procedures showed that 40G10 and 41H2 are the most pathogenic *GT1* mutants, whereas the pathogenicity of 45F10 is reduced. The capacity of 21D5 to induce symptoms is extremely attenuated because the mutation apparently affects both the ability to invade the plant tissues and the production of morphogens.

4.A.4. The regulation of *fas* gene expression is impaired *in vitro* and *in planta* affecting the level of cytokinin production by 21D5

Although the virulence of 21D5 was extremely weak, on wounded excised leaves occasionally small leafy galls developed suggesting that cytokinin production is not completely shut down in this strain. To get more insight into cytokinin gene expression in 21D5, an available *fasA:GUS* reporter plasmid pJDGV5 (Temmerman et al., 2000) was introduced into 21D5 cells by electroporation. The resulting strain 21D5(pJDGV5) and the wild-type strain D188(pJDGV5) carrying the same plasmid, were subsequently grown under particular conditions known to induce *fas* gene expression (Temmerman et al., 2000). As shown in Figure 4.8.A, especially the combination of 5 mM histidine or leafy gall extract (20 µl/ml) with 20 mM pyruvate induced *fasA* expression in the D188 background, confirming previous reports (Temmerman et al., 2000). In contrast, in the 21D5 mutant, no differential expression of the *fas* genes could be measured, suggesting that cytokinin production would be impaired in this strain.

Then, both reporter strains were used to infect excised leaves and 7 days later *in planta* expression was quantified using MUG as a substrate (Figure 4.8.B) or visualized by histochemical staining (Figure 4.8.C-F). In D188-infected plants, *fasA* expression could be measured (Figure 4.8.B) and was localized in distinct patches on the leaf lamina and in the axillary regions (Figure 4.8.C and D). In contrast, no *fasA* expression was detectable with either of the assays in the 21D5 background (Figure 4.8.B, E and F). These results are consistent with the *in vitro* expression and virulence data and indicate that this mutant has severe difficulties to interact in an appropriate way with its host.

To substantiate this finding, Petr Tarkowski, our collaborator at Palacký University (Olomouc, Czech Republic), grew D188-5, D188, and 21D5 *in vitro* under inducing conditions (5 mM His/20 mM Pyr) and quantified the cytokinins secreted into the supernatant. Although the analysis was done only once, his results showed that the

cytokinin profile of the three strains was different (Figure 4.8.G). Whereas no large differences were observed between D188 and 21D5 for the *c*Z-type cytokinins, the level of 2-iP-type cytokinins was considerably lower in 21D5 compared to D188, resulting in a 34% lower total cytokinin amount secreted by 21D5 under these conditions (Table 4.2). As reported before, D188-5 is able to secrete a low amount of cytokinins as well (Figure 4.8.G and Table 4.2).

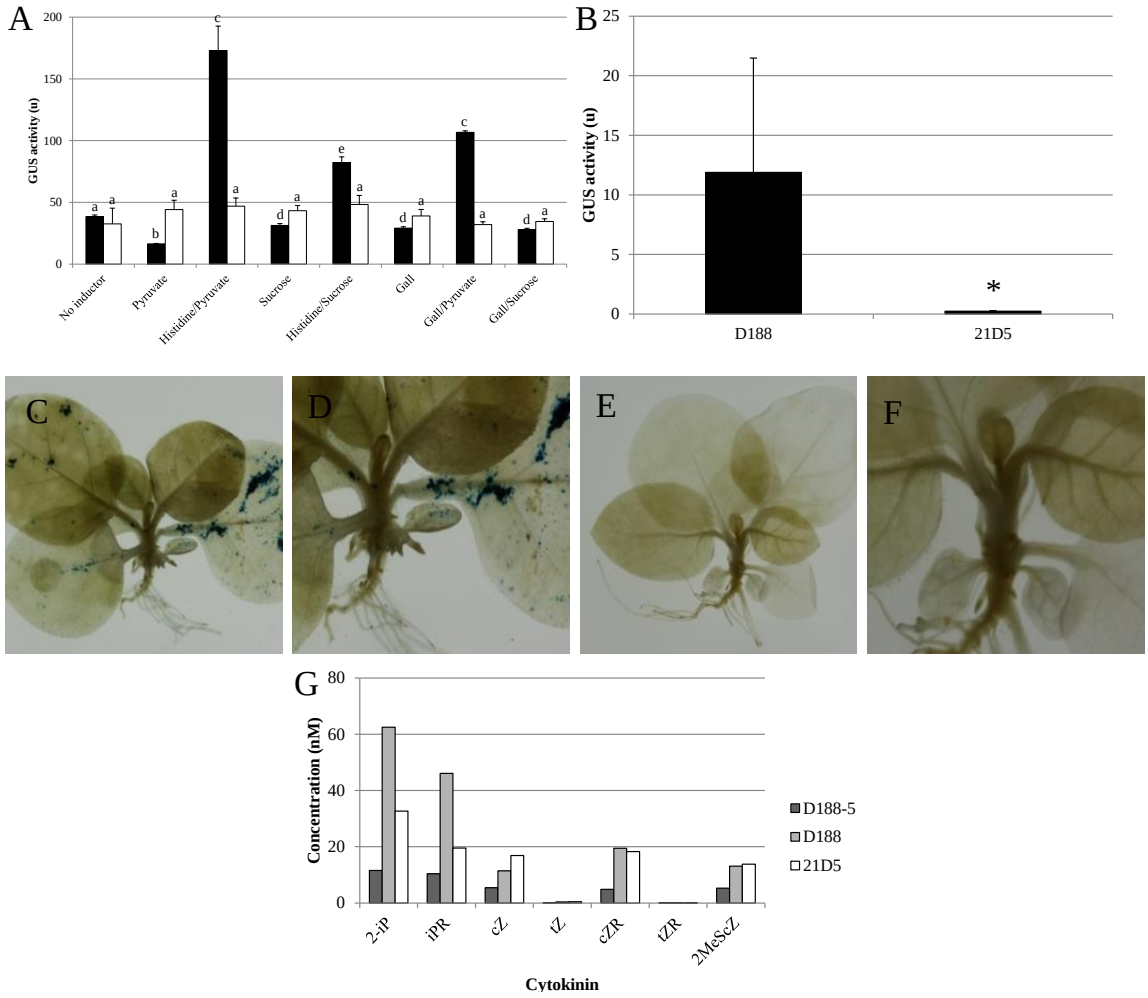

Figure 4.8 Expression of *fasA* and cytokinin production in different *R. fascians* strains.
(A) Effect of different conditions on *fasA* expression *in vitro* in D188 (black bars) and 21D5 (white bars) measured with the reporter plasmid pJDGV5 and MUG as substrate. Inductions were performed in IM medium in the presence of 20 mM pyruvate, 5 mM histidine, 20 mM sucrose and 20 µl/ml leafy gall extract. Statistical differences within each strain indicated by different letters were evaluated with Student's *t*-tests ($p<0.05$). Error bars represent SE (n=3). (B) Expression of *fasA* in the D188 and 21D5 background *in planta* 7 days after infection of excised leaves and measured with MUG as substrate. The asterisk marks the statistical difference between both conditions according to Student's *t*-tests ($p<0.05$). Error bars represent SE (n=4). (C-F) Histochemical staining visualizing *in planta fasA* expression in the D188 (C-D) and 21D5 (E-F) background. D and F are details of C and E, respectively. Photos were taken with a Canon OS 50D ISO 100 (Diaphragm 16 and closing time 1/100sec). (G) Preliminary data on the cytokinin production by D188-5, D188 and 21D5 grown under inducing conditions (20 mM pyruvate and 5 mM histidine).

Table 4.2 Preliminary data on the cytokinin content of the supernatant of different *R. fascians* strains grown under inducing conditions (20 mM pyruvate and 5 mM histidine).

Strain	cZ-type cytokinins (nM)	2-iP-type cytokinins (nM)	Total cytokinin content (nM)	Relative total cytokinin content (%)
D188-5	44	108	153	100
D188	15	52	37	24
21D5	49	21	101	66

4.A.5. Impaired *att* gene expression affects the *in planta* production of the Att compound by 21D5

Since expression of the *att* genes and the production of Att compound is tightly linked to the invasion capacity of *R. fascians* and to *fas* gene regulation (Maes et al., 2001), the phenotypes of 21D5 might suggest that the *att* autoregulatory system is defective in this mutant. To test this hypothesis, we first introduced an available *attA:GUS* reporter plasmid pRFTM3 (Maes et al., 2001) into 21D5 cells by electroporation and measured the GUS activity after *in vitro* growth of the resulting strain 21D5(pRFTM3) and D188(pRFTM3) under several *att*-inducing conditions (Maes et al., 2001). As shown in Figure 4.9.A, *attA* expression in the D188 background was highly induced by combining 5 mM histidine with 20 mM pyruvate or 20 mM sucrose or leafy gall extract (20 µl/ml) with 20 mM pyruvate. Although a similar expression pattern was obtained in the 21D5 mutant, the overall expression level was significantly lower (Figure 4.9.A).

To verify whether this defect also occurred *in planta*, excised leaves were infected with both reporter strains and *in planta attA* expression was quantified after 7 days. Surprisingly, the *attA g*ene was highly expressed when 21D5 was present on the host (Figure 4.9.B). To obtain further evidence for this finding, we evaluated whether the Att compound could be detected in infected plants. Therefore, *Arabidopsis* plants were infected with different *R. fascians* strains and, 28 days after infection, extracts were prepared from these plants. These extracts were subsequently used to quantify their inducing capacity on *attA* expression in the absence or presence of 20 mM pyruvate. The presence of pyruvate strongly enhances gall-induced virulence gene expression and can be used to detect low amounts of Att compound (Maes et al., 2001; Temmerman et al., 2000). In accordance with the *in planta* expression data, extracts obtained from 21D5-infected plants indeed had inducing activity, indicating that the Att compound is produced and secreted into the plant tissues by 21D5 (Figure 4.9.C). However, just as for extracts of plants infected with strain D188-*att1*, in the absence of pyruvate, the inducing activity was

lower than that of extracts from D188-infected plants, suggesting that production of the Att compound is partly compromised (Figure 4.9.C).

Finally, the localization of *attA* expression in the 21D5 and D188 background was visualized using histochemical staining of tobacco plants infected with both reporter strains. In D188, extensive *attA* expression was apparent in the complete epiphytic population (Figure 4.9.D and E), corroborating previous reports (Cornelis et al., 2002). Unexpectedly, almost no *attA* expression could be detected in the 21D5 background (Figure 4.9.F and G). The discrepancy between both *in planta* expression results (Figure 4.9.B and F) might be caused by the different infection procedures that were used. Indeed, for the quantification of the *in planta* expression excised leaves were infected. These leaves were placed on MS medium which might support 21D5 growth. In contrast, the localization of *in planta* expression was done on intact plants, so in that case 21D5 growth has to be supported by the plant only.

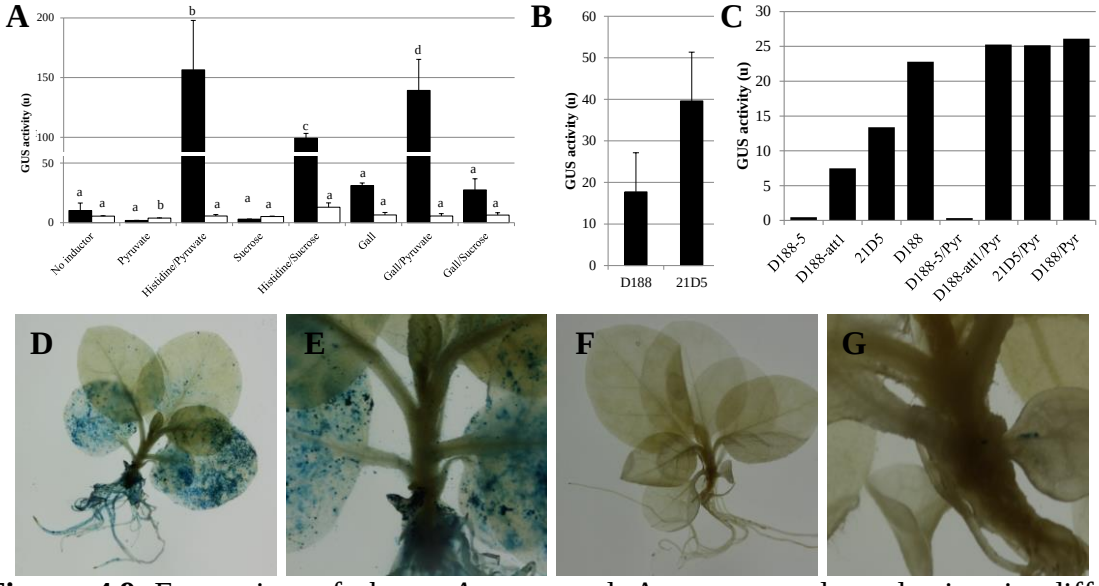

Figure 4.9 Expression of the *attA* gene and Att compound production in different *R. fascians* strains.

(A) Effect of different conditions on *attA* expression *in vitro* in D188 (black bars) and 21D5 (white bars) measured with the reporter plasmid pRFTM3 and pNPG as substrate. Inductions were performed in IM medium in the presence of 20 mM pyruvate, 5 mM histidine, 20 mM sucrose and 20 µl/ml leafy gall extract. Statistical differences within each strain indicated by different letters were evaluated with Student's *t*-tests ($p<0.05$). Error bars represent SE (n=3). (B) Expression of *attA* in the D188 and 21D5 background *in planta* 7 days after infection of excised leaves and measured with MUG as substrate. Both conditions were not statistically different according to Student's *t*-tests ($p<0.05$). Error bars represent SE (n=4). (C) Effect of extracts from *A. thaliana* plants infected with different *R. fascians* strains on *attA* expression in the presence or absence of 20 mM pyruvate measured in strain D188(pRFTM3) with pNPG as substrate. (D-G) Histochemical staining visualizing *in planta attA* expression in the D188 (D-E) and 21D5 (F-G) background. E and G are details of D and F, respectively. Photos were taken with a Canon OS 50D ISO 100 (Diaphragm 16 and closing time 1/100sec).

4.A.6. 21D5 is unable to persist on the plant host

From the *fasA* and *attA* expression data and the cytokinin and Att compound production results, we can conclude that both these essential virulence factors are not completely shut down in strain 21D5, but they are not functioning optimally. To get more insight into why the mutation in *GT1* causes this partial defect, we evaluated the persistence of 21D5 on its host in time, by quantifying at 2, 7 and 21 dpi the establishment of the total and the endophytic subpopulations on tobacco leaves dissected from plants that were infected by dipping. For comparison, similar manipulations were done with D188 and D188-5. To assure a comparable initial inoculum, for each bacterial strain, the washed bacterial solution was set to the same OD600. The total D188-5 population did not change much with time, whereas the contribution of the endophytic subpopulation increased with one log between 2 and 7 dpi (Figure 4.10). The total population of D188 increased with one log by 21 dpi, but the endophytic subpopulation remained stable throughout the experiment (Figure 4.10). The initial 21D5 total population was one log lower than those of D188-5 and D188 and dropped another log by the end of the experiment (Figure 4.10). Moreover, the endophytic subpopulation of 21D5 dropped 2 logs between 2 and 7 dpi, but stayed stable thereafter, ending 3-3.5 logs lower than the endophytic populations of D188-5 and D188 (Figure 4.10).

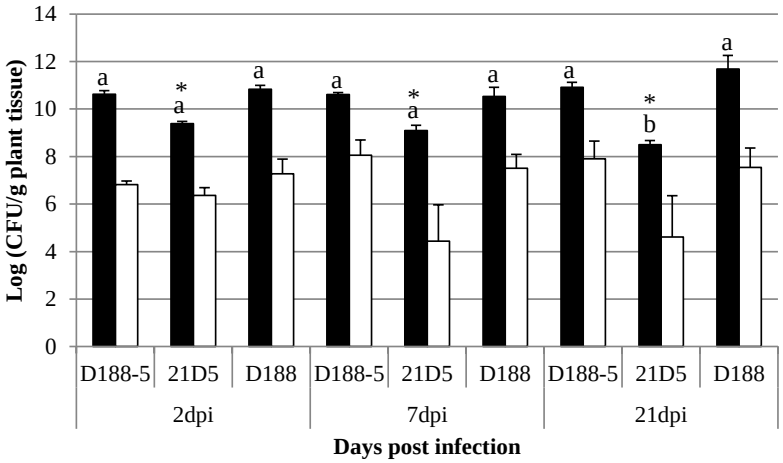

Figure 4.10 Colonization capacities of *R. fascians* strains D188-5, 21D5 and D188.
Infected leaves were used as such (total population) or first submitted to a bleach treatment (endophytic subpopulation); after several time points the leaves were crushed and serial dilution were made and plated on YEB medium to determine the colony forming units per gram fresh plant tissue. Black bars: total population; white bars: endophytic subpopulation. Statistical differences between time points for total population of each strain indicated by different letters were evaluated with Student's t-tests ($p<0.05$). Endophytic subpopulations were not statistically different according to Student's *t*-tests ($p<0.05$). For each time point, the asterisks indicate significant differences with D188 according to Student's t-tests ($p<0.05$). Error bars are SE (n=4).

These data suggested that 21D5 experiences difficulties to maintain itself on the host. To verify whether this was indeed the case, excised tobacco leaves infected for 5 weeks with D188 or 21D5 were observed by scanning electron microscopy without sample pre-treatment. In agreement with previous reports (Cornelis et al., 2001), strain D188 formed large epiphytic colonies covered by a layer on the leaf blade (Figure 4.11.A and B), almost appearing like a crust (Figure 4.11.C). Also the leaf edges contacting the medium were heavily colonized by D188 (Figure 4.11.D). In contrast, it was very difficult to find sites extensively colonized by 21D5 (Figure 4.11.E and F) and a thick crusty biofilm was not found either (Figure 4.11.G). However, small patches of bacteria (Figure 4.11.I) and peculiar globular structures (Figure 4.11.J) were occasionally observed. 21D5 was apparently only able to efficiently colonize the leaf margins that were in contact with the medium (Figure 4.11.H), supporting the hypothesis stated to explain the discrepancy between the *in planta att* expression data in the 21D5 background (Figure4.9).

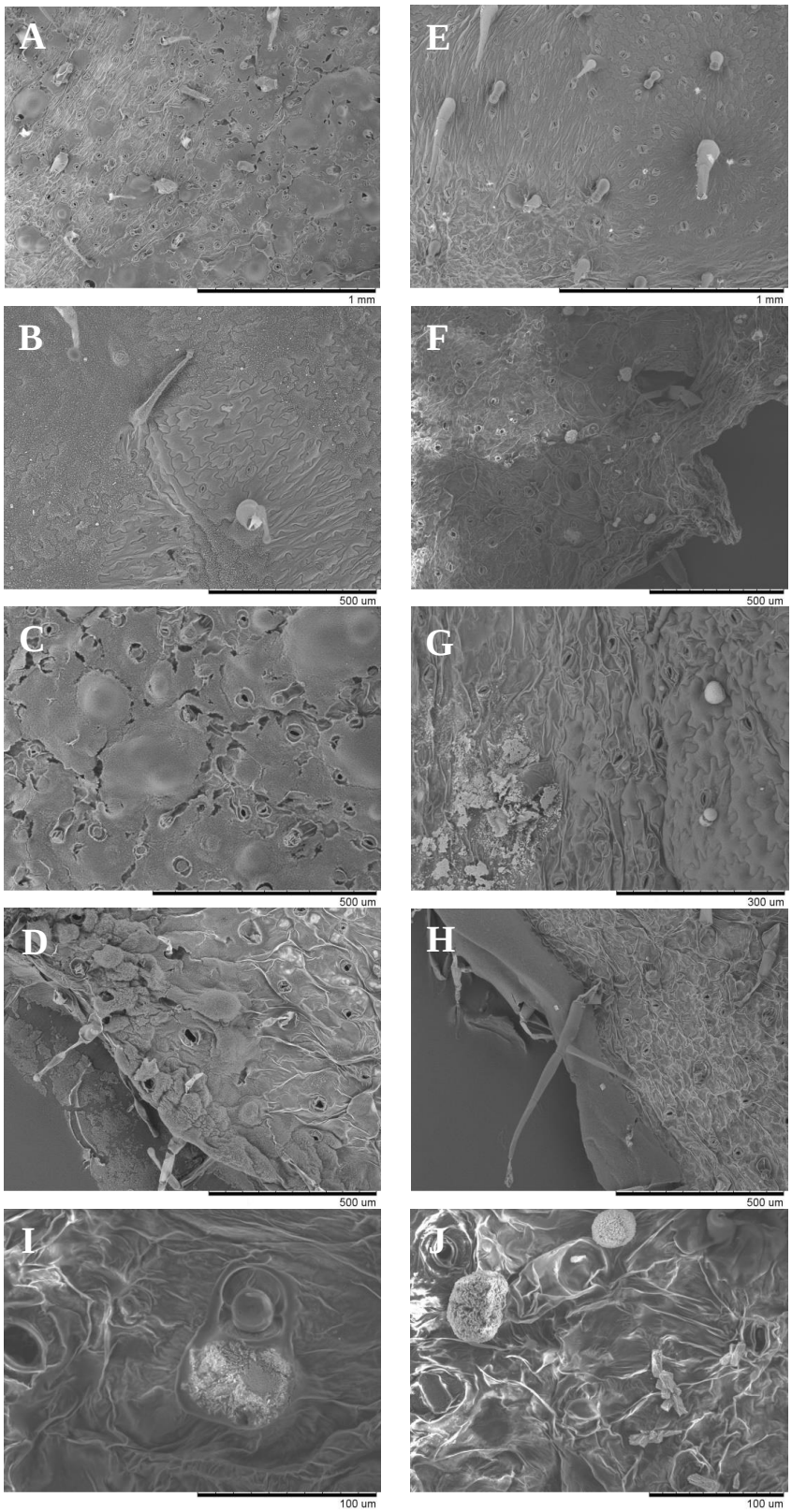

Figure 4.11 Epiphytic colonization of excised tobacco leaves by *R. fascians* strain D188 (A-D) and 21D5 (E-J) 5 weeks after infection.

At least 3 regions from several infected leaves were analyzed for each strain. (A-B) Large epiphytic D188 colonies; (C) Epiphytic D188 biofilm resembling a bacterial crust; (D) Extensive D188 colonization at the leaf edge; (E-F) Absence of extensive epiphytic colonization by 21D5; (G) Marginal crust-like colonization by 21D5; (H) Extensive 21D5 colonization at the leaf edge. (I) Small patches of epiphytic 21D5 bacteria; (J) Peculiar global colonization structures observed during 21D5 infection; Images were taken with a Tabletop Microscope TM-1000 (Hitachi) without sample processing.

4.A.7. Expression of *GT1* is possibly induced by carbon sources that accumulate in infected plants and might be controlled by AttR

Altogether, the colonization data indicate that strain 21D5 has difficulties to establish itself on the plant host. Moreover, the *in planta fas* and *att* expression data suggest that the limited amount of bacteria that do persist on the plant are not in the appropriate physiological condition to express these essential virulence factors to the level that is required to achieve full pathogenicity. This finding is supported by the complete inability of 21D5 to grow on a medium with minimal nutritional resources. To get more insight into the timing at which the GT1 function is required during the interaction with the host and into the regulation of the *GT1* gene expression, an available transcriptional *GT1:GUS* fusion was cloned into a bifunctional vector (see Material an Methods) and the resulting construct pRFGT2-1 was introduced into *R. fascians* D188 and D188-5, but also in D188-Δ*attR* and D188-Δ*fasR*, two mutants carrying a deletion in the master regulators AttR and FasR (Maes et al., 2001; Temmerman et al., 2000).

One of the earliest responses of the plant on infection with *R. fascians* is the modulation of its primary metabolism, leading to the accumulation of carbon sources related to the Krebs cycle, such as pyruvate, succinate, fumarate, malate, glucose, and fructose (Depuydt et al., 2009b) (Figure 8.3 in the Annexes). Since *GT1* might be required at the onset of the interaction, we first tested whether *GT1* expression in the D188 background was modulated by these carbon compounds. In this experiment, we also included the standard inducers histidine and uninfected plant and leafy gall extracts, and acetate and citrate, two additional compounds of the Krebs cycle. The data are the result of a single experiment and should be considered as preliminary. As shown in Figure 4.12, all of the carbon sources that accumulate in infected plants, as well as histidine and leafy gall extracts, induced the *GT1* expression. One exception was fumarate, but this compound was toxic to *R. fascians* at the concentrations used (data not shown). Extract from uninfected plants and citrate, which does not accumulate in infected plants, did not induce *GT1* expression (Figure 4.12). Interestingly, acetate, which was used in the primary screen as a carbon source to identify 21D5 as a mutant, activated *GT1* expression as well (Figure 4.12). These data suggest that the GT1 function is activated in response to the modulation of the primary metabolism of the plant and is likely required at the onset of the interaction.

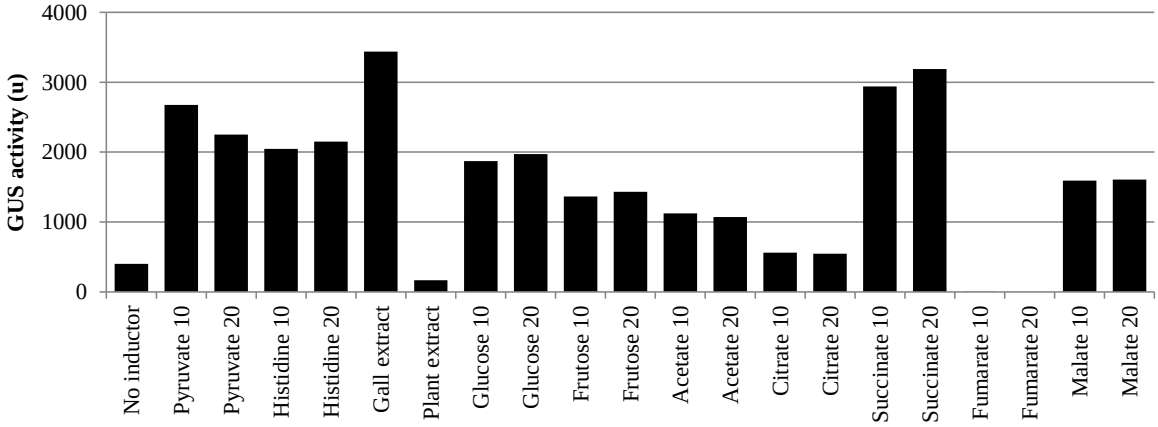

Figure 4.12 Effect of different conditions on *in vitro GT1* expression measured in D188(pRFGT2-1) with MUG as a substrate.
Inductions were done in IM medium with the different compounds (10 mM and 20 mM) and plant-derived extracts (20 µl/ml). The data are the results of a single experiment and should be considered as preliminary.

Next, we evaluated the expression of *GT1* in different regulatory mutants under conditions typically used to determine virulence gene expression. In the D188 background, pyruvate, histidine/pyruvate, and leafy gall extract induced *GT1* expression, whereas plant extract did not (Figure 4.13), confirming the data of the previous experiment (Figure 4.12). Similar results were obtained in D188-Δ*fasR* (Figure 4.13), indicating that *GT1* expression is independent from the FasR master regulator and the GT1 function likely unrelated to cytokinin production. The complete loss of *GT1* expression in the D188-Δ*attR* background (Figure 4.13), suggests that the autoregulatory system encoded by the *att* operon would control *GT1* expression, supporting the requirement of the GT1 function at the first steps of the interaction. However, if this were the case, no *GT1* expression would be expected in the plasmid-free D188-5 background. Surprisingly, in D188-5, *GT1* expression was as high as in D188 and not differential compared to the negative control (Figure 4.13). To get more insight into these conflicting results, the plasmid content of the different strains will have to be verified and the experiment repeated.

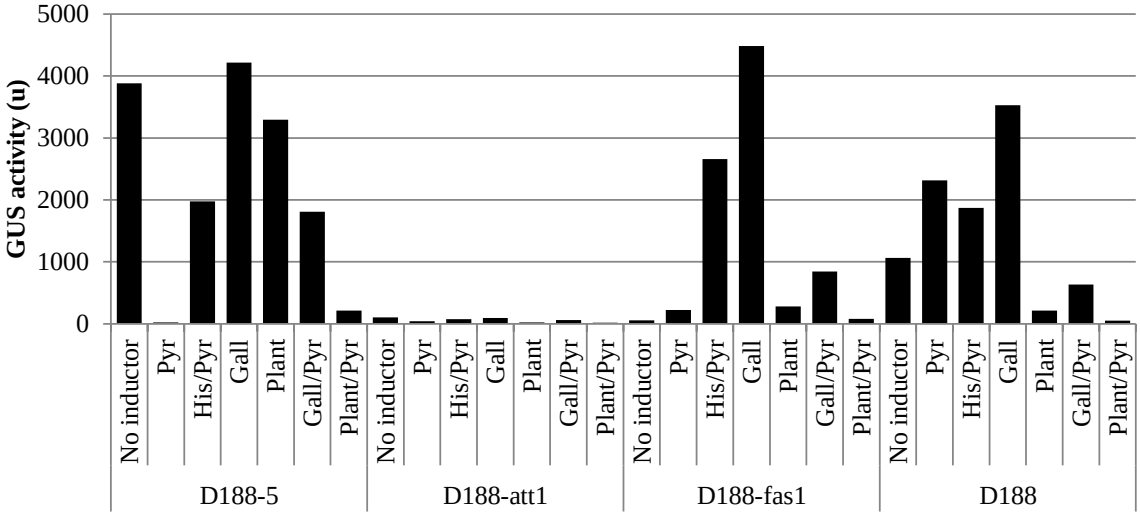

Figure 4.13 Effect of different regulators on *in vitro GT1* expression measured from the reporter plasmid pRFGT2-1 in different *R. fascians* strains with MUG as a substrate.
Inductions were done in IM medium with 20 mM pyruvate (Pyr), 5 mM histidine (His), 20 µl/ml leafy gall extract (Gall) and 20 µl/ml plant extract (Plant). The data are the results of a single experiment and should be considered as preliminary.

Nevertheless, when we analyzed the promoter region of the *pFi_135-136* operon, a typical LysR-type binding motif could be detected (Figure 4.14), suggesting that AttR regulation might indeed occur.

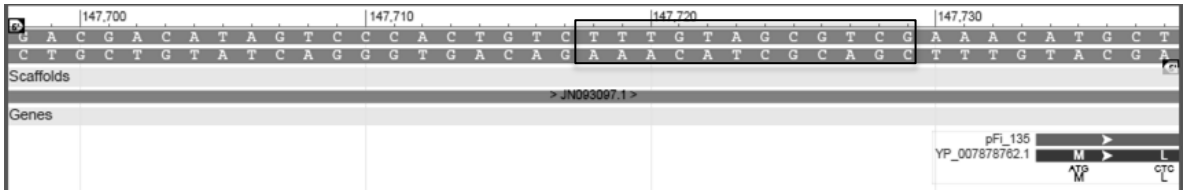

Figure 4.14 Presence of the T-N_{11}-A motif in the upstream sequence of the *pFi_135_136* operon. This motif is typically present in promoters regulated by LysR-type proteins (Goethals et al., 1992).

B. Methylated cytokinins: the secret weapon of R. fascians?

As explained in the Introduction, the two phytopathogenic actinomycetes *R. fascians* and *Streptomyces turgidiscabies*, that are known to induce leafy galls, have related SAM-dependent methyltransferase genes (*mtr*) associated with their *fas* operons (Figure 1.9). Their location in the *fas* locus and the loss of virulence of *R. fascians mtr* mutants, suggests their involvement in the biosynthesis of an essential methylated cytokinin. To

analyze the impact of the mutations in the *mtr* genes on the cytokinin production in *R. fascians*, the cytokinin profile of the supernatant of D188-5, D188, D188-*mtr1* and D188-*mtr2* grown under *fas*-inducing conditions was determined by Petr Tarkowski, our collaborator at Palacký University (Olomouc, Czech Republic). The data presented in Figure 4.15 are preliminary and still incomplete, but they support the hypothesis that the MTRs are apparently not involved in the production of 2MeS*c*Z or any other of the detected cytokinins.

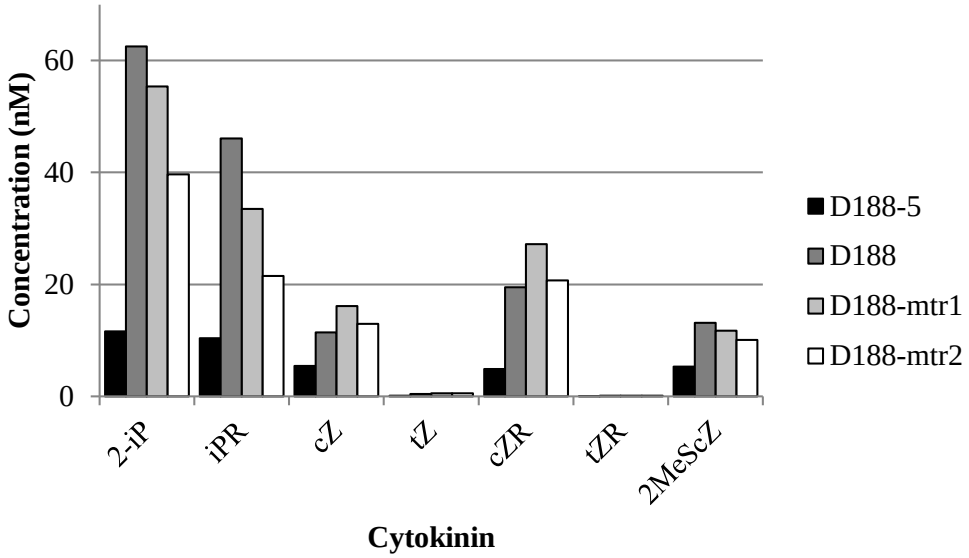

Figure 4.15 Preliminary data on the cytokinin production of different *R. fascians* strains induced with 20 mM pyruvate and 20 µl/ml leafy gall extract.

So, to visualize the reaction product(s) of the MTR proteins, different bacterial strains were grown under *fas*-inducing conditions in IM medium in the presence of ^{14}C-labelled Adenine or ^{14}C-labelled SAM. The bacterial pellets and the supernatants were extracted and the extracts analyzed on silica thin layers using butanol/water/25% ammonia (4/2/1) as mobile phase (see Materials and Methods for details). The labelled compounds were visualized with a phosphor-imager and the UV fluorescence by irradiation at 365 nm. The comparison of the pattern obtained in D188-5, D188-*fas1*, D188-*mtr1*, and D188-*mtr2* with that of D188 should allow the identification of *fas*- and *mtr*-dependent compounds. These compounds are expected to be present in the *S. turgidiscabies* DSM41990 and DSM41997 as well, because they carry the *fas* operon and the *mtr* genes (Aittamaa et al., 2010). The labeling experiments revealed clear patterns, both for the cellular extracts (Figure 4.16) and for the extracts of the supernatants (Figure 4.17), but unfortunately none of the compounds could be linked to the *fas* or the *mtr* genes.

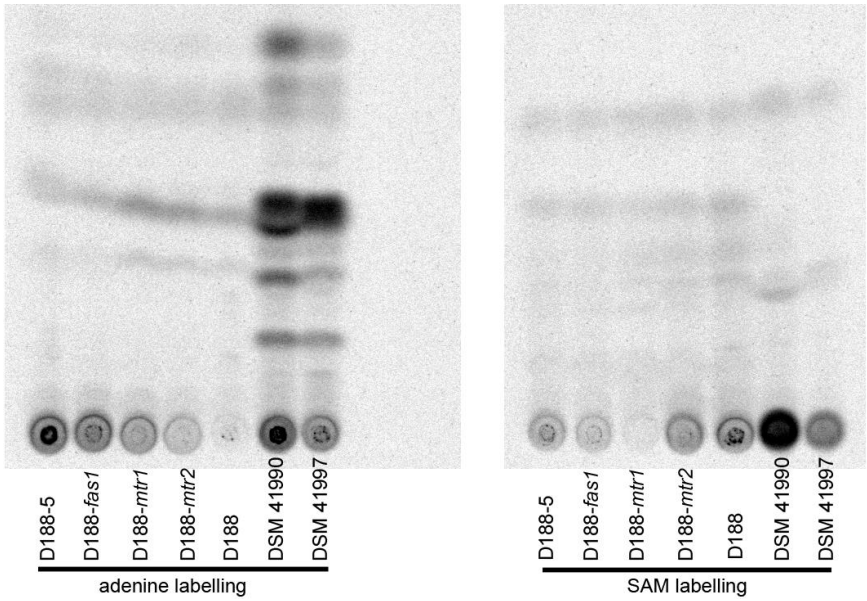

Figure 4.16 Thin layer chromatography analysis of ^{14}C-adenine- and ^{14}C-SAM-labelled compounds produced by different *R. fascians* and *S. turgidiscabies* strains.
Analysis of the butanol fraction of the bacterial cells. *R. fascians* strains were induced in IM medium with pyruvate (20 mM) combined with leafy gall extract (20 µl/mL); the *S. turgidiscabies* strains were not induced.

No UV-fluorescent compounds were detected in the cellular extracts (data not shown) and none of the UV-fluorescent compounds secreted in the supernatants were *fas*- or *mtr*-dependent (Figure 4.17).

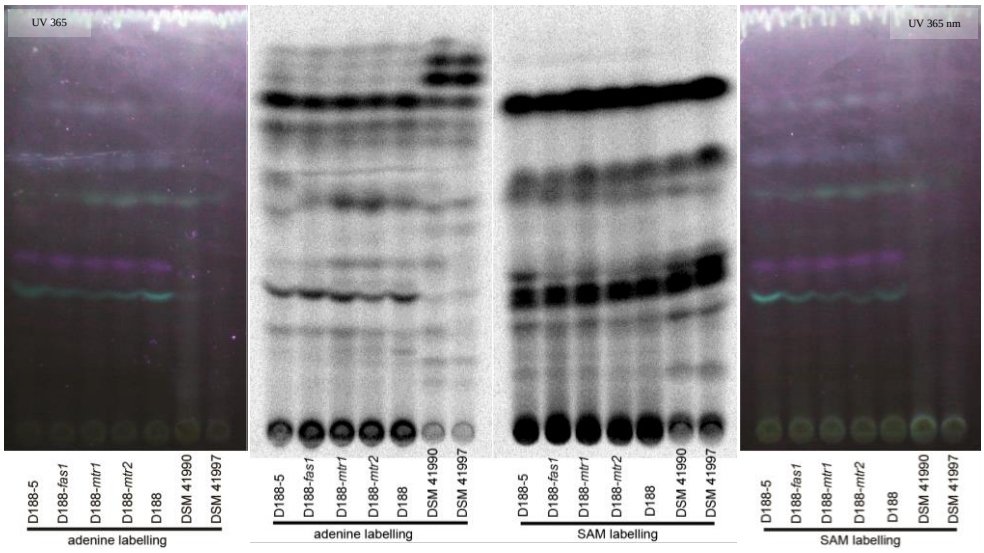

Figure 4.17 Thin layer chromatography and UV-fluorescence analysis of ^{14}C-adenine- and ^{14}C-SAM-labelled compounds produced by different *R. fascians* and *S. turgidiscabies* strains.
Analysis of extracts of the supernatants of the different strains. *R. fascians* strains were induced in IM medium with pyruvate (20 mM) combined with leafy gall extract (20 µl/mL); the *S. turgidiscabies* strains were not induced.

To understand this unexpected result, we decided to analyze the *in vitro* expression of the *mtr* genes and compare it to that of *fasA*. Therefore, D188-*mtr1*, D188-*mtr2*, and D188(pJDGV5) were grown under the typical inducing conditions and the expression of the GUS reporter gene was quantified with MUG as a substrate. Whereas for *fasA* a significant expression was measured with histidine/pyruvate and gall/pyruvate, hardly no expression was measured for both *mtr* genes (Figure 4.18). These data explain the TLC results and indicate that the *mtr* genes are not co-expressed with the *fas* genes *in vitro*. We reasoned that the *mtr* gene expression might be substrate dependent and so inductions were set with 2-iP, *c*Z and *t*Z, but again no expression could be measured (Figure 4.18).

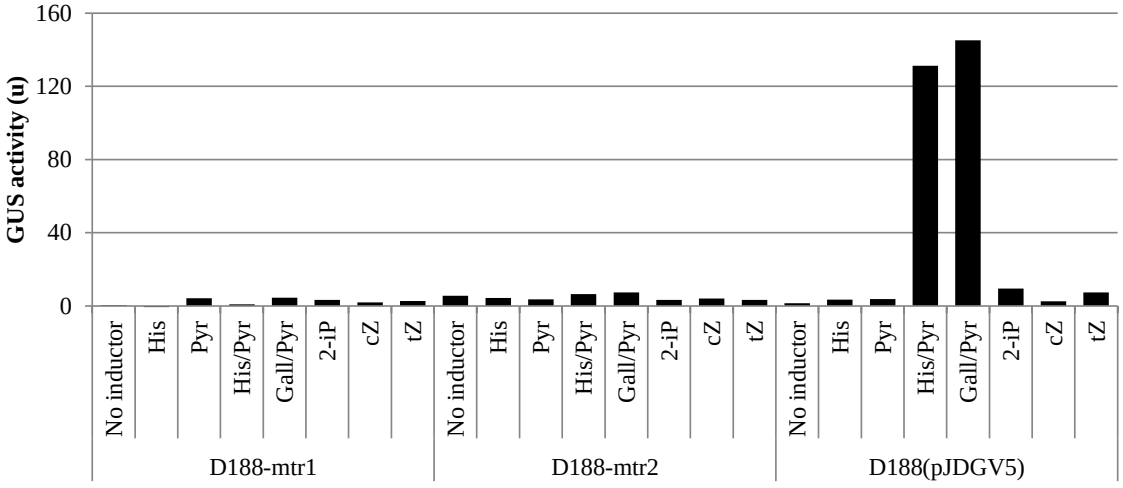

Figure 4.18 Effect of different conditions on *in vitro mtr1*, *mtr2*, and *fasA* expression measured in D188-*mtr1*, D188-*mtr2*, and D188(pJDGV5), respectively, with MUG as a substrate.
Inductions were performed in IM medium in the presence of 20 mM pyruvate (Pyr), 5 mM histidine (His), 20 µl/ml leafy gall extract, 20 µl/ml plant extract, 10 µM 2-iP, 10 µM *c*Z and 10 µM *t*Z. The data are the results of a single experiment and should be considered as preliminary.

Finally, excised leaves from 4-week old tobacco plants were infected by dipping with D188-*mtr1*, D188-*mtr2*, and D188(pJDGV5) and *in planta* expression was quantified after 7 days with MUG as a substrate (Figure 4.19.A). Interestingly, both *mtr* genes were expressed *in planta* and their expression level was comparable or even exceeded that of *fasA* (Figure 4.19.A). To confirm the obtained results, the localization of *mtr1*, *mtr2*, and *fasA* expression was visualized using histochemical staining of 4-week old tobacco plants infected for 7 days with the reporter strains. The expression level of all three genes was comparable and it was localized in distinct patches on the leaf lamina and in the axillary

regions (Figure 4.19.B-D). Altogether, the expression results show that the *fas* and *mtr* genes are controlled by different regulatory mechanisms. Apparently, the ones that determine *mtr* expression are even more stringent that those controlling *fas* expression. The results also highlight the complication to identify the MTR-dependent cytokinins.

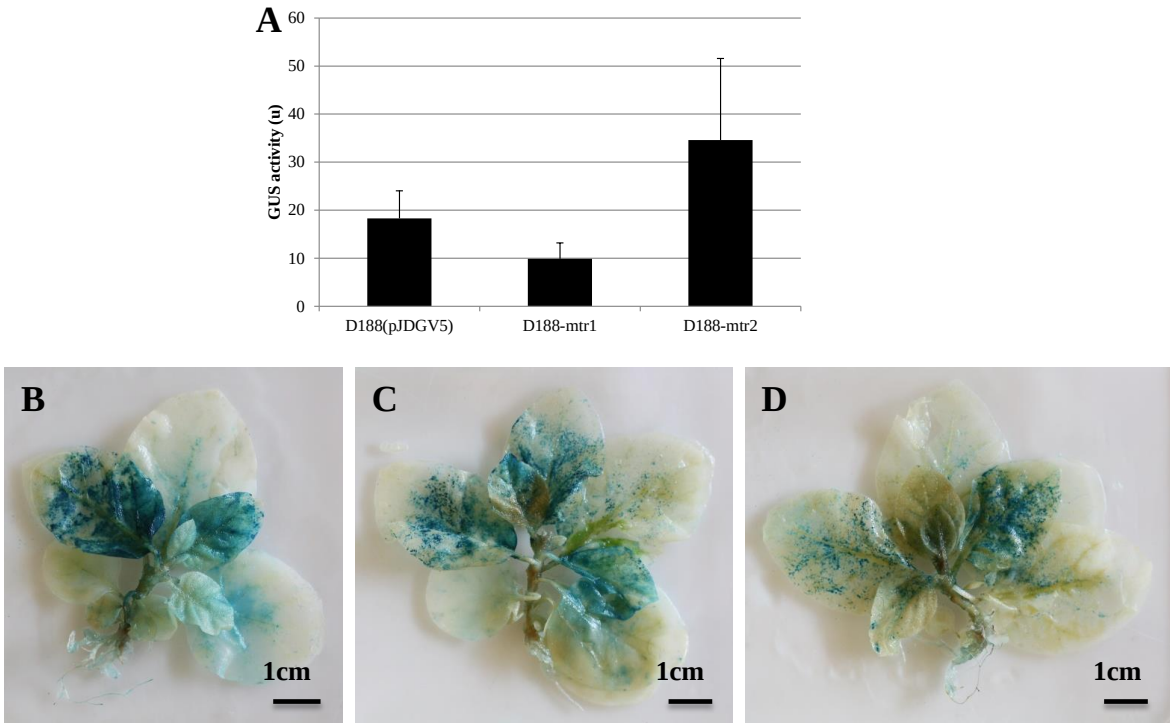

Figure 4.19 *In planta* expression of *fasA*, *mtr1* and *mtr2* using different assays.
(A) Quantification of the expression of *fasA*, *mtr1* and *mtr2* in the D188 background *in planta* 7 days after infection of excised leaves and measured with MUG as substrate. *fasA* and *mtr* expression were not statistically different according to Student's *t*-tests ($p<0.05$). Error bars represent SE (n=4). (B-D) Histochemical staining visualizing *in planta fasA* (B), *mtr1* (C) and *mtr2* (D) expression in the D188 background. Photos were taken with a Canon OS 50D ISO 100 (Diaphragm 16 and closing time 1/100sec).

To find a solution for this problem, we then tried if we could bring the *in planta* expression *in vitro* so that the labelling experiments could be repeated under conditions in which the *mtr* genes are expressed. Therefore, 4-week old tobacco plants and excised leaves of plants of the same age were infected with D188-*mtr1* by dipping. After 7 days, these plant tissues were used to set *in vitro* inductions. Therefore, the plant material was either crushed or cut in pieces and placed in IM medium overnight to evaluate whether *mtr1* expression from the bacteria present on the plants could be detected. We also wondered if the supplementation of additional D188-*mtr1* cells that were grown *in vitro* to such samples, would positively affect the *mtr1* expression levels. Therefore, inductions were performed

in the presence of dissected infected leaves, crushed or cut leaves from infected plants, and D188-*mtr1* diluted two times. As control for the previous experiment, *in vitro* grown D188-*mtr1* cells were induced with leafy gall extract. Importantly, in this assay, significant *mtr1* expression could be measured in all the samples taken from the infected excised leaves (Figure 4.20). Expression in most of the samples from intact plants was much lower (Figure 4.20). Generally, addition of *in vitro* grown D188-*mtr1* cells did not strongly increase the measured *mtr1* expression, except in the case of cut leaves from infected complete plants (Figure 4.20). Based on these results, the labelling experiment can be repeated starting from infected crushed plant material that is incubated overnight in IM medium in the presence of ^{14}C-labelled Adenine or ^{14}C-labelled SAM. Unfortunately, due to time constraints, I was unable to perform this experiment myself, but, hopefully, future work on this subject will allow to discover the methylated cytokinins of *R. fascians*.

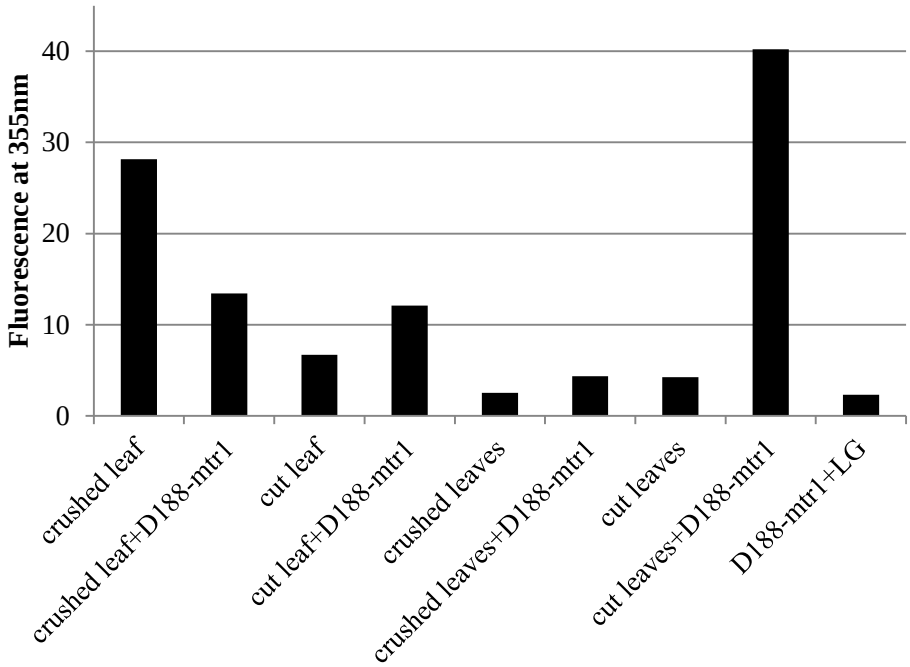

Figure 4.20 Bringing *in planta* expression of the *mtr1* gene to an *in vitro* system.
Effect of different conditions on *in vitro mtr1* expression measured in D188-*mtr1* with MUG as substrate. Inductions were performed in IM medium on a single crushed or cut D188-*mtr1* infected excised leaf, or 3 small crushed or cut leaves dissected from entire D188-*mtr1* infected plants. *In vitro* grown D188-*mtr1* cells induced with 20 µl/ml leafy gall extract (LG) were used as a control. The data are the results of a single experiment and should be considered as preliminary.

5. Discussion

In this work we analyzed the putative function of two new pFiD188-located loci in the pathology of *R. fascians* strain D188: the glycosyltransferase GT1 encoded by *pFi_136* and two SAM-dependent methyltransferases MTR1 and MTR2 encoded by *pFi_075* and *pFi_076*, respectively.

Glycosyltransferase enzymes play an important role in the biosynthesis of cell wall components, including peptidoglicans, arabinogalactans and lipoarabinomannans (Wagner and Pesnot, 2010), and the bacterial cell wall has proven to be essential for the virulence in multiple pathogens (Bizzini et al., 2007; Paterson et al., 2009). When *R. fascians* initiates an interaction with a host plant, it first goes through an epiphytic growth stage. Several characteristics of the bacterium indicate that it is well adapted for this phase of its life cycle, suggesting that it is important for the subsequent success of the pathological phase (Stes et al., 2011). However, to date, almost no information is available on the molecular determinants that control the epiphytic behavior. Similarly, the putative role of the cell wall of *R. fascians* during the interaction with its host is largely unknown. Nevertheless, the attenuated virulence of the *att* mutants coincides with their inability to cause symptoms when the plants are intact, implying that active penetration of the plant tissues is controlled by this autoregulatory system either directly or indirectly (Maes et al., 2001). Moreover, Lacey (1961) suggested that *R. fascians* would lose its cell wall during the interaction with the host and these L-forms would be difficult to re-isolate from infected tissues. Based on the differential visualization of the bacterial populations living in and on the plant with *in situ* hybridization and immuno-localization, Cornelis and colleagues concluded that major reorganizations of the cell wall likely occur during the interaction with the host (Cornelis et al., 2002; Cornelis et al., 2001).

With the identification of the 21D5 mutant, it became possible, for the first time, to get insight into factors that are vital for the very early steps of the interaction with the host and that are unrelated to molecular signaling through phytohormones. One important finding was that the colony morphology of *R. fascians* was strongly dependent of the growth conditions. Especially on the defined minimal media, but not on the minimal media with plant-derived extracts which are complex mixtures of many compounds, the bacteria produced a very peculiar colony shape characterized by a distinctive protrusion layer

(Figure 4.1). It has been shown that the leaf surface is a hostile and patchy nutrient-poor environment for epiphytic bacteria (Beattie and Lindow, 1995; Beattie and Lindow, 1999) and surface properties are known to affect adhesion and biofilm formation (Lorite et al., 2013). Thus, it is very likely that the behavior of *R. fascians* on the plant host will depend on their position on the leaf and will change as the interaction proceeds. The 21D5 mutant has a very strong colony morphology defect: it exhibits the protrusion layer on rich medium and is unable to grow on defined minimal media (Figures 4.1 and 4.2). Based on our results, we can conclude that although this modified growth behavior does not affect growth capacity when sufficient nutrients are available (Table 4.1), it has a very severe impact on the epiphytic fitness of *R. fascians* and, consequently, on its pathogenicity. Indeed, the mutation in the *GT1* gene lead to an almost complete loss of virulence illustrated by the strongly attenuated ability of 21D5 to induce symptoms on *Arabidopsis* and tobacco (Figures 4.3 – 4.7). This reduction in pathogenic capacity coincided with a strongly reduced ability to establish epiphytic colonies (Figures 4.8.E, 4.9.F, and 4.11) and a sustained endophytic population (Figure 4.10). The importance of the endophytic subpopulation on symptom maintenance had been illustrated before by the identification of the *vic* mutant, which is unable to grow on the C2 carbons provided by infected plant tissues (Vereecke et al., 2002a; Vereecke et al., 2002b), but the absolute requirement of extensive epiphytic colonization for the pathology is new. Moreover, the defective colonization potential of 21D5 also resulted in a strongly impaired *in planta* expression of the *att* and *fas* genes (Figures 4.8.E and 4.9.F), which would inevitably lead to an uncoordinated and inadequate production of cytokinins. A comparable effect of a defective attachment on virulence factor production has been reported in other phytopathogens as well (Anand and Mysore, 2007; Gelvin, 2000; Gelvin, 2010; Hsiao et al., 2011). Finally, although the results are only preliminary, the expression pattern of the *GT1* gene was shown to be rather unique (Figure 4.12): a *GT1:GUS* transcriptional fusion was activated upon incubation with the carbon sources that accumulate when plants perceive the colonization by *R. fascians* (Depuydt et al., 2009b). Such a pattern indicates that the GT1 function is most likely required very early during the interaction, which is in agreement with the colonization data. The observation that *GT1* expression would be controlled by the *att* autoregulatory system (Figures 4.13 and 4.14), extends the *att* regulon and identifies the GT1 function as a putative invasion factor.

Concerning the *fas*-associated *mtr* genes, the most important question we wanted to address was what are the reaction products of the encoded MTR proteins. Previous work has shown that *R. fascians* produces a mixture of six cytokinins (Pertry et al., 2009) and this offers a variety of potential benefits during the interaction with the plant host, amongst which their synergistic action is thought to explain the strong morphogenic activity of the bacteria (Stes et al., 2011). Nevertheless, the observation that the complete loss of pathogenicity of the *mtr* mutants (Pertry, 2009) is not correlated with a strong reduction in the level of a subset of the six cytokinins (Figure 4.15) is very intriguing and might indicate that there are still new *R. fascians* cytokinins to be discovered. Therefore, we took an approach to feed a set of bacteria with ^{14}C-labelled adenine and ^{14}C-labelled SAM, both thought to be precursors of the elusive MTR-cytokinins. Unfortunately, none of the compounds visualized by TLC were *fas*- or *mtr*-dependent (Figures 4.16 and 4.17). Determination of the expression profile of the *mtr* genes showed that also these genes were regulated in a novel way: *mtr* expression could not be obtained *in vitro* under any of the conditions tested (Figure 4.18), albeit that their *in planta* expression was comparable to that of the *fas* genes (Figure 4.19). This result illustrates that laboratory media do not necessarily mimic the physiological conditions of plants, a conclusion that has been drawn before by Marco and colleagues for *Pseudomonas syringae*, another intimate plant-pathogen interaction (Marco et al., 2005). Nevertheless, till now, there always seemed to be a nice correlation between *in vitro* and *in planta* data (Pertry, 2009), but with the results on the *mtr* genes, caution should be taken when making firm hypotheses or conclusions based on *in vitro* results only. We succeeded in developing a system by which the *in planta* expression could be brought *in vitro* (Figure 4.20) so that the feeding experiments can be repeated and the *mtr*-dependent cytokinins will hopefully be identified. Finally, based on reports on other pathogens, an alternative hypothesis could be formulated in which the *R. fascians* MTR's would function in cell wall formation (Lissina et al., 2014; Nishiuchi et al., 2000; Whitfield et al., 1997) or in adhesion (Lissina et al., 2014). However, the lack of a colony phenotype (data not shown) and the good epiphytic colonization (Figure 4.19) rule out this possibility.

Altogether, the results obtained during this master thesis have illustrated clearly that a lot remains to be discovered on the bacterial side of the interaction between *R. fascians* and its plant host. Although some data are still preliminary and await confirmation, we have

identified the *GT1* gene as a putative novel member of the *att* regulon and a first invasion factor that acts at the very onset of the interaction with the host. The finding that the bacterial behavior is strongly dependent of the growth conditions was novel as well and adds another interaction parameter to this multifaceted pathology. The results on the *mtr* genes revealed that the regulation of the *fas* genes is even more complex than previously anticipated (Pertry, 2009) and identification of the elusive MTR-cytokinins will require novel and imaginative approaches.

6. Summary and perspectives

Until now all the identified pathogenicity factors in *R. fascians* were located in unique region U1 of the linear plasmid pFiD188. However, the function of the majority of genes on the linear plasmid is still unknown. In this thesis two loci on pFiD188 were proven to be essential for the pathogenicity of the bacteria: the glycosyltransferase *GT1*, situated in unique region U2, and two SAM-dependent methyltransferases *mtr1* and *mtr2*, located immediately upstream of the *fas* operon in unique region U1.

Glycosyltransferase mutants were identified in a collection of transposon mutants of the wild-type *R. fascians* strain D188 and strain 21D5 was selected based on its growth impairment in LB medium supplemented with acetate. In this work, we further developed this line of research and could show that the medium composition has a strong impact on the appearance of the bacterial colonies. This finding illustrates that *R. fascians* can adjust its shape in response to particular conditions, which might be of significant importance during the interaction with the plant host. The mutant 21D5 exhibited a strong colony morphology phenotype and coagulated when grown in liquid medium. Whereas these phenotypes did not affect the growth potential of this mutant on rich media, it did result in a complete inability to grow under nutrient deprivation, which might affect its epiphytic fitness. Indeed, when we analyzed the virulence capacity of 21D5, a very severe attenuation was revealed. The impaired symptom development induced by this mutant coincided with a reduced *fas* gene expression resulting in a lower cytokinin production and a defective *att* autoregulation affecting both the invasion ability and virulence gene expression. Finally, the mutation in the *GT1* gene strongly compromised the survival of *R. fascians* on and in the plant tissues, indicating that the GT1 function is likely essential at the onset of the interaction. This hypothesis was supported by the unique expression profile: *GT1* expression was induced by all the Krebs cycle intermediates that accumulate in plants that sense the presence of *R. fascians* and this induction might be controlled by AttR.

Although some of the generated data are still preliminary, based on all available information, we would like to postulate a speculative working hypothesis for the role of the GT1 locus in the *R. fascians* pathology. When *R. fascians* makes contact with a plant, this host quickly reacts by altering its primary metabolism. The differential accumulation of

Krebs cycle intermediates is sensed by the bacteria through the sensor histidine kinase encoded by *pFi_133* located upstream of the *GT1* locus and leads to the activating phosphorylation of the response regulator encoded by *pFi_134*. As a result, pFi_134 protein activates the transcription of the *pFi_135-pFi_136* operon. Expression of this operon is also controlled by AttR which is known to be activated upon perception of a compatible host. As such, GT1 is produced and glycosylates the integral membrane protein encoded by *pFi_135* leading to the modification of the cell wall which determines biofilm formation and adaptation to life on and in its host. Because this modification cannot occur in 21D5, the way in which the bacterial cells interact with each other is modified, the mutant is unable to adapt to the plant host environment, exhibits a strong loss of epiphytic fitness, resulting in inadequate production of virulence factors an consequently, a very poor pathogenicity.

Clearly, many aspect of this model remain to be substantiated by data, but if this is successful, the *GT1* locus will be identified as the earliest determinant of pathology of *R. fascians*. The most important issues that need to be addressed are: 1) analyzing the virulence of mutants in the 2-component regulatory system encode by *pFi_133-pFi_134* and determining the expression profile of both genes; 2) establishing that the phenotypes of 21D5 are caused by the transposon mutation by doing complementation assays; 3) confirming the expression profile of *GT1* and its dependence of AttR; 4) demonstrating the GT activity of GT1 and showing that pFi_135 is its substrate; 5) identifying the defect in the 21D5 cell wall.

The two *mtr* mutants that have been created in previous work, were shown to be non-pathogenic albeit that the levels of none of the *fas*-dependent cytokinins were strongly altered. Moreover, *S. turgidiscabies*, the only other known microorganism know to induce leafy galls, also has the *mtr* genes associated with its *fas* operon. These finding led us to postulate that the *R. fascians* pathogenicity was determined by unidentified methylated cytokinins. Because we anticipated that the *mtr* genes would be co-regulated with the *fas* genes, we initiated a feeding experiment in which different *R. fascians* strains were grown under *fas*-inducing conditions in the presence of ^{14}C-labelled adenine and ^{14}C-labelled SAM; two *S. turgidiscabies* strains were included in the analysis as well. The supernatants were extracted and the extracts analyzed by TLC. Unexpectedly, no *fas*- or *mtr*-dependent compounds could be identified amongst the secreted compounds. When we evaluated the

expression of the *mtr* genes grown *in vitro* under the *fas*-inducing conditions, much to our surprise, both *mtr*'s were not expressed at all, showing that their expression is even more tightly controlled than that of the *fas* genes. However, when the bacteria colonized the host, a strong *in planta* expression, comparable to that of *fasA*, was observed. To permit the identification of the *mtr*-dependent cytokinins, we set out to develop an assay in which the *in planta* conditions could be brought to an *in vitro* system. By infecting plants and crushing the infected tissue after 7 days in induction medium, we were able to detect a considerable level of *mtr* gene expression after an overnight *in vitro* incubation period, opening the path to the identification of the elusive methylated cytokinins. Unfortunately, due to a lack of time, new feeding experiments could not be done during this thesis. A very important implication of these results is the interpretation of the *in vitro* obtained data on the spectrum of cytokinins produced by *R. fascians*. Indeed, in view of the current results it seems very likely that the full capacity of cytokinin production and even of other plant growth regulators is completely different and underestimated than what we think it is based on all previous data.

Thus, the *mtr* genes and especially their reaction products hold great putative potential for tissue culture, as they may represent very potent and novel plant growth regulators. However, to finalize the *mtr* story, several topics will have to be tackled: 1) the feeding experiment has to be repeated with crushed infected plant tissue and the extracts have to be analyzed in multiple TLC systems with different mobile phases; 2) the labeled *mtr*-dependent compounds have to be identified and traced back in infected plant tissues; 3) the MTR proteins have to be expressed in a heterologous system and the SAM-dependent methyl transfer to a cytokinin has to be demonstrated; 4) the *mtr* genes in *S. turgidiscabies* have to be mutated and the effect on leafy gall development and the production of methylated cytokinin has to be assessed; 5) the activity of the elusive methylated cytokinins has to be tested on diverse and recalcitrant plants in tissue culture practices.

Altogether, the work described in this report is a considerable contribution to the understanding of the pathogenicity process of *R. fascians*. Moreover, it opens new and exciting research perspectives that might enable the use of *R. fascians* or its morphogens in tissue culture practices or help horticulturists in safe guarding their ornamental crops from this pathogen.

7. References

Aittamaa M, Somervuo P, Laakso I, Auvinen P, Valkonen JP. Microarray-based comparison of genetic differences between strains of *Streptomyces turgidiscabies* with focus on the pathogenicity island Molecular Plant Pathology 2010; 11: 733-746.

Albesa-Jové D, Giganti D, Jackson M, Alzari PM, Guerin ME. Structure-function relationships of membrane-associated GT-B glycosyltransferases. Glycobiology 2014; 24: 108-124.

Anand A, Mysore KS. *Agrobacterium* biology and crown gall disease. Dordrecht: Springer, 2006.

Badreddine I, Lafitte C, Heux L, Skandalis N, Spanou Z, Martinez Y, et al. Cell wall chitosaccharides are essential components and exposed patterns of the phytopathogenic oomycete *Aphanomyces euteiches*. Eukaryotic cell 2008; 7: 1980-1993.

Bailey R, Schönrogge K, Cook JM, Melika G, Csóka G, Thuróczy C, et al. Host niches and defensive extended phenotypes structure parasitoid wasp communities. Plos Biology 2009; 7: 1-12.

Bartholdson SF, Brown AR, Mewburn BR, Clarke DJ, Fry SC, Campopiano DJ, et al. Plant host and sugar alcohol induced exopolysaccharide biosynthesis in the *Burkholderia cepacia* complex. Microbiology 2008; 154: 2513-2521.

Beattie GA, Lindow SE. The secret life of foliar bacterial pathogens on leaves. Annual Review of Phytopathology 1995; 33: 145-172

Beattie GA, Lindow SE. Bacterial colonization of leaves: a spectrum of strategies. Phytopathology 1999; 89: 353-359.

Berg S, Kaur D, Jackson M, Brennan PJ. The glycosyltransferases of *Mycobacterium tuberculosis* - roles in the synthesis of arabinogalactan, lipoarabinomannan, and other glycoconjugates. Glycobiology 2007; 17: 35R-56R.

Birch RG. *Xanthomonas albilineans* and the antipathogenesis approach to disease control. Molecular Plant Pathology 2001; 2: 1-11.

Bizzini A, Majcherczyk P, Beggah-Möller S, Soldo B, Entenza JM, Gaillard M, et al. Effects of α-phosphoglucomutase deficiency on cell wall properties and fitness in *Streptococcus gordonii*. Microbiology 2007; 153: 490-498.

Boher B, Nicole M, Potin M, Geiger JP. Extacellular polysaccharides from *Xanthomonas axonoplodis pv. manihotis* interact with cassava cell walls during pathogenesis. Molecular Plant-Microbe Interactions Journal 1997; 10: 803-811.

Campbell JA, Davies GJ, Bulone V, Henrissat B. A classification of nucleotide-diphospho-sugar glycosyltransferases based on amino acid sequence similarities. Biochemical Journal 1997; 326: 929-939.

Cantaloube S, Veyron-Churlet R, Haddache N, Daffé M, Zerbib D. The *Mycobacterium tuberculosis* FAS-II dehydratases and methyltransferases define the specificity of the mycolic acid elongation complexes. Plos One 2011; 6: 1-11.

CBI. The plants and young plant material market in the EU, Centre for the promotion of imports from developing countries (Ed) CBI, Rotterdam, The Netherlands.: Available online: www.cbi.nl/marketinfo/cbi/, 2006.

Champion MD. Host-pathogen o-methyltransferase similarity and its specific presence in highly virulent strains of *Francisella tularensis* suggests molecular mimicry. Plos One 2011; 6: 1-12.

Chou FL, Chou HC, Lin YS, Yang BY, Lin NT, Weng SF, et al. The *Xanthomonas campestris* gumD gene required for synthesis of xanthan gum is involved in normal pigmentation and virulence in causing black rot. Biochemical and Biophysical Research Communications 1997; 233: 265–269.

Collmer A. Determinants of pathogenicity and avirulence in plant pathogenic bacteria. Current Opinion in Plant Biology 1998; 1: 329-335.

Cornelis K, Ritsema T, Nijsse J, Holsters M, Goethals K, Jaiziri M. The plant pathogen *Rhodococcus fascians* colonizes the exterior and interior of the aerial parts of plants. Molecular Plant-Microbe Interactions Journal 2001; 14: 599-608.

Cornelis K, Maes T, Jaziri M, Holsters M, Goethals K. Virulence genes of the phytopathogen *Rodococcus fascians* show specific spatial and temporal expression patterns during plant infection. Molecular Plant-Microbe Interactions Journal 2002; 15: 398-403.

Coutinho PM, Deleury E, Davies GJ, Henrissat B. An evolving hierarchical family classification for glycosyltransferases. Journal of Molecular Biology 2003; 328: 307-317.

Crespi M, Messens E, Caplan AB, van Montagu M, Desomer J. Fasciation induction by the phytopatogen *Rhodococcus fascians* depends upon a linear plasmid encoding a cytokinin synthase gene. EMBO Journal 1992; 11: 795-804.

Crespi M, Vereecke D, Temmerman W, Van Montagu M, Desomer J. The *fas* operon of *Rhodococcus fascians* encodes new genes required for efficient fasciation of host plants. Journal of Bacteriology 1994; 176: 2492-2501.

Cuccui J, Wren BW. Bacteria like sharing their sweets. Molecular Microbiology 2013; 89: 811-815.

de Boer SH, Wieczorek A, Kummer A. An ELISA test for bacterial ring rot of potato with a new monoclonal antibody. Plant Disease 1988; 72: 874-878.

de O Manes CL, Beeckman T, Ritsema T, Van Montagu M, Goethals K, Holsters M. Phenotypic alterations in *Arabidopsis thaliana* plants caused by *Rhodococcus fascians* infection. Journal of Plant Research 2004; 117: 139-145.

Depuydt S, Dolezal K, Van Lijsebettens M, Moritz T, Holsters M, Vereecke D. Modulation of the hormone setting by *Rhodococcus fascians* results in ectopic KNOX activation in *Arabidopsis*. Plant Physiology 2008; 146: 1267-1281.

Depuydt S, De Veylder L, Holsters M, Vereecke D. Eternal youth, the fate of developing *Arabidopsis* leaves upon *Rhodococcus fascians* infection. Plant Physiology 2009a; 149: 1387-1398.

Depuydt S, Trenkamp S, Fernie AR, Elftieh S, Renou J, Vuylsteke M, et al. An integrated genomics approach to define niche establishment by *Rhodococcus fascians*. Plant Physiology 2009b; 149: 1366-1386.

Desaki Y, Miya A, Venkatesh B, Tsuyumu S, Yamane H, Kaku H, et al. Bacterial lipopolysaccharides induce defense responses associated with programmed cell death in rice cells. Plant and Cell Physiology 2006; 47: 1530–1540.

Desomer J, Dhaese P, Van Montagu M. Conjugative transfert of cadmium resistance plasmids in *Rhodococcus fascians* strains. Journal of Bacteriology 1988; 170: 2401-2405.

Donnelly PM, Bonetta D, Tsukaya H, Dengler NG. Cell cycling and cell enlargement in developing leaves of *Arabidopsis*. Developmental Biology 1999; 215: 407-419.

Dover LG, Cerdeño-Tárraga AM, Pallen MJ, Parkhill J, Besra GS. Comparative cell wall core biosynthesis in the mycolated pathogens, *Mycobacterium tuberculosis* and *Corynebacterium diphtheriae*. FEMS Microbiology Reviews 2004; 28: 225-250.

Dow JM, Crossman L, Findlay K, He YQ, Feng JX, Tang JL. Biofilm dispersal in *Xanthomonas campestris* is controlled by cell–cell signaling and is required for full virulence to plants. PNAS 2003; 100: 10995–11000.

Dyakov Y, Dzhavakhiya V, Korpela T. Comprehensive and molecular phytopathology, 2007.

Forizs L, Lestrade S, Mol A, Dierick JF, Gerbaux C, Diallo B, et al. Metabolic shift in the phytopathogen *Rhodococcus fascians* in response to cell-free extract of infected tobacco plant tissues. Current Microbiology 2009; 58: 483-487.

Forizs L. Metabolism and pathogenicity in the phytopathogen *Rhodococcus fascians*. PhD thesis. Université Libré de Bruxelles, Brussels, Belgium, 2012, pp. 171.

Francis I, Gevers D, Karimi M, Holsters M, Vereecke D. Linear plasmids and phytopathogenicity. Vol 7: Microbial Linear Plasmids. Berlin: Springer-Verlag, 2007.

Francis I, Holsters M, Vereecke D. The Gram-positive side of plant-microbe interactions. Environmental Microbiology 2010; 12: 1-12.

Francis I, De Keyser A, De Backer P, Simón-Mateo C, Kalkus J, Pertry I, et al. pFiD188, the Linear Virulence Plasmid of *Rhodococcus fascians* D188 Molecular Plant-Microbe Interactions Journal 2012; 25: 637-647.

Galbraith DW, Bourque DP, Bohnert HJ. Methods in plant cell biology - Part B. Vol 50. London: Academi Press, inc., 1995.

Galuszka P, Popelková H, Werner T, Frébortová J, Pospísilová H, Mik V, et al. Biochemical characterization of cytokinin oxidases/dehydrogenases from *Arabidopsis thaliana* expressed in *Nicotiana tabacum* L. Journal of Plant Growth Regulation 2007; 26: 255-267.

Gelvin SB. *Agrobacterium* and plant genes involved in T-DNA transfer and integration. Annual Review of Plant Physiology and Plant Molecular Biology 2000; 51: 223-256.

Gelvin SB. Plant proteins involved in *Agrobacterium*-mediated genetic transformation. Annual Review of Phytopathology 2010; 48: 45-68.

Goethals K, Montagu M, Holsters M. Conserved motifs in a divergent nod box of *Azorhizobium caulinodans* ORS571 reveal a common structure in promoters regulated by LysR-type proteins. PNAS 1992; 89: 1646-1650.

Goethals K, Vereecke D, Jaziri M, Van Montagu M, Holsters M. Leafy gall formation by *Rhodococcus fascians*. Annual Review of Phytopathology 2001; 39: 27-52.

Goodfellow M. Reclassification of *Corynebacterium fascians* (Tilford) Dowson in the Genus *Rhodococcus*, as *Rhodococcus fascians* comb. nov. Systematic and Applied Microbiology 1984; 5: 225-229.

Gottwald TR, Graham JH, Schubert TS. Citrus canker: The pathogen and its impact. Plant Health Progress 2002.

Guerin M, Kordulakova J, Schaeffer F, Svetlikova Z, Gicquel B, Mikusova K, et al. Molecular recognition and interfacial catalysis by the essential phosphatidylinositol mannosyltransferase PimA from mycobacteria. The Journal of Biological Chemistry 2007; 282: 20705-20714.

Gürtler V, Mayall BC, Seviour R. Can whole genome analysis refine the taxonomy of the genus *Rhodococcus*? FEMS Microbiology Reviews 2004; 28: 377-403.

Hashimi SM, Birch RG. Functional analysis of genes for benzoate metabolism in the albicidin biosynthetic region of *Xanthomonas albilineans*. Applied Microbiology and Biotechnology 2010; 87: 1475–1485.

Hayward A, Stone G. Oak gall wasp communities: Evolution and ecology. Basic and Applied Ecology 2005; 6: 435-443.

Hsiao YM, Liu YF, Fang MC, Song WL. XCC2731, a GGDEF domain protein in *Xanthomonas campestris*, is involved in bacterial attachment and is positively regulated by Clp Microbiological research 2011; 166: 548-565.

Hu Y, Chen L, Ha S, Gross B, Falcone B, Walker D, et al. Crystal structure of the MurG:UDP-GlcNAc complex reveals common structural principles of a superfamily of glycosyltransferases. PNAS 2003; 100: 845-849.

Ichiyama S, Shimokata K, Tsukamura M. Carotenoid pigments of genus *Rhodococcus*. Microbiology and Immunology 1989; 33: 503-508.

Joshi M, Loria R. *Streptomyces turgidiscabies* possesses a functional cytokinin biosynthetic pathway and produces leafy galls. Molecular Plant-Microbe Interactions Journal 2007; 20: 751–758.

Katz JE, Dlakic M, Clarke S. Automated identification of putative methyltransferases from genomic open reading frames. Molecular & Cellular Proteomics 2003; 2: 525-540.

Kers JA, Cameron KD, Joshi MV, Bukhalid RA, Morello JE, Wach MJ, et al. A large, mobile pathogenicity island confers plant pathogenicity on *Streptomyces* species. Molecular Microbiology 2005; 55: 1025–1033.

Kevers C, Franl T, Strasser RJ, Dommes J, Gaspar T. Hyperhydricity of micropropagated shoots: a typically stress-induced change of physiological state. Plant Cell, Tissue and Organ Culture 2004; 77: 181-191.

Kuramitsu HK. Proprieties of a mutant of *Streptococcus mutans* altered in glucosyltransferase activity. Infection and Immunity 1976; 13: 345-353.

Lacey MS. The development of filter-passing organisms in *Corynebacterium fascians* cultures. Annals of Applied Biology 1961; 49: 634-644.

Li J, Wang N. The gpsX gene encoding a glycosyltransferase is important for polysaccharide production and required for full virulence in *Xanthomonas citri* subsp. *citri*. BMC Microbiology 2012; 12: 31.

Lissina E, Weiss D, Young B, Rella A, Cheung-Ong K, Del Poeta M, et al. A novel small molecule methyltransferase is important for virulence in *Candida albicans*. ACS Chemical Biology 2014; 8: 2785-2793.

Loria R, Kers J, Joshi M. Evolution of plant pathogenicity in *Streptomyces*. Annual Review of Phytopathology 2006; 44: 469-487.

Lorite GS, Richard J, Clerici JH. Surface Physicochemical Properties at the Micro and Nano Length Scales: Role on Bacterial Adhesion and *Xylella fastidiosa* Biofilm Development Plos One 2013; 8: e75247.

Maes T, Vereecke D, Ritsema T, Cornelis K, Thi Thu HN, Van Montagu M, et al. The *att* locus of *Rhodococcus fascians* strain D188 is essential for full virulence on tobacco through the production of an autoregulatory compound. Molecular Microbiology 2001; 42: 13-28.

Marco ML, Legac J, Lindow SE. *Pseudomonas syringae* genes induced during colonization of leaf surfaces. Environmental Microbiology 2005; 7: 1379-1391.

Miller ML, Putnam ML, Kraus J. Survival and spread of *Rhodococcus fascians* in greenhouse grown herbaceous perennials. Phytopathology 2007; 97 (Suppl.).

Miller ML, Putnam ML. Pathogenicity testing of *Agrobacterium tumefaciens* and *Rhodococcus fascians* isolates on micropropagated plants. Phytopathology 2008; 98 (Suppl.).

Nester EW, Kosuge T. Plasmids specifying plant hyperplasias. Annual Review of Microbiology 1981; 35: 531-565.

Netea MG, Brown GD, Kullberg BJ, Gow NA. An integrated model of the recognition of *Candida albicans* by the innate immune system. Nat. Rev. Microbiol. 2008; 6: 67–78.

Nishiuchi Y, Baba T, Yano I. Mycolic acids from *Rhodococcus*, *Gordonia*, and *Dietzia*. Journal of microbiological methods 2000; 40: 1-9.

Paterson GK, Cone DB, Peters SE, Maskell DJ. The enzyme phosphoglucomutase (Pgm) is required by *Salmonella enterica* serovar Typhimurium for O-antigen production, resistance to antimicrobial peptides and *in vivo* fitness. Microbiology 2009; 155: 3403-3410.

Pertry I. How the *fas* locus contribues to *Rhodococcus fascians* cytokinin production: an in-depth molecular and biochemical analysis. PhD thesis. Ghent University, Ghent, Belgium, 2009, pp. 170.

Pertry I, Václavíková K, Depuydt S, Galuska P, Spíchal L, Temmerman W, et al. Identification of *Rhodococcus fascians* cytokinins and their modus operandi to reshape the plant. Proc Natl Acad Sci USA 2009; 106: 929-934.

Pertry I, Václavíková K, Gemrotová M, Spíchal L, Galuszka P, Depuydt S, et al. *Rhodococcus fascians* impacts plant development through the dynamic Fas-mediated production of a cytokinin mix. Molecular Plant-Microbe Interactions Journal 2010; 23: 1164-1174.

Pitzschke A, Hirt H. New insights into an old story: *Agrobacterium*-induced tumour formation in plants by plant transformation. EMBO J. 2010; 29: 1021-1032.

Putnam ML, Miller ML. It is crown gall or leafy gall? Digger 2006; 50: 39-46.

Putnam ML, Miller ML. *Rhodococcus fascians* in herbaceous perennials. Plant Dis. 2007; 91: 1064-1076.

Putnam M. Demystifying *Rhodococcus fascians*. Digger 2014: 33-37.

Rajaoson S, Vandeputte OM, Vereecke D, Kiendrebeogo M, Ralambofetra E, Stévigny C, et al. Virulence quenching with a prenylated isoflavonone renders the Malagasy legume *Dalbergia pervillei* resistant to *Rhodococcus fascians*. Environmental Microbiology 2011; 13: 1236-1252.

Rédei GP. Encyclopedia of genetics, genomics, proteomics, and informatics, 2008.

Schaeffer ML, Khoo KH, Besra GS, Chatterjee D, Brennan PJ, Belisle JT, et al. The *pimB* gene of *Mycobacterium tuberculosis* encodes a mannosyltransferase involved in

lipoarabinamannan biosynthesis. The Journal of Biological Chemistry 1999; 274: 31625-31631.

Simeone R, Huet G, Constant P, Malaga W, Lemassu A, Laval F, et al. Functional characterisation of three O-methyltransferases involved in the biosynthesis of phenolglycolipids in *Mycobacterium tuberculosis*. Plos One 2013; 8: 1-13.

Simón-Mateo C, Depuydt S, de Oliveira Manes CL, Cnudde F, Holsters M. The phytopathogen *Rhodococcus fascians* breaks apical dominance and activates axillary meristems by inducing plant genes involved in hormone metabolism. Molecular Plant Pathology 2006; 7: 103-112.

Stes E, Holsters M, Vereecke D. Phytopathogenic strategies of *Rhodococcus fascians*. Vol 16: Biology of *Rhodococcus*. Berlin: Springer-Verlag, 2010.

Stes E, Vandeputte OM, El Jaziri M, Holsters M, Vereecke D. A successful bacterial coup d'état: how *Rhodococcus fascians* redirects plant development. Annual Review of Phytopathology 2011; 49: 1-118.

Stes E, Prinsen E, Holsters M, Vereecke D. Plant-derived auxin plays an accessory role in symptom development upon *Rhodococcus fascians* infection. The Plant Journal 2012; 70: 513-527.

Stes E, Francis I, Pertry I, Dolzblasz A, Depuydt S, Vereecke D. The leafy gall syndrome induced by *Rhodococcus fascians*. FEMS Microbiology Letters 2013; 342: 187-194.

Struck AW, Thompson ML, Wong LS, Micklefield J. S-adenosyl-methionine-dependent methyltransferases: highly versatile enzymes in biocatalysis, biosynthesis and other biotechnological applications. Chembiochem 2012; 13: 2642-2655.

Sundin GW, Jacobs JL. Ultraviolet radiation (UVR) sensitivity analysis and UVR survival strategies of a bacterial community from the phyllosphere of field-grown peanut (*Arachis hypogeae L.*). Microbial Ecology 1999; 38: 27-38.

Taniguchi N, Honke K, Fukuda M. Handbook of Glycosyltransferase and Related Genes. Tokyo, 2002.

Taniguchi N, Nakano K, Nomura R, Naka S, Kojima A, Matsumoto M, et al. Defect of glucosyltransferases reduces platelet aggregation activity of *Streptococcus mutans*: analysis of clinical strains isolated from oral cavities. Archives of Oral Biology 2010; 55: 410-416.

Tarkowski P, Vereecke D. Threats and opportunities of plant pathogenic bacteria. Biotechnol Advances 2014; 32: 215-229.

Temmerman W, Vereecke D, Dreesen R, Montagu M, Holsters M, Goethals K. Leafy gall formation is controlled by fasR, an AraC-type regulatory gene in *Rhodococcus fascians*. Journal of bacteriology 2000; 182: 5832-5840.

Tilford PE. Fasciation of sweet peas caused by *Phytomonas fascians* n.sp. . African

Journal of Agricultural Research 1936; 53: 383-394.

Vandeputte OM, Öden S, Mol A, Vereecke D, Goethals K, El Jaziri M, et al. Biosynthesis of auxin by the Gram-positive phytopathogen *Rhodococcus fascians* is controlled by compounds specific to infected plant tissues. Applied and Environmental Microbiology 2005; 71: 1169-1177.

Vereecke D, Burssens S, Simón-Mateo C, Inzé D, Van Montagu M, Goethals K, et al. The *Rhodococcus fascians* - plant interaction: morphological traits and biotechnological applications. Planta 2000; 210: 241-251.

Vereecke D, Cornelis K, Temmerman W, Holsters M, Goethals K. Versatile persistence pathways for pathogens of animals and plants. Trends in Microbiology 2002a; 10: 485-488.

Vereecke D, Cornelis K, Temmerman W, Jaziri M, Van Montagu M. Chromosomal locus that affects the pathogenicity of *Rhodococcus fascians*. Journal of Bacteriology 2002b; 184: 1112-1120.

Wagner GK, Pesnot T. Glycosyltransferases and their assays. Chembiochem 2010; 11: 1939-1949.

Whitfield C, Amor PA, Koplin R. Modulation of the surface architecture of gram-negative bacteria by the action of surface polymer:lipid A-core ligase and by determinants of polymer chain length. Molecular Microbiology 1997; 23: 629-638.

8. Annexes

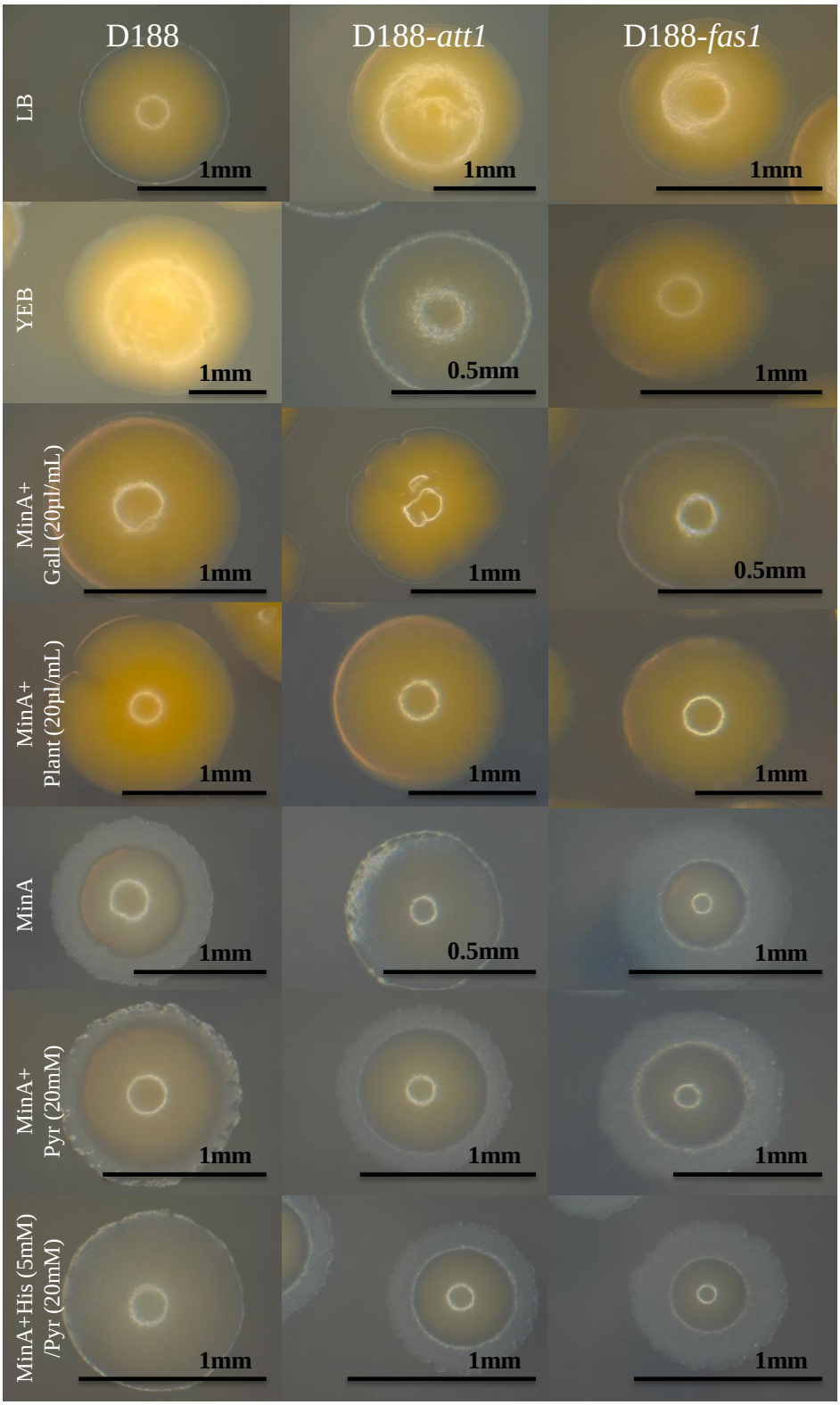

Figure 8.1 Colony morphology of the wild-type *R. fascians* strain D188, the attenuated mutant D188-*att1*, and the non-pathogenic mutant D188-*fas1* grown on different media. Photos of representative colonies after 4 days of growth at 28°C were taken with a binocular and the ProRes®CapturePro 2.8 software (exposure time of 650ms).

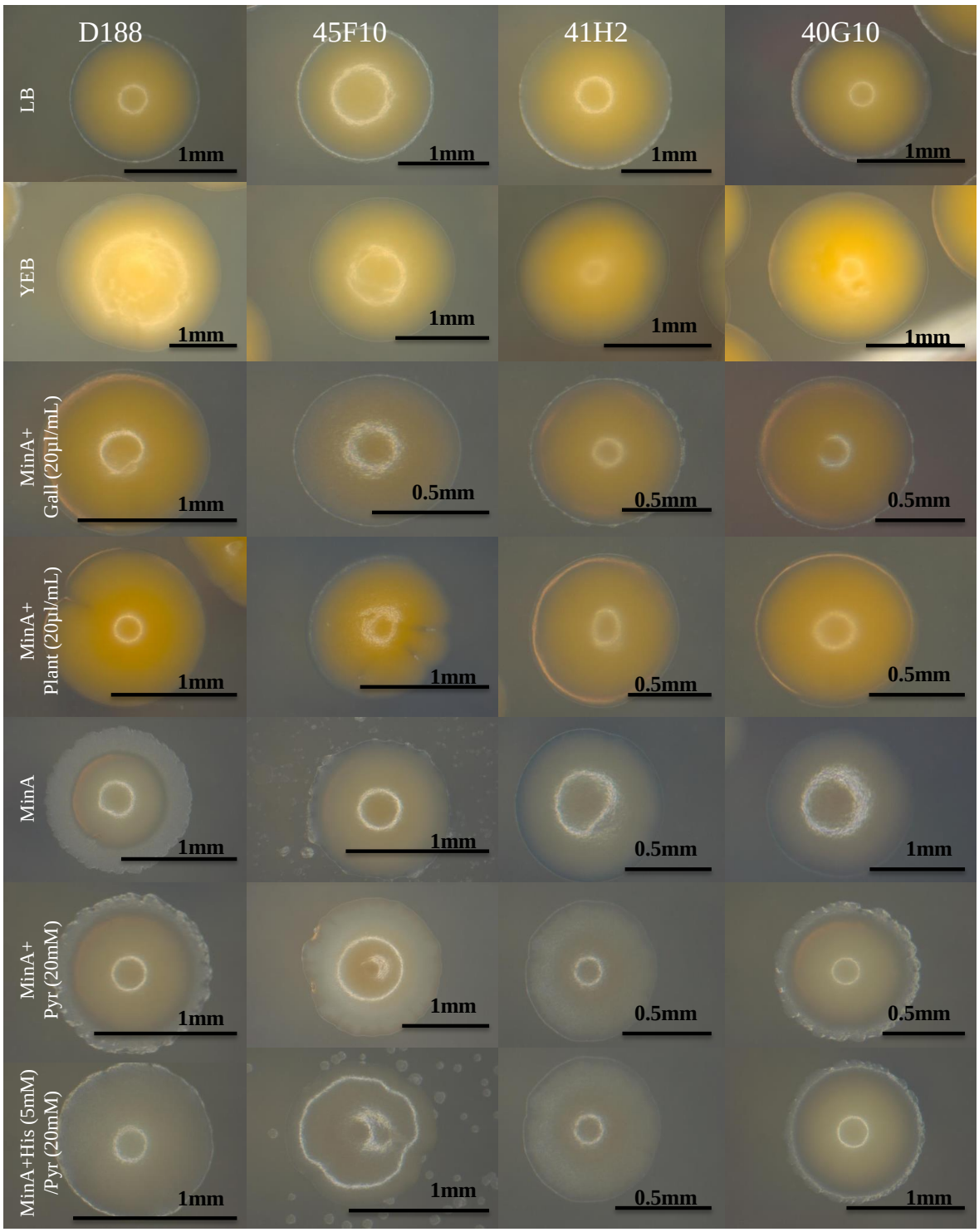

Figure 8.2 Colony morphology of the wild-type *R. fascians* strain D188 and three *GT1* transposon mutants 45F10, 41H2 and 40G10, grown on different media.
Photos of representative colonies after 4 days of growth at 28°C were taken with a binocular and the ProRes®CapturePro 2.8 software (exposure time of 650ms).

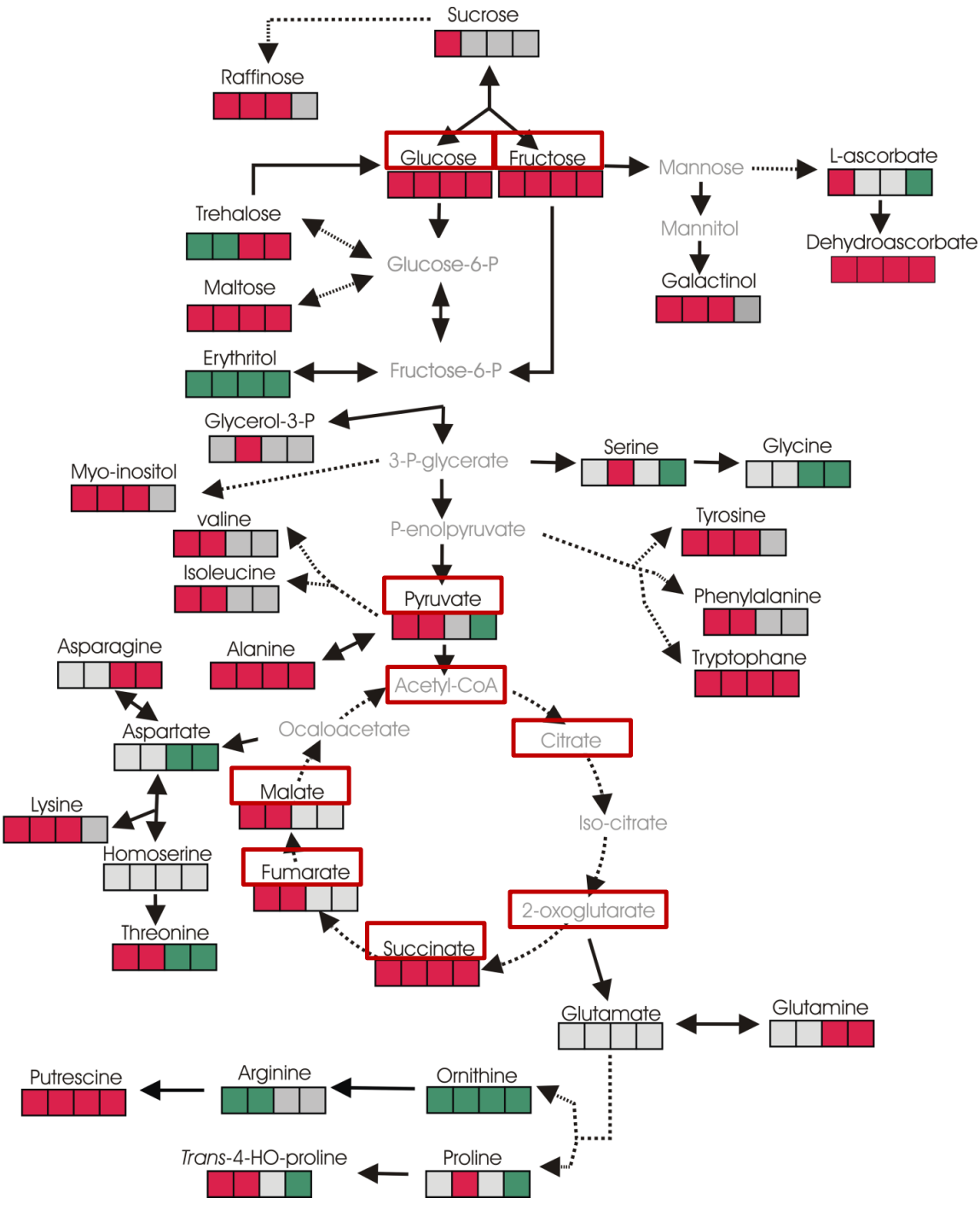

Figure 8.3 Overview of significant changes in the primary metabolism upon infection with *R. fascians* D188 when compared with D188-5 infection.
Green and red represent compounds of which the concentration increases or decreases with time, respectively. Grey indicates no significant changes. Red boxes are the C-sources used in the induction assays. Acetate is in the form of Acetyl-CoA and Histidine can be transformed in 2-oxoglutarate (Depuydt et al., 2009b).